1979 AUTHOR INDEX

Asterisk indicates abstract

Abbud, Y. see Balachandran, S.

Abdel-Razzak, M. and Christie, J. H. Thyroid carcinoma in an autonomously functioning nodule, 1001

Abrams, H. L. Federation of American Societies of Radiological Science, 1318

Abreau, C. see Kleinmann, R. E.

Abrenio, J. K., Jhingran, S. G. and Johnson, P. C. Ga-67 citrate abdomen image in starch granulomatous disease, 902

Aburano, T., Tonami, N. and Hisada, K. CEA radioimmunoassay in liver metastases detection, 232

Ackerman, R. H. see Goodman, M. M.

Ackery, D. M. see Karran, S. J.

Adams, R. and Hine, G. J. Deadtime correction for radionuclide angiocardiography, 168

Adkinson, N. F. see Hamilton, R. G.

Adolph, R. see Nishiyama, H.

Agress, H. Decision making and Bayesian analysis, 622*

Ahluwalia, B., Javaheri, S., Eldred, E., Pappagianopoulos, P., Elmaleh, D. R., Hales, C. A., Brownell, G. L. and Kazemi, H. Regional delivery of radioaerosol, 272

Ahmad, D. see Chamberlain, M. J.

Ahmad, M., Fletcher, J. W., Pur-Shariari, A. A., George, E. A. and Donati, R. M. Radionuclide venography and lung scanning, 291

Ahmad, M., Perrillo, R. P., Sunwoo, Y. C. and Donati, R. M. Xe-133 retention in hepatic steatosis, 397

Ahmad, M., Sullivan, T., Haibach, H., Sandock, K., Logan, K. and Holmes, R. Exercise induced change in left ventricular function, 640*

Akashi, Y. see Miyamae, T.

Alavi, A., Desai, A., Esterhai, J., Brighton, C. and Dalinka, M. Bone scanning of nonunited fractures, 647*

Alavi, A., Reivich, M., Greenberg, J., Christman, D., Fowler, J. S., Hand, P., Rosenquist, A., Rintelman, W. and Wolf, A. P. Mapping of functional brain activity with F-18 fluorodeoxyglucose, 612*

Alavi, A., Ring, E. and Baum, S. Radioisotopic demonstration of acute intestinal bleeding, 631*

Alavijeh, H. S. see Sherbini, S.

Alazraki, N. P. see Verba, J. W.

Albro, P. C. see Ritchie, J. L.

Alderson, P. O. Book review; *Clinical Nuclear Cardiology*, 465

Alderson, P. O., Douglass, K. H., Mendenhall, K. G., Guadini, V. A., Watson, D. C., Links, J. M. and Wagner, H. N. Deconvolution analysis in left-to-right cardiac shunt quantitation, 502

Alderson, P. O., Lee, H., Summer, W. R., Motazedi, A. and Wagner, H. N. Comparison of Xe-133 washout and single-breath lung imaging, 917

Alderson, P. O., Vieras, F., Housholder, D. F., Mendenhall, K. G. and Wagner, H. N. Gated and cinematic perfusion imaging in experimental pulmonary embolism, 407

Alderson, P. O.
see Boonyaprapa, S.
see Bradley, W. P.
see Camargo, E. E.
see Chipps, B. E.
see Katz, R. D.
see Yang, S. L.

Ali, A.
see Fordham, E.
see Tetalman, M.

Ali, F. A. see Faraj, B. A.

Allan, A. see Ell, P. J.

Allen, D. R.
see Larson, S. M.
see Rudd, T. G.

Allen, E. W.
see Leonard, J. C.
see Venkatesh, N.

Allen, S. I. see Ostrow, H. G.

Allison, K. J. see Katzenellenbogen, J. A.

Almaraz, B. see Perlstein, M.

Almasi, J. see Verba, J.

Alpert, J. S. see Wynne, J.

Alpert, N. M.
see Bingham, J. B.
see Konstam, M. A.

Alter, W. A., Grissom, M., Hill, J., Vieras, F., Eckelman, W. C. and Phillips, J. Receptor binding radiopharmaceuticals for myocardial imaging, 671*

Alter, W. A., Grissom, M., Hill, J., Vieras, F., Eckelman, W. C. and Phillips, J. Receptor binding radiopharmaceuticals for myocardial imaging, 683*

Alter, W. A. see Grissom, M.

Altman, R. P. see Majd, M.

Anderson, J. see Hilts, S. V.

Ando, Y. see Kubo, A.

Andrews, G. A. see Hübner, K. F.

Angelberger, P. F. Comparison of Tc-99m HSA and in vivo labeled Tc-99m RBC for cardiac studies, 1214

Appledorn, C. R. and Oppenheim, B. E. Biexponential curve fitting algorithm, 614*

Appledorn, C. R., Oppenheim, B. E. and Wellman, H. N. An adaptive filter for computer processing of digital images, 665*

Appledorn, C. R. see Oppenheim, B. E.

Applegate, G.
see Fisher, R. S.
see Malmud, L. S.

Armas, R. R., Thakur, M. L., and Gottschalk, A. Selective spleen scanning with Tc-99m RBC, 683*

Armstrong, C. J., Brown, T. F., Kirchner, P. T. and Brunsden, B. S. Right-to-left shunt quantitation, 670*

Armstrong, J. D. see Lavender, J. P.

Arnold, J. S., Barnes, W. E., Khedkar, N. and Milo, T. Kinetic studies of a new Tc-99m diphosphonate, 653*

Arnold, J. S., Barnes, W. E., Khedkar, N. and Nelson, M. Computer analysis of hepatobiliary studies, 686*

Arnold, J. S. see Khedkar, N.

Aronow, W. see Lyons, K. P.

Ash, J. M., Kass, E. and Gilday, D. L. Diuretic renal scans in pediatric hydronephrosis, 623*

Ashare, A. B. Amount of information transmitted by medical images, 609*

Ashare, A. B. Automated ROC curves, 609*

Ashburn, W. L.
see Pfisterer, M. E.
see Slutsky, R.

Ashkar, F. S., Block, F., Hourani, M. and Serafini, A. Radioassay for antibody to hepatitis B core antigen, 676*

Ashkar, F. S., Buehler, R. J., Chan, T. and Hourani, M. Radioimmunoassay of free thyroxine, 956

Ashkar, F. S., Hourani, M., Block, F. and Serafini, A. Radioassay of bile acids, 676*
Athanasoulis, C. A. see Brownell, G. L.
Atkins, F. B. and Beck, R. N. Scatter response function of collimated imaging systems, 608*
Atkins, F. B., Harper, P. V., Scott, R. and Beck, R. N. Analysis of coincident scatter for large area detector positron cameras, 635*
Atkins, F. B. see Metz, C. E.
Atkins, H. L. and Som, P. Effect of growth hormone and somatostatin on pancreas uptake of Se-75 selenomethionine, 543
Atkins, H. L.
see Hui, J. C. K.
see McAfee, J. G.
see Schachner, E. R.
see Som, P.
see Srivastava, S. C.
Atlan, H., Tzivoni, D., Weiss, A., Rod, J. L., Saloman, J., Warshaw, D., Samuels, L. D. and Gotsman, M. MUGA atrial pacing in myocardial ischemia, 668*
Atlan, H., Weiss, A., Tzivoni, D., Rein, A., Saloman, J., Warshaw, D., Samuels, L. D. and Gotsman, M. Tc-99m RBC MUGA for optimization of pacemaker rate, 660*

Babbitt, D. P. see Sty, J. R.
Bacharach, S. L., Green, M. V., Borer, J. S., Hyde, J. E., Farkas, S. P. and Johnston, G. S. Frame rate requirements for rest and stress cardiac studies, 189
Bacharach, S. L. see Ostrow, H. G.
Baehner, R. L. see Siddiqui, A. R.
Baer, K. see Fernandez-Pol, J. A.
Bahn, R. C. see Singh, M.
Bahr, G. H. see Lewis, J. T.
Bailey, M. see Blum, M.
Bails, R. P. see Myers, R. W.
Baker, W. J. see Welch, D. M.
Bakker, A. and Terpstra, I. Estimation of total binding capacity of thyroxine binding globulin, 995
Balachandran, S., Abbud, Y., Prince, M. J. and Chausmer, A. B. Tumoral calcinosis, 675*
Baldwin, R. D.
see Levinson, E. D.
see Spencer, R. P.
Ball, J. D. see Kelly, R. J.
Baltaxe, H. A. see Quaife, M. A.
Bandyopadhyay, D. see Som, P.
Banim, S. see Dymond, D. S.
Banka, V. S. see Bodenheimer, M. M.
Baran, D. see Vandevivere, J.
Baranczuk, R. J. see Spicer, J. A.
Bard, R. see Blaufox, M. D.
Bardfeld, P. A., Goldsmith, S. J. and Lipsyck, H. Beta thromboglobulin radioimmunoassay, 664*
Barnes, W. E.
see Arnold, J. S.
see Khedkar, N.
Barron, E. L. see Vieras, F.
Bar-Sella, P. see Front, D.
Basilico, F. C. see Folland, E. D.
Basmadjian, G. P., Gilliland, D. L., Leonard, J. C., Kirschner, A. S. and Ice, R. D. Para-aortic lymph node visualization with Tc-99m $SnPO_4$, 654*
Bassano, D. A. and McAfee, J. G. Cellular radiation doses of labeled neutrophils and platelets, 255
Bassingthwaighte, J. B. Kinetics of blood-to-cell uptake of tracers, 605*
Bateman, J. see Waxman, A. D.
Bateman, J. M. see Steckley, R. A.
Battler, A.
see Pfisterer, M. E.
see Slutsky, R.
Baum, S. see Alavi, A.
Baumert, J. E., Lantieri, R. L., Fawcett, H. D. and Goris, M. L. Thresholding algorithm for ventilation-perfusion studies, 613*
Baumert, J. E. see Doherty, P. W.
Baumgartner, A. M., Jones, P. F., Baumgartner, W. A. and Black, C. T. Radioimmunoassay of hair in opium abuse, 748
Baumgartner, W. A. see Baumgartner, A. M.
Baxter, B. S., Christian, P. E., and Coleman, R. E. Precision computer display techniques, 607*
Baxter, C. see Lewis, S. E.
Baxter, R. H. see Camargo, E. E.
Baylink, D. J. see Chesnut, C. H.
Beaucaire, J. see Espinola, L. G.
Beck, J. W., Tatum, J. L., Cobb, F. R., Harris, C. C. and Goodrich, J. K. Background activity calculation algorithm for T1-201 myocardial perfusion imaging, 1294
Beck, R. N.
see Atkins, F. B.
see Metz, C. E.
Becker, D. V. Radioiodine treatment in childhood hyperthyroidism, 890
Becker, D. V. see Carter, J.
Becker, E. L. see Sripada, P. K.
Becker, G. P. see Clements, I. P.
Becker, L. see Burow, R. D.
Beckers, C. see Pauwels, S.
Beekhuis, H., van Luyk, W. H. J. and Piers, D. A. Differential renal function using Tc-99m DMSA, 898
Beg, K. see Keim, H. J.
Beierwaltes, W. H. Book review; *Thyroid Cancer*, 811
Beierwaltes, W. H.
see Carey, J. E.
see Freitas, J. E.
see Gross, M. D.
see Wieland, D. M.
see Wu, J. L.
Beightol, R. W. see Welch, D. M.
Beihn, R. and Vannier, M. Pharmacokinetic Ga-67 imaging in tumors, 614*
Beller, G. A. see Nichols, A. B.
Beneventano, T. and Freeman, L. M. Book review; *Radiological Atlas of Biliary and Pancreatic Disease*, 1218
Bennett, L. R.
see Horn, N. L.
see Khentigan, A.
see Mena, I.
Bennett, M. C. see Koral, K. F.
Benua, R. S. see Gelbard, A. S.
Berger, H. J., Johnstone, D. E., Sands, M. J. and Gottschalk, A. Exercise right ventricular response in coronary artery disease, 624*
Berger, H. J. see Johnstone, D. E.
Berggren, M. J. see Singh, M.
Berman, D. S., Maddahi, J., Freeman, M., Staniloff, H., Elkayam, U., Charuzi, Y., Tanasescu, D. E., Brachman, M. B., Swan, H. J. C., Forrester, J. and Waxman, A. D. Variable time to redistribution in T1-201 exercise myocardial scintigraphy, 688*
Berman, D. S.
see Chapman, D.
see Elkayam, U.
see Maddahi, J.
see Shah, P. K.
see Staniloff, H.
see Tanasescu, D.
see Waxman, A. D.
Berridge, M., Jiang, V. W. and Welch, M. J. Local effects in labeled molecules following I-125 decay, 616*
Bertrand, A. see Pierrez, J.
Bessent, R. G., Fogelman, I., Citrin, D. L., McKillop, J. H., Turner, J. G. and Greig, W. R. Clinical comparison of Tc-99m HEDP and MDP, 896
Bessent, R. G.
see Fogelman, I.
see McKillop, J. H.
Bessman, A. see Siegel, M. E.
Bevan, J. A. see Tofe, A. J.
Bhargava, V. see Verba, J. W.
Bhaskar, G. see Rao, G. M.
Bianco, J. A., Makey, D. G., Laskey, W. K. and Shafer, R. B. Left ventricular dV/dT in coronary disease, 1
Bianco, J. A. see Shafer, R. B.
Bidani, N., Kirchner, P. T., Ryan, J. W. and Cooper, M. Impact of bone marrow imaging on bone and Ga scan interpretation, 602*
Bifolck, L. V. see Holman, B. L.
Bighi, S. M. see Feggi, L. M.
Bigler, R. E., Kostick, J. A., Laughlin, J. S. and Gillespie, J. R. Compartmental analysis of steady state $H_2{}^{15}O$ and $^{15}O_2$ distribution, 606*
Bilde, T. see Dahlager, J. I.
Billinghurst, M. W. Colloidal particle size determination by gel filtration, 1098
Billinghurst, M. W. and Jette, D. Colloidal particle size determination by gel filtration, 133
Billinghurst, M. W., Rempel, S. and Westendorf, B. A. Radiation decomposition of Tc-99m radiopharmaceuticals, 138
Bingham, J. B., Cochavi, S., Moore, R. H.,

Strauss, H. W., McKusick, K. A. and O'Brien, H. A. Rb-82 for the determination of renal blood flow, 619*
Bingham, J. B., Frega, N. S., Leaf, A., McKusick, K. A. and Strauss, H. W. Tl-201 and Tc-99m DTPA imaging in experimental tubular necrosis, 630*
Bingham, J. B., Taroli, E. J., Alpert, N. M., Boucher, C. A., Okada, R. D., McKusick, K. A., Pohost, G. M. and Strauss, H. W. Left ventricular end-diastolic volume from gated cardiac images, 667*
Birnholz, J. C. see Wynne, J.
Bishop, H. see Mena, I.
Black, C. T. see Baumgartner, A. M.
Blatt, C. J. see Hayt, D. B.
Blau, M.
see Chang, W.
see Rosenspire, K.
see Wicks, R.
Blaufox, M. D., Iloreta, F., Heller, S., Bard, R. and Freeman, L. M. Evaluation of renal function reserve with cortical regions of interest, 620*
Blaufox, M. D.
see Chervu, L. R.
see McAfee, J. G.
Blei, C. L., Cano, R. A., Johnston, G. S. and Jones, A. E. Calvarial markings on bone scan, 621*
Block, F. see Ashkar, F. S.
Block, P. C. see Boucher, C. A.
Bloom, C. Y. see Goldstein, H. A.
Bloss, R. S., McConnell, R. W., McConnell, B. G., Floyd, M., Conner, W. T., Henry, R. G. and Kahan, B. D. Imaging of a possible vascular steal from a renal transplant, 1053
Blue, J. see Nishiyama, H.
Blum, M., Harley, N. H., Kolber, A. B., Melnikoff, L. and Bailey, M. Long-term Se-75 selenomethionine retention, 365
Blumfield, D. E. see Hecht, H. S.
Blumhagen, J. D., Rudd, T. G. and Christie, D. L. Detection of gastroesophageal reflux in children, 636*
Bobba, V. R. see Krishnamurthy, G. T.
Bode, R. F. see Sonnemaker, R. E.
Bodenheimer, M. M., Banka, V. S., Fooshee, C. M., Hermann, G. A., and Helfant, R. H. Wall motion and regional ejection fraction at rest and during isometric exercise, 724
Boedecker, R. A. see Sty, J. R.
Bogren, H. G. see DeNardo, S. J.
Bohlman, W. see Stanton, T.
Bonte, F. J. see Datz, F. L.
Boon, R. see Galkin, B. M.
Boonyaprapa, S., Alderson, P. O., Garfinkel, D. J. and Wagner, H. N. Detection of pulmonary aspiration in children, 636*
Borer, J. S.
see Bacharach, S. L.
see Ostrow, H. G.
Born, M. L.
see Price, R. R.
see Steckley, R. A.
Bornstein, I. see Verba, J. W.
Boschult, P. see Quaife, M. A.
Bossuyt, A. see Deconinck, F.
Botvinick, E.
see Seder, J.
Botvinick, E. H. Pathophysiology of persistently positive myocardial images, 895
Boucher, C. A., Strauss, H. W., Okada, R. D., Kirshenbaum, H. D., Kushner, F. G., McKusick, K. A., Block, P. C., Leask, J. and Pohost, G. M. Bifocal diverging collimator for biplane heart imaging, 651*
Boucher, C. A.
see Kirshenbaum, H. D.
see Kushner, F. G.
see Okada, R. D.
Bourguignon, M. H. and Wagner, H. N. Measurement of right and left ventricular pressure, 648*
Bourguignon, M. H. see Camargo, E. E.
Bove, K. E. see Silberstein, E. B.
Bowen, R. D.
see Grove, R. B.
see Powers, T. A.
Bowerman, H. Book review; *Atlas of Xeroradiographic Anatomy of Normal Skeletal Systems*, 907
Boyd, C. M. Book review; *Textbook of Nuclear Medicine: Basic Science*, 1108
Boyd, G. S. and Merrick, M. V. New radiopharmaceuticals for hepatic and GI function, 684*
Brachman, M. B., Tanasescu, D. E., Wolfstein, R. S. and Waxman, A. D. Renal function evaluation using Tc-99m glucoheptonate and I-131 Hippuran, 623*
Brachman, M. B.
see Berman, D. S.
see Tanasescu, D. E.
see Waxman, A. D.
Bradley, W. P., Alderson, P. O. and Weiss, J. F. Effect of iron deficiency on Ga-67 citrate biodistribution and tumor uptake, 243
Bradley-Moore, P. R. and Doppman, J. L. Liver scan patterns in partial Budd-Chiari syndrome, 679*
Bradley-Moore, P. R. see Stibolt, T. B.
Bradshaw, D. L. see Spicer, J. A.
Brady, L. W. see Markoe, A. M.
Brady, T. J., Thrall, J. H., Lo, K., Clare, J., Rogers, W. L. and Pitt, B. Exercise radionuclide ventriculography in coronary artery disease, 687*
Brady, T. J., Thrall, J. H., Lo, K., Walton, J. A., Brymer, J. F. and Pitt, B. Radionuclide and contrast exercise ventriculography, 640*
Branch, R. A. see Price, R. R.
Braverman, L. E. see Kleinmann, R. E.
Bray, S. T., Partain, C. L., Teates, C. D., Guilford, W. B., Williamson, B. R. J. and McLaughlin, R. C. Bone scanning in idiopathic regional migratory osteoporosis, 1268
Bray, S. T. see Williamson, B. R. J.
Breslow, K. see Study, K. T.
Bridgeman, J. R. see Vieras, F.
Brighton, C. see Alavi, A.
Brill, A. B.
see Pickens, D.
see Price, R. R.
Brinzendine, M. see Jengo, J. A.
Brock, P. see Kleinmann, R. E.
Bronskill, M. J. Analog-circuit motion correction for liver imaging, 803
Bronskill, M. J. see Harauz, G.
Brookes, M. see Charkes, N. D.
Brown, D. H., Carlton, J. E., Rafter, J. J. and Hayes, R. L. Extraction purification of a Ga-67 binding glycoprotein, 682*
Brown, D. W. I-125 fibrinogen test complicated by allergy, 808
Brown, L. E.
see Wieland, D. M.
see Wu, J. L.
Brown, M. see Covitz, W.
Brown, M. L., Hay, I. D., Wahner, H. W. and Hammell, T. C. Comparison of the tomographic scanner and large field camera for adrenal studies, 609*
Brown, M. L.
see Bruschwein, D. A.
see Clements, I. P.
see Wahner, H. W.
Brown, N. J. G. see Jarritt, P. H.
Brown, P. see Krishnamurthy, G. T.
Brown, P. H. and Royal, H. D. Distortion of bar phantom image by collimator, 1100
Brown, P. H. see Royal, H. D.
Brown, T. F.
see Armstrong, C. J.
see Brunsden, B. S.
Brownell, G. L., Cochavi, S., Elmaleh, D. R. and Athanasoulis, C. A. Transverse section perfusion imaging in peripheral disease, 619*
Brownell, G. L.
see Ahluwalia, B.
see Goodman, M. M.
Bruns, D. J. see Siddiqui, A. R.
Brunsden, B. S., Kirchner, P. T., Charleston, D. and Harper, P. V. Optimal back-projection of 7-pinhole collimator images, 608*
Brunsden, B. S., Kirchner, P., Lands, E., Brown, T. F. and Cooper, M. Spatial resolution in depth of tomographic and non-tomographic instruments, 636*
Brunsden, B. S.
see Armstrong, C. J.
see Harper, P. V.
Bruschwein, D. A., Brown, M. L. and McLeod, R. A. Ga scintigraphy for disc space infection, 601*
Brymer, J. F. see Brady, T. J.
Buchanan, J. W. and Wagner, H. N. Editorial; Cardiovascular nuclear medicine teamwork, 377
Buchanan, J. W.
see Katz, R. D.
see Langan, J. K.
Budinger, T. F. and Gulberg, G. T. Attenuation compensation in computerized

emission tomography, 658*

Budinger, T. F., Yano, Y., Derenzo, S. E., Huesman, R. H., Cahoon, J. L., Moyer, B. R., Greenberg, W. L. and O'Brien, H. A. Rb-82 myocardial positron emission tomography, 603*

Budinger, T. F. see Yano, Y.

Buehler, R. J. see Ashkar, F. S.

Buell, U. and Kazner, E. Transmission computerized tomography and scintigraphy in intracranial tumor, 806

Buffkin, D. C., Chang, B., Webber, M. M. and Verma, R. C. Recovery and separation of radiolabeled platelets, 685*

Buffkin, D. C.
see Verma, R. C.
see Webber, M. M.

Buja, L. M. see Datz, F. L.

Bull, J. Book review; *Cancer Therapy by Hyperthermia and Radiation,* 1218

Bunow, B., Line, B. R., Horton, M. R. and Weiss, G. H. Regional ventilatory clearance by Xe scintigraphy, 703

Buoncore, E. see Hübner, K. F.

Burdine, J. A., DePuey, E. G., Orzan, F., Mathur, V. S. and Hall, R. J. Scintigraphic, EEG and enzymatic diagnosis of myocardial infarction, 711

Burdine, J. A., Murphy, P. H. and DePuey, E. G. Clinical applications of radionuclide computed tomography, 108

Burdine, J. A.
see Murphy, P. H.
see Procianoy, R. S.
see Sonnemaker, R. E.

Burgess, E. C. see Leonard, J. M.

Burns, G. S. see Thomas, S. R.

Burns, H. D., Dannals, R. F., Marzilli, L. G. and Wagner, H. N. Aminoethane complexes of carrier free Tc-99m, 641*

Burns, H. D., Manspeaker, H., Miller, R., Risch, V., Emrich, J. and Heindel, N. D. Preparation and biodistribution of Tc-99m complexes of bis(2-mercaptoethyl)-amines, 654*

Burns, H. D.
see Dannals, R. F.
see Marzilli, L. G.

Burow, R. D., Pond, M., Schafer, A. W. and Becker, L. Computer analysis of Tl-201 myocardial perfusion images, 771

Burt, R. see Park, H.

Buse, M. G. see Gordon, L.

Bushberg, J. T. see Hoffer, P. B.

Butler, T. A. see Washburn, L. C.

Buttfield, I. Australian and New Zealand Society of Nuclear Medicine, 571

Byrd, B. L.
see Hayes, R. L.
see Hübner, K. F.
see Washburn, L. C.

Cahill, P., McGovern, R., Sterrett, R., Tapia, L., Ho, L. and Hurley, J. I-131 Hippuran kinetics for renal transplant evaluation, 629*

Cahill, P. see Carter, J.

Cahoon, J. L. see Budinger, T. F.

Caldwell, J. H., Ritchie, J. L., Hamilton, G. W. and Kennedy, J. W. Exercise radionuclide ventriculography and rest-exercise Tl-201 imaging, 687*

Caldwell, J. H.
see Ritchie, J. L.
see Sorensen, S. G.

Callery, P. S. see Loberg, M. D.

Callow, A. D. see Hotte, C. E.

Calvin, J. see Driedger, A. A.

Camargo, E. E., Harrison, K. S., Wagner, H. N., Bourguignon, M. H., Reid, P. R., Alderson, P. O. and Baxter, R. H. Monitoring of left ventricular function in arrhythmia, 669*

Camargo, E. E. and Wagner, H. N. Fatty acid metabolism and drug susceptibility of *M. tuberculosis,* 676*

Camp, M. see Faraj, B. A.

Camp, V. M. see Tarcan, Y.

Cano, R. A. see Blei, C. L.

Cantor, R. E. see Friedman, M. L.

Cantrell, J. B. see Tarcan, Y.

Carey, J. E. and Swanson, D. P. Thyroid contamination from airborne I-131, 362

Carey, J. E., Thrall, J. H., Freitas, J. E. and Beierwaltes, W. H. Absorbed dose to the human adrenals from I-131 iodomethylnorcholesterol, 60

Caride, V. J. see Espinola, L. G.

Carlile, T. In memoriam; Asa E. Seeds, M. D., 573

Carlson, K. E. see Katzenellenbogen, J. A.

Carlton, J. E. see Brown, D. H.

Carpenter, J. see Hellman, C.

Carpenter, P. C. see Wahner, H. W.

Carr, D. H. see Fogelman, I.

Carretta, R. F. see Matin, P.

Carril, J. M., MacDonald, A. F., Dendy, P. P., Keyes, W. I., Undrill, P. E. and Mallard, J. R. Emission computed tomography combined with $^{99m}TcO_4^-$ brain scanning, 1117

Carson, J. J. see Sarkar, S. D.

Carter, J., Ho, S. L., Cahill, P. and Becker, D. V. Inexpensive portable data collection and image analysis, 666*

Casarett, G. W. see King, M. A.

Casey, D. L. see Digenis, G. A.

Cash, A. G. see Russell, C. D.

Casper, S. see DeLand, F. H.

Caston, N. J. see Ter-Pogossian, M. M.

Castonguay, A. see Pozderac, R. V.

Castronovo, F. P., Kopiwoda, S. Y. and Strauss, H. W. Envenomation of mice with I-125 cobra venom, 655*

Causer, D. A. see Singh, H.

Cerf, M. see Syrota, A.

Chackett, K. F. Calculation of radioactive decay with a pocket calculator, 1317

Chamberlain, C. C. see Grossman, Z. D.

Chamberlain, M. J., Mathur, P., Ahmad, D. and Kostuk, W. J. Right and left ventricular function in chronic pulmonary disease, 669*

Chan, D. W. see Perlstein, M.

Chan, T. see Ashkar, F. S.

Chanamolu, V. B. see O'Mara, R. E.

Chandler, H. L. and DeMaster, D. R. Value of Tc-99m brain scans, 620*

Chandler, H. L. see Goldstein, H. A.

Chang, B.
see Buffkin, D. C.
see Verma, R. C.
see Webber, M. M.

Chang, C. C. see Spolter, L.

Chang, W. and Blau, M. Gray scale for photoscan transparencies, 1216

Chang, W. and Blau, M. Optimization of gray scale for photoscanners, 997

Chang, W. and Blau, M. Optimization of the gray scale for photoscanners, 57

Chang, W. and Henkin, R. E. Multiple-gated tomographic blood pool imaging, 644*

Chapman, D., Newcomer, K., Berman, D. S. and Waxman, A. D. Half-inch vs quarter-inch Anger camera crystals, 610*

Charache, P. see D'Antonio, R.

Charkes, N. D. Mechanisms of skeletal tracer uptake, 794

Charkes, N. D. The bone scan in thyroid cancer, 999

Charkes, N. D., Brookes, M. and Makler, P. T. Five-compartmental model of F-18 kinetics in rats, 1150

Charkes, N. D., Makler, P. T., Malmud, L. S., Dessel, S. and Reilley, J. Optimizing bone scan timing, 614*

Charkes, N. D. see Sagar, V. V.

Charleston, D. B.
see Brunsden, B. S.
see Harper, P. V.
see Tsui, B. M. W.

Charpak, G. see Hoan, N. N.

Charuzi, Y.
see Berman, D. S.
see Maddahi, J.
see Staniloff, H.

Chatterjee, S. see Swanson, M. A.

Chaudhuri, T. see Sorensen, S. G.

Chausmer, A. B. see Balachandran, S.

Chayes, Z. see Strashun, A.

Chen, C-T. see Tsui, B. M. W.

Chen, I. W., Sperling, M. and Maxon, H. R. Modification of a digoxin radioassay for stat procedure, 664*

Chen, M. F., Whipple, J. M. and McIntyre, P. A. Radiometric assays of nutrients in food, 616*

Chen, M. F. see Kertchner, J. A.

Chervu, L. R., Robbins, E. B., Huq, S. S. and Blaufox, M. D. In vivo and in vitro studies of Tc-99m HIDA uptake, 655*

Chesnut, C. H., Baylink, D. J. and Nelp, W. B. Activation analysis of bone mass in calcitonin therapy for osteoporosis, 677*

Chesnut, C. H., Baylink, D. J. and Nelp, W. B. Activation analysis of bone mass in stanozolol therapy for osteoporosis, 677*

Chiang, G. see Yano, Y.

Chiang, L-C. see Yeh, E-L.

Chiles, J. see Tetalman, M.
Chilton, H. and Ekstrand, K. Photochromic and glass lenses for radiation protection, 898
Chilton, H., Lewis, J. C., Motsinger, S. F. and Cowan, R. J. Altered biodistribution of *I-131* iodomethylnorcholesterol, 806
Chilton, H., Lewis, J. C., Motsinger, S. F. and Cowan, R. J. *RES distribution of an impurity in* I-131 iodomethylnorcholesterol, 803
Chilton, H. see Kelly, R. J.
Chin, E. V. see Steigman, J.
Chipps, B. E., Alderson, P. O., Roland, J-M. A., Yang, S., van Aswegen, A., Rosenstein, B. L. and Wagner, H. N. Ventricular function at rest and exercise in cystic fibrosis, 637*
Chisholm, P. M., Danpure, H. J., Healey, G. and Osman, S. Cell damage resulting from In-111 oxine labeling, 1308
Christian, P. E. see Baxter, B. S.
Christie, D. L. see Blumhagen, J. D.
Christie, J. H. see Abdel-Razzak, M.
Christman, D. see Alavi, A.
Chua, K. G. see Harper, P. V.
Citrin, D. L.
see Bessent, R. G.
see Fogelman, I.
Clancy, B. see Hnatowich, D.
Clare, J. see Brady, T. J.
Clark, O. see Okerlund, M. D.
Claunch, B. C. see Royal, H. D.
Clay, M. M. see Fazio, F.
Clements, I. P., Strelow, D. A., Becker, G. P., Vlietstra, R. E. and Brown, M. L. Venous *volume changes assessed by blood pool* imaging, 633*
Clorius, J. H., Dreikorn, K., Zelt, J., Raptou, E., Weber, D., Rubinstein, K., Dahm, D. and Georgi, P. Renal graft evaluation with $^{99m}TcO_4^-$ and I-131 Hippuran, 1029
Clorius, J. H., Iio, M. and McCready, V. R. Abstracts of current literature, 585
Clorius, J. H., Ostertag, H. and Raptou, E. *I-131 Hippuran* renograms in orthostatic hypertension, 462
Clorius, J. H.
see Coupal, J. J.
see Domstad, P.
Cloutier, R. J. see Watson, E. E.
Coates, G. Xe-127 or Xe-133 for ventilation studies, 461
Coates, G. and Garnett, E. S. Ventilation studies and the perfusion lung scan, 268
Cobb, F. R.
see Beck, J. W.
see McEwan, P.
Cochavi, S., Pohost, G. M., Elmaleh, D. R. and Strauss, H. W. Transverse-sectional F-18 myocardial imaging in infarct, 1013
Cochavi, S.
see Bingham, J. B.
see Brownell, G. L.
see Nichols, A. B.
Coffey, J. L., Cristy, M. and Warner, G. G. Estimates of specific absorbed fractions for photon sources in heart, 607*
Coffey, J. L. see Watson, E. E.
Cohen, J. see Kronenberg, M. W.
Cohen, M. B. see Spolter, L.
Cohen, M. S. see Zakhireh, B.
Cohen, W. N. see Grossman, Z. D.
Cohn, S. H. see Vartsky, D.
Coleman, R. E.
see Baxter, B. S.
see Khentigan, A.
see Welch, D. M.
Collice, M. see Fazio, F.
Collier, B. D. and Drum, D. E. Radionuclide *and ultrasound liver imaging, 601**
Collier, B. D., Treves, S., McAfee, J., Subramanian, G., Davis, M. A. and Heyman, S. Tc-99m parabutyl-IDA and I-131 rose bengal studies in jaundiced *neonates*, 637*
Collins, R. see Lyons, K. P.
Collman, I. R. see Hübner, K. F.
Colombetti, L. G., Goldman, J., Patel, G. C., Goldman, M. and Pinsky, S. M. Rapid labeling of IgG with Tc-99m, 652*
Colsher, J. G. see Stoub, E. W.
Comar, D.
see Mazière, B.
see Syrota, A.
Conant, R. see Jengo, J. A.
Conner, W. T. see Bloss, R. S.
Conway, J. J., Weiss, S. C., Khentigan, A., Tofe, A. J. and Thane, T. T. Gallbladder and bowel localization of bone agents, 622*
Conway, J. J., Weiss, S. C., Luck, S. R. and Goldstein, R. I. Gastroesophageal reflux in children, 680*
Conway, J. J. see Khentigan, A.
Cook, S. A. see Fouad, F. M.
Cooper, M.
see Bidani, N.
see Brunsden, B. S.
see Harvey, E.
see Rezai-Zadeh, K.
see Ryan, J.
Corder, E. H. see Loberg, M. D.
Corgan, R. L. see DeLand, F. H.
Counsell, R. E. see Pozderac, R. V.
Coupal, J. J. Book review: *Quality Control in Nuclear Medicine; Radiopharmaceuticals, Instrumentation and In Vitro Assays*, 811
Coupal, J. J., Domstad, P., Fried, A., Kim, E. E. and Clorius, J. H. Abstracts of current literature, 370, 1321
Coupal, J. J., Domstad, P., Fried, A., Kim, E. E., Clorius, J. H. and Iio, M. Abstracts of current literature, 467
Coupal, J. J., Domstad, P., Fried, A., Simmons, G., Clorius, J. H. and McCready, V. R. Abstracts of current literature, 177
Coupal, J. J. and Kim, E. E. Clinical comparison of Tc-99m HEDP and MDP, 896
Coupal, J. J. see Smith, R. B.
Covitz, W., Eubig, C., Truman, A. T., Shelnutt, R., Sellers, B. B., Moore, H. V. and Brown, M. Monitoring cardiac function after heart surgery, 661*
Cowan, R. J.
see Chilton, H.
see Kelly, R. J.
Cowley, M. J., Mantle, J. A., Rogers, W. J., Russell, R. O., Rackley, C. E. and Logic, J. R. Diffuse activity patterns in Tc-99m pyrophosphate myocardial studies, 496
Cradduck, T. D. see Manyari, D. E.
Craig, W. E. see Sonnemaker, R. E.
Cristy, M. see Coffey, J. L.
Croft, B. Y. Safe handling of radioiodine, 362
Croft, B. Y. see Williamson, B. R. J.
Cronin, J. C. see Glass, E. C.
Cuarón, A. and Cuarón, C. H. Estimation of *total binding capacity of thyroxine binding* globulin, 996
Cuarón, A. and Cuarón, C. H. *Total binding* capacity of thyroxine-binding globulin, 67
Cuarón, C. H. see Cuarón, A.
Dab, I. see Vandevivere, J.
Dahlager, J. I. and Bilde, T. Renographic evaluation of kidney preservation with *chlorpromazine, 18*
Dahm, D. see Clorius, J. H.
Daley, K. see Sarkar, S. D.
Dalinka, M. see Alavi, A.
Daly, M. J., Jones, W., Rudd, T. G. and Tremann, J. Differential renal function using Tc-99m DMSA, 63
Daniels, D. L. see Sonnemaker, R. E.
Daniller, A. see Rudavsky, A. Z.
Dannals, R. F., Burns, H. D., Marzilli, L. G., Dannals, T. E., Trageser, T. C. and Wagner, H. N. Radiolabeled acetylcholinesterase inhibitors for myocardial imaging, 671*
Dannals, R. F. see Burns, H. D.
Dannals, T. E. see Dannals, R. F.
Danpure, H. J. see Chisholm, P. M.
D'Antonio, R., Charache, P., Wagner, H. N. and Gedra, T. Radiometric serum test for antibiotic activity, 616*
Datz, F. L., Buja, L. M., Lewis, S. E., Bonte, F. J., Parkey, R. W. and Willerson, J. T. Pathophysiology of persistently positive myocardial images, 895
Datz, F. L., Gordon, M., Lewis, S. E., Hickey, D. C., Krupski, W. and Parkey, R. W. Tc-99m S colloid angiography for evaluation of vascular trauma, 633*
Davis, M. A. and Taube, R. A. Toxicity and safety in lung perfusion studies with particles, 1099
Davis, M. A.
see Collier, B. D.
see Jones, A. G.
see Kaplan, W. D.
see Neirinckx, R. D.
see Orvig, C.
Davison, A., Jones, A. G. and Trop, H. S. New complexes of Tc-99m in lower oxidation states, 652*

Davison, A., Sohn, M., Orvig, C., Jones, A. G. and LaTegola, M. R. A tetradentate ligand to coordinate technetium, 641*
Davison, A.
see Jones, A. G.
see Orvig, C.
Deacon, J. M.
see Ell, P. J.
see Jarritt, P. H.
Deconinck, F., Bossuyt, A., Lepoudre, R. and Jonckheer, M. Dynamic densitography and tomography of the lung, 665*
de Graaf, J. see de Graaf, P.
de Graaf, P., Schicht, I. M., Pauwels, E. K. J., Souverijn, J. H. M. and de Graaf, J. Bone scintigraphy in uremic pulmonary calcification, 201
Dehmer, G. J. see Lewis, S. E.
DeLand, F. H. Book review; *Atlas of Human Anatomy*, 368
DeLand, F. H. Editorial; copyright policy, 83
DeLand, F. H. Editorial; 25th anniversary, 475
DeLand, F. H. Book review; *A Color Atlas of Sectional Anatomy*, 1319
DeLand, F. H., Kim, E. E., Corgan, R. L., Casper, S., Primus, F. J., Spremulli, E., Estes, N. and Goldenberg, D. M. Axillary lymphoscintigraphy with I-131 antibody to CEA, 1243
DeLand, F. H., Kim, E. E., Primus, F. J., Corgan, R. L., Spremulli, E., Estes, N. and Goldenberg, D. M. Cancer lymphoscintigraphy by radioimmuno-detection, 645*
DeLand, F. H.
see Kim, E. E.
see Smith, R. B.
DeLuca, S., McKusick, K. A., Winzelberg, G. G. and Strauss, H. W. Increased specificity of vertebral bone scans, 674*
Delude, D. see Gewirtz, H.
DeMaster, D. R. see Chandler, H. L.
DeMeester, T. R. see Rezai-Zadeh, K.
DeNardo, G. L.
see DeNardo, S. J.
see Glass, E. C.
DeNardo, S. J., Bogren, H. G. and DeNardo, G. L. I-123 fibrinogen scintigraphy and radiopaque venography in thrombophlebitis, 633*
DeNardo, S. J., DeNardo, G. L., Swanson, M. A., Trelford, J. D. and Krohn, K. A. Highly iodinated fibrinogen tumor imaging, 645*
DeNardo, S. J., Twardock, A. R., DeNardo, G. L. and Steffen, S. M. I-123 fibrinogen imaging of intracardiac thrombi, 604*
DeNardo, S. J. see Swanson, M. A.
Dendy, P. P. see Carril, J. M.
DePamphilis, B. V.
see Jones, A. G.
see Orvig, B. V.
DePuey, E. G.
see Burdine, J. A.
see Sonnemaker, R. E.
Derenzo, S. E. Optimization of shielding depth for circular positron tomographs, 635*
Derenzo, S. E. see Budinger, T. F.
DeRoo, M. see Devos, P. G.
Desai, A. see Alavi, A.
Dessel, S. see Charkes, N. D.
Deutchman, A. H., Hunter, W. W., Schlosser, P. A., Miller, D. W., Steidley, J. W., Profant, R. T., Gerber, M. S., Yocum, K. M. and Hyland, J. R. A multi-detector high purity germanium camera, 629*
Deutchman, A. H. see Steidley, J. W.
Devaux, J-Y. Deadtime correction for radionuclide angiocardiography, 168
Devos, P. G., Forget, P., DeRoo, M. and Eggermont, E. Evaluation of gastroesophageal reflux in children, 636*
Dewan, S. S. The bone scan in thyroid cancer, 271
Dewanjee, M. K., Fuster, V., Kaye, M. P. and Josa, M. Platelet deposition in coronary artery bypass grafts, 604*
Dewanjee, M. K. see Singh, M.
Dhawan, V. and Yeh, S. D. J. Tc-99m methylene diphosphonate labeling efficiency and stomach concentration, 791
Dhawan, V. M., Spencer, R. P. and Sziklas, J. J. Reversible functional asplenia in chronic aggressive hepatitis, 34
Diamond, G. see Staniloff, H.
Dickson, E. R. see Wahner, H. W.
Digenis, G. A., Casey, D. L., Wesner, D. A., Washburn, L. C. and Hayes, R. L. Preparation of optically active C-11 amino acids, 662*
Dilts, C. A. see Folland, E. D.
Dindogru, A. see Muz, J.
Dinerstein, R. see Huang, C. C.
Dinsmore, R. E. see Okada, R. D.
Djordjevic, L. see Ehrhardt, G. J.
Doerr, D. R. see Siddiqui, A. R.
Doherty, P. W., Fawcett, D., Goodwin, D. A., Heckman, J. R., Baumert, J. E., Lantieri, R. L. and McDougall, I. R. In-111 leukocyte scans in inflammatory disease, 659*
Dohi, Y. see Miyamae, T.
Domstad, P. Book review; *A User's Guide to Diagnostic Ultrasound*, 1003
Domstad, P. Book review; *Atlas of Abdominal Ultrasonography in Children*, 175
Domstad, P., Fried, A., Kim, E. E. and Clorius, J. H. Abstracts of current literature, 1110, 1220
Domstad, P., Fried, A., Kim, E. E., Clorius, J. H., Ganatra, R. D. and McCready, V. R. Abstracts of current literature, 75
Domstad, P., Fried, A., Kim, E. E., Clorius, J. H. and Iio, M. Abstracts of current literature, 813, 909, 1005
Domstad, P., Fried, A., Kim, E. E., Simmons, G., Clorius, J. H. and McCready, V. R. Abstracts of current literature, 275
Domstad, P. see Coupal, J. J.
Donati, R. M.
see Ahmad, M.
see Fernandez-Pol, J. A.
Donoghue, G. D. see Steinbach, J. J.
Donovan, I. A. see Harding, L. K.
Doppman, J. L. see Bradley-Moore, P. R.
D'Orsi, C. J. see Kaplan, W. D.
dos Remedios, L. V. see Khentigan, A.
Douglass, K. H. see Alderson, P. O.
Dowsett, D. J.
see Morley, T. R.
see Short, M. D.
Drasin, E. see Myers, R. W.
Dreikorn, K. see Clorius, J. H.
Drew, H. M. see Lipson, A.
Driedger, A. A., Sibbald, W. J., Moffat, J., Calcin, J., Reid, B. D. and Holliday, R. L. Alveocapillary permeability in septic pulmonary edema, 612*
Driedger, A. A. see Manyari, D. E.
Drum, D. E. see Collier, B. D.
Dubovsky, E. V. see Goldenberg, D. J.
Duick, D. S. see Wahner, H. W.
Durakovic, A. see Owunwanne, A.
Durie, B. G. M. see Woolfenden, J. M.
Dwaliby, J. M. see Freedman, G. S.
Dworkin, H. J. and Ferry, J. D. Book review; *Radioimmunoassay and Related Procedures in Medicine*, 1107
Dworkin, H. J. see Freitas, J. E.
Dye, S. F., Lull, R. J., McAuley, R. J., VanDam, B. E. and Young, W. Bone and Ga-67 scan changes in acute osteomyelitis, 647*
Dymond, D. S., Elliott, A. T., and Banim, S. Detection of a false left ventricular aneurysm, 851
Dzindzio, B. see Quaife, M. A.

Eacho, P. I. see Porter, D. W.
Eagles, C. J. see Karran, S. J.
Eckelman, W. C., Reba, R. C., Gibson, R. E., Rzeszotarski, W. J., Vieras, F., Mazaitis, J. K. and Francis, B. Receptor-binding radiotracers, 350
Eckelman, W. C.
see Alter, W. A.
see Gibson, R. E.
see Grissom, M.
see Paik, C. H.
Eckfeldt, J. H. see Shafer, R. B.
Effeney, D. J. see Seder, J.
Effros, R. M. see Uszler, J. M.
Eggermont, E. see Devos, P. G.
Ehrhardt, G. J., Head, R., Djordjevic, L. and Welch, M. J. Automated (Ge-68)-(Ga-68) solvent generator, 682*
Eichling, J. O. see Mullani, N. A.
Eigen, H. see Thirunavukkarasu, S.
Eikman, E. A. Book review; *Pulmonary Macrophage and Epithelial Cells*, 74
Eikman, E. A. Computer-assisted liver mass estimation, 808
Eikman, E. A. Teaching editorial; Radionuclide hepatobiliary procedures, 358
Eikman, E. A., Jain, V. K., Mack, G. A., Madden, J. A., Flower, D. L. and Witenhafer, S. R. Computer-assisted measure-

ment of liver inhomogeneity, 664*
Eikman, E. A., Mack, G. A., Jain, V. K. and Madden, J. A. Liver mass estimation from gamma camera images, 144
Eikman, E. A., Williams, J. W., Zander, J. D., Wheeler, J. C. and Okulski, T. A. Cholecystokinin cholescintigraphy in acute abdominal disease, 686*
Eisenberg, J. see Maayan, M. L.
Eisenman, J. I. see Verma, R. C.
Eisner, R. see Verba, J.
Eklem, M. see Krishnamurthy, G. T.
Ekstrand, K. see Chilton, H.
Elam, D. see Taplin, G. V.
Eldred, E. see Ahluwalia, B.
Elkayam, U., Berman, D. S., Freeman, M., Staniloff, H., Maddahi, J., Swan, H. J. C., Forrester, J. and Waxman, A. D. Noninvasive assessment of latent mechanical function, 667*
Elkayam, U.
see Berman, D. S.
see Maddahi, J.
see Staniloff, H.
Ell, P. J., Deacon, J. M., Jarritt, P. H., Pearce, P. C. and Allan, A. Tc-99m plasmin and I-125 fibrinogen deep vein thrombus detection, 633*
Ell, P. J. see Jarritt, P. H.
Elliott, A. T. see Dymond, D. S.
Ellis, K. J. see Vartsky, D.
Elmaleh, D. R.
see Ahluwalia, B.
see Brownell, G. L.
see Cochavi, S.
see Goodman, M. M.
Elson, M. K. see Shafer, R. B.
Emrich, J.
see Burns, H. D.
see Markoe, A. M.
Ensminger, W. D. see Kaplan, W. D.
Entine, G. see Mauderli, W.
Erickson, P. see Touya, J. J.
Ernst, J. see Kagan, A.
Espinola, L. G., Beaucaire, J., Gottschalk, A. and Caride, V. J. Distribution of Tc-99m and In-111 labeled liposomes in mice, 434
Esquerré, J. P. and Guiraud, R. Tc-99m heparin and thromboembolism, 652*
Essington, B. see Khaw, B. A.
Esterhai, J. see Alavi, A.
Estes, N. see DeLand, F. H.
Ettinger, U. R. see Kronenberg, M. W.
Eubig, C. see Covitz, W.
Evans, H. J. see LeBlanc, A. D.
Evans, R. see Lyons, K. P.
Eyler, E. R. see Hricak, H.

Fairchild, R. G. see Hui, J. C. K.
Faith, W. see Harvey, E.
Fajman, W. see Tarcan, Y.
Falkoff, M. see Lewis, S. E.
Fallon, J. T. see Khaw, B. A.
Faraj, B. A., Nixon, D., Murray, D., Tarcan, Y., Camp, M., Ali, F. A. and Stacciarini, W. Urinary excretion of L-Dopa, dopamine and methyldopamine in melanoma, 664*
Faraj, B. A. see Tarcan, Y.
Farkas, S. P. see Bacharach, S. L.
Fawcett, D. see Doherty, P. W.
Fawcett, H. D. see Baumert, J. E.
Fawwaz, R. A., Hardy, M. A., Oluwole, S., Nowygrod, R., Sung, D. I., Reemtsma, K. and Johnson, P. M. Pb-109 hematoporphyrin radiation effect on cardiac allograft, 659*
Fawwaz, R. A. and Johnson, P. M. Ga-67 localization in normally functioning kidney transplant, 207
Fawwaz, R. A.
see Johnson, P. M.
see Wang, T. S. T.
Fawzi, M. B. see Tofe, A. J.
Fay, R. see Handmaker, H.
Fazio, F., Fieschi, C., Nardini, M., Collice, M., Possa, M. and Spinelli, F. Regional cerebral blood flow by continuous Kr-81m and emission computed tomography, 611*
Fazio, F., Miniati, M., Greening, A. P. and Clay, M. M. Continuous recording of mucociliary clearance, 613*
Fazio, F., Pratt, T. A., McKenzie, C. C. and Steiner, R. E. Regional ventilation and perfusion after radiotherapy for lung carcinoma, 638*
Fazio, F. see Gordon, I.
Feggi, L. M. and Bighi, S. M. Scintigraphy of Meckel's diverticulum, 888
Feinendegen, L. E.
see Reske, S. N.
see Vyska, K.
Ferguson, D. L. see Francis, M. D.
Fernandes, P. see Grossman, Z. D.
Fernandez-Pol, J. A., Klos, D., Baer, K. and Donati, R. M. Transferrin receptors in cell culture, 672*
Ferry, J. D. see Dworkin, H.J.
Fester, A. see Janowitz, W. R.
Fields, A. T. see Loberg, M. D.
Fieschi, C. see Fazio, F.
Figiel, S. J. see Muz, J.
Finberg, H. see Wynne, J.
Fine, E. J. see Maayan, M. L.
Fink, E. J. see Waxman, A. D.
Fisher, R. S., Malmud, L. S., Stelzer, F. A., Phaosawasdi, K., Tolin, R. D., Reilley, J. and Applegate, G. Cholinergic effects in dynamic esophageal scintigraphy, 685*
Fisher, R. S.
see Malmud, L. S.
see Stelzer, F. A.
Fitzgerald, J. F. see Thirinavukkarasu, S.
Fitzgerald, L. T. see Mauderli, W.
Fitzgibbons, A. K. see Gewirtz, H.
Fleming, J. S. see Karran, S. J.
Flesh, L. H. see Kishore, R.
Fletcher, J. W. see Ahmad, M.
Flickinger, F. W. Disappearance of a hyperfunctioning thyroid nodule, 579
Flower, D. L. see Eikman, E. A.
Floyd, J. L. see Sonnemaker, R. E.
Floyd, M. see Bloss, R. S.
Fogelman, I. and Carr, D. H. Bone scanning and radiology in metabolic disease, 602*
Fogelman, I., Citrin, D. L., McKillop, J. H., Turner, J. G., Bessent, R. G. and Greig, W. R. Tc-99m HEDP and Tc-99m MDP in detection of bone metastases, 98
Fogelman, I. see Bessent, R. G.
Folland, E. D., Tow, D. E., Parisi, A. F., Karaffa, S., Dilts, C. A. and Basilico, F. C. Comparison of echocardiogram and first pass radionuclide ventriculogram for determination of LVEF, 651*
Follett, D. A. see Keim, H. J.
Fooshee, C. M. see Bodenheimer, M. M.
Fordham, E., Ali, A., Rayudu, G., Knospe, W., Richards, P. and Ku, T. H. Hemopoietic vs reticuloendothelial marrow distribution, 675*
Fordham, E. see Tetalman, M.
Forget, P. see Devos, P. G.
Forrester, J.
see Berman, D. S.
see Elkayam, U.
see Maddahi, J.
see Staniloff, H.
Forstrom, L., Hoogland, D. R., Gomez, L., Saecker, G., Weiblen, B., McCullough, J. and Loken, M. In-111 oxine labeled leukocytes in occult inflammation abscess, 659*
Forstrom, L. A. see Williams, L. E.
Forwand, S. A. see Zir, L. M.
Fossel, E. T. see Goldman, M. R.
Fouad, F. M., Houser, T., MacIntyre, W. J., Cook, S. A. and Tarazi, R. C. Automated computer program for radionuclide cardiac output determination, 1301
Fowler, J. S.
see Alavi, A.
see Som, P.
Fox, W. see Harper, P. V.
Francis, B. see Eckelman, W. C.
Francis, M. D., Ferguson, D. L. and Tofe, A. J. Comparative evaluation of three diphosphonates, 655*
Francis, M. D. see Tofe, A. J.
Franco, J. see Stanton, T.
Frank, M. S. see Weissman, H. S.
Franken, E. A. see Thirunavukkarasu, S.
Fraser, L. M. see Vieras, F.
Freedman, G. S., Knobelman, R. A., Dowaliby, J. M. and LaVallee, C. A. Salivary gland imaging, 679*
Freeman, L. M.
see Beneventano, T.
see Blaufox, M. D.
see Keim, H. J.
see Weissman, H. S.
Freeman, M.
see Berman, D. S.
see Elkayam, U.
see Maddahi, J.
see Staniloff, H.
Freeman, M. J. see Miller, I. D.
Freeman, R. see Jengo, J. A.

Frega, N. S. see Bingham, J. B.
Freitas, J. E. I-131 iodomethylnorcholesterol adrenal imaging in primary aldosteronism, 897
Freitas, J. E. and Dworkin, H. J. Optimizing the detection of hepatic metastases, 264
Freitas, J. E., Grekin, R. J., Thrall, J. H., Gross, M. D., Swanson, D. P. and Beierwaltes, W. H. Adrenal imaging with I-131 iodomethylnorcholesterol in aldosteronism, 7
Freitas, J. E., Gross, M. D., Swanson, D. P. and Beierwaltes, W. H. Cost of adrenal imaging in Cushing's syndrome, 677*
Freitas, J. E., Swanson, D. P., Gross, M. D. and Sisson, J. C. I-131 therapy for hyperthyroidism in children, 847
Freitas, J. E.
see Carey, J. E.
see Gross, M. D.
see Koral, K. F.
Freundlieb, C. see Vyska, K.
Frick, M. P., Knight, L. C., Ponto, R. A. and Loken, M. K. Evaluation of imaging instruments in canine liver hematomas, 448
Frick, M. P. see Williams, L. E.
Fried, A.
see Coupal, J. J.
see Domstad, P.
Fried, W. see Kagan, A.
Friedman, A. M. see Huang, C. C.
Friedman, M. I. see Pierson, R. N.
Friedman, M. L. and Cantor, R. E. Left ventricular aneurysm detection from gated heart scintigrams, 720
Friesinger, G. C. see Steckley, R. A.
Fritzberg, A. R., Whitney, W. P. and Klingensmith, W. C. Hepatobiliary transport mechanism of Tc-99m diethyl-IDA, 642*
Fritzberg, A. R. see Klingensmith, W. C.
Froelicher, V. see Pfisterer, M. E.
Front, D., Bar-Sella, P., Hardoff, R. and Nir, I. $^{99m}TcO_4^-$ uptake and capillary ultrastructure in brain tumors, 612*
Frost, H. see Frost, P.
Frost, P. and Frost, H. Recirculation of lymphocytes and use of In-111, 169
Fujioka, M. see Miyamae, T.
Fukuchi, M., Kido, A., Hyodo, K., Tachibana, K., Onoue, K., Morita, T. and Nagai, K. Tl-201 uptake in enlarged thyroid glands, 827
Fuster, V. see Dewanjee, M. K.

Gabel, M. see Nishiyama, H.
Gaede, J. T. see Wilkinson, R. H.
Gagne, G. M.
see Grossman, Z. D.
see McAfee, J. G.
Galambos, J. see Tarcan, Y.
Galante, M. see Okerlund, M. D.
Galkin, B. M., Gilliam, R. V., Boon, R., Shaber, G. S. and Park, C. H. Color modification of syringe shields, 1101
Ganatra, R. D.
see Domstad, P.
see Patel, M. C.
Garcia, M. M. see Witherspoon, L. R.
Garcia-Prats, J. A. see Procianoy, R. S.
Gard, M. F. and Morris, C. R. Pulse-mode photographic image development, 789
Garfinkel, D. J. see Boonyaprapa, S.
Garner, T. see Hellman, C.
Garnett, E. S. see Coates, G.
Gates, G. F. Gallium bone scan in acute leukemia, 854
Gatley, S. J. see Lieberman, L. M.
Gaulden, M. E. Book review; *Radiological Protection,* 1003
Gedra, T. see D'Antonio, R.
Gelbard, A. S., Benua, R. S., Laughlin, J. S., Rosen, G., Reiman, R. E. and McDonald, J. M. Quantitative N-13 glutamate scanning of osteogenic sarcoma, 782
Gelbard, A. S., Benua, R. S., McDonald, J. M., Reiman, R. E., Vomero, J. J. and Laughlin, J. S. Organ imaging with N-13 L-glutamate, 663*
Gelfand, M. J. see Thomas, S. R.
Genna, S. and Pang, S. C. Design and performance of a digital camera, 628*
Genna, S. see Pang, S. C.
George, E. A. see Ahmad, M.
Georgi, P. see Clorius, J. H.
Gerber, F. H. see Kmet, J. P.
Gerber, M. S. see Deutchman, A. H.
Gergans, G. see Khedkar, N.
German, P. A., Patil, A., Lumia, F. J. and Maranhao, V. Radionuclide angiography diagnosis of tricuspid regurgitation, 670*
Gewirtz, H., Sullivan, M. J., Shearer, D. R., Delude, D., Fitzgibbons, A. K. and Most, A. S. Analysis of normal zones in Tl-201 scans in coronary artery disease, 649*
Gewirtz, H.
see Kirshenbaum, H. D.
see Zir, L. M.
Gibbs, W. D. see Hübner, K. F.
Gibson, R. E., Eckelman, W. C., Vieras, F. and Reba, R. C. Biodistribution of muscarinic acetylcholine receptor antagonists, 865
Gibson, R. E. see Eckelman, W. C.
Gil, C. see Schachner, E. R.
Gilday, D. L.
see Ash, J. M.
see Renaud, L.
Gildenhorn, H. Book review; *Atlas of Radiologic Anatomy,* 74
Gillespie, J. R. see Bigler, R. E.
Gilliam, R. V. see Galkin, B. M.
Gilliland, D. L. see Basmadjian, G. P.
Gilson, A. J.
see Janowitz, W. R.
see Zusmer, N. R.
Gittes, R. F. see Kaplan, W. D.
Giwa, L. O. see Hui, J. C. K.
Glass, E. C., Hines, H. H., Cronin, J. C., Smith, A. L. and DeNardo, G. L. Kidney studies using Tc-99m methylene diphosphonate, 623*
Glass, E. C. see Matin, P.
Glober, G. see Wasnich, R.
Godfrey, S. see Samuels, L. D.
Goin, J. see Leonard, J. C.
Gold, H. K. see Khaw, B. A.
Goldenberg, D. J., Russell, C. D., Mihas, A. A., Dubovsky, E. V. and Logic, J. R. Ga-67 citrate scanning in Crohn's disease, 215
Goldenberg, D. M. see DeLand, F. H.
Goldman, J. see Colombetti, L. G.
Goldman, J. K. see Steinbach, J. J.
Goldman, M. see Colombetti, L. G.
Goldman, M. R., Fossel, E. T., Ingwall, J. and Pohost, G. M. F-19 for NMR imaging of myocardial infarction, 604*
Goldman, S. M. see Hayt, D. B.
Goldsmith, S. J. see Bardfeld, P. A.
Goldstein, H. A., Bloom, C. Y. and Hansell, J. R. Diagnosis of temporomandibular joint disease, 603*
Goldstein, H. A. and Chandler, H. L. Testicular torsion demonstration by scintigraphy, 173
Goldstein, N. P. see Wahner, H. N.
Goldstein, R. I. see Conway, J. J.
Goldstone, J. see Seder, J.
Goliash, T. see Verba, J.
Golomb, H. see Rezai-Zadeh, K.
Gomez, L. see Forstrom, L.
Goodman, J. see Harper, P. V.
Goodman, M. M., Elmaleh, D. R., Strauss, H. W., Ackerman, R. H. and Brownell, G. L. F-18 deoxyfluoroglucose tomography of canine head and heart, 606*
Goodrich, J. K. see Beck, J. W.
Goodwin, D. A. Recirculation of lymphocytes and use of In-111, 169
Goodwin, D. A. see Doherty, P. W.
Gooneratne, N. S. see Leman, R. B.
Gordon, D. G.
see Pfisterer, M. E.
see Slutsky, R.
Gordon, I., Helms, P. and Fazio, F. Ventilation/perfusion scanning in pediatrics, 639*
Gordon, L., Levine, J. H., Mayfield, R. K. and Buse, M. G. I-131 iodomethylnorcholesterol adrenal imaging in primary aldosteronism, 897
Gordon, L., Mayfield, R. K., Levine, J. H., Lopes-Virella, M. F., Sagel, J. and Buse, M. G. False-negative adrenal imaging, 677*
Gordon, M. see Datz, F. L.
Goris, M. L. Teaching editorial; Non-target activities, 1312
Goris, M. L. see Baumert, J. E.
Gorten, R. J. and Kelly, P. J. Cerebral perfusion scintigraphy in ruptured intracranial aneurysms, 611*
Goswami, R. see Katzenellenbogen, J. A.
Gotsman, M. see Atlan, H.
Gottschalk, A.
see Armas, R. R.
see Berger, H. J.
see Espinola, L. G.
see Johnstone, D. E.

see Zakhireh, B.
Gould, L. see Schelbert, H. R.
Grady, E. D. Yt-90 resin sphere internal radiation therapy, 674*
Grant, P. M. see Yano, Y.
Gray, R. see Maddahi, J.
Green, F. A. see Rosenspire, K.
Green, M. V.
see Bacharach, S. L.
see Ostrow, H. G.
Greenberg, J. see Alavi, A.
Greenberg, J. H. see Jones, S. C.
Greenberg, W. L. see Budinger, T. F.
Greene, R. E. see Konstam, M. A.
Greenfield, A. J. see Winzelberg, G. G.
Greenfield, L. Book review; *Nuclear Radiology (Second Series) Syllabus,* 465
Greenfield, L. D. Book review; *Secondary Spread in Breast Cancer,* 1319
Greening, A. P. see Fazio, F.
Greenwald, E. B. see Hart, H. E.
Greig, W. R.
see Bessent, R. G.
see Fogelman, I.
see McKillop, J. H.
Grekin, R. J. see Freitas, J. E.
Griffin, D. W. see Harding, L. K.
Grissom, M., Alter, W. A., Hill, J., Vieras, F., Eckelman, W. C. and Phillips, J. First-pass and equilibrium characteristics of Tc-99m vascular markers, 656*
Grissom, M. see Alter, W. A.
Groch, M. W., Von Behren, P. L. and Lewis, G. K. Effects of extrinsic cardiac motion on heart imaging, 657*
Grosfeld, J. L. see Thirunavukkarasu, S.
Gross, M. D., Freitas, J. E., Swanson, D. P. and Beierwaltes, W. H. Dexamethasone suppression adrenal scintigraphy, 621*
Gross, M. D., Freitas, J. E., Swanson, D. P., Brady, T. and Beierwaltes, W. H. The normal dexamethasone suppression adrenal scintiscan, 1131
Gross, M. D.
see Freitas, J. E.
see Swanson, D. P.
Grossman, Z. Book review; *Obstetrical Diagnosis by Radiographic, Ultrasonic and Nuclear Methods,* 74
Grossman, Z. D., Gagne, G. M., Zens, A. L., Thomas, F. D., Chamberlain, C. C., Singh, A., Cohen, W. N. and Heitzman, E. R. Computerized tomography of experimental acute pulmonary arterial occlusion, 601*
Grossman, Z. D., Gagne, G. M., Zens, A.L., Thomas, F. D., Chamberlain, C.C., Singh, A., Cohen, W. N. and Heitzman, E. R. Transmission computed tomography, Tc-99m MAA imaging, chest radiography in experimental pulmonary occlusion, 1251
Grossman, Z. D., McAfee, J. G., Gagne, G. M., Zens, A. L., Thomas, F. D., Fernandes, P. and Roskopf, M. L. Renal extraction efficiency of radioactive agents, 629*
Grossman, Z. D. see Wistow, B. W.
Grove, R. B., Harolds, J. A., Powers, T. A., Pederson, R. W. and Bowen, R. D. RV function by three methods, 668*
Grove, R. B., Powers, T. A., Harolds, J. A., Jones, W. B., Orr, S. C., Melton, R. E. and Bowen, R. D. Detection of obstructive uropathy using Tc-99m DTPA, 623*
Grove, R. B.
see Powers, T. A.
see Price, R. R.
Groves, B. see Sorensen, S. G.
Grunbaum, Z.
see Larson, S. M.
see Srivastava, S. C.
Guadini, V. A. see Alderson, P. O.
Guffey, M. M. see Spicer, J. A.
Guilarte, T. R. and McIntyre, P. A. Radiometric assay for Vitamin B_6, 676*
Guilarte, T. R. see Kertchner, J. A.
Guilford, W. B. see Bray, S. T.
Guinto, F. C. see Partain, C. L.
Guiraud, R. see Esquerré, J. P.
Gullberg, G. T. Constant attenuation compensation in emission computed tomography, 658*
Gullberg, G. T. and Huesman, R. H. Noise propagation in positron emission computed tomography, 609*
Gullberg, G. T. see Budinger, T. F.
Gunnar, R. see O'Connell, J.
Guruprakash, G. H. see Rao, G. M.
Gustafson, D. E. see Singh, M.

Haase, G. M. see Sfakianakis, G. N.
Haber, E. see Khaw, B. A.
Hackshaw, B. T. see Kelly, R. J.
Hagan, P. L.
see Halpern, S. E.
see Taylor, A.
Haibach, H. see Ahmad, M.
Halama, J. R., Simpkin, D. J. and Nickles, R. J. Dynamic phantom for nuclear cardiology, 610*
Hales, C. A.
see Ahluwalia, B.
see Nichols, A. B.
Hall, R. J. see Burdine, J. A.
Halpern, S. E. and Hagan, P. L. Effect of carrier on Ga-67 and Mn-54 in a tumor model I, 656*
Halpern, S. E. and Hagan, P. L. Effect of carrier on Ga-67 and Mn-54 in a tumor model II, 656*
Halpern, S. E., Preisman, R. and Hagan, P. L. Scanning dose and detection of thyroid metastases, 1099
Hamanaka, D. see Suzuki, T.
Hamilton, G. W. Tl-201 myocardial imaging in ischemic heart disease, 1201
Hamilton, G. W.
see Caldwell, J. H.
see Ritchie, J. L.
see Sorensen, S. G.
Hamilton, R. G. and Adkinson, N. F. IgG anti-insulin antibody fluctuations in diabetics, 673*
Hammell, T. C. see Brown, M. L.
Hand, P. see Alavi, A.
Handmaker, H., Young, B. and Fay, R. Nuclear renal imaging in pyelonephritis, 623*
Hansell, J. R. and Haven, G. T. Changes in precision levels of common ligand assays, 617*
Hansell, J. R. see Goldstein, H. A.
Hapke, B. see Ithakissios, D. S.
Harauz, G. and Bronskill, M. J. Respiratory motion in supine and upright liver imaging, 733
Harding, L. K., Griffin, D. W. and Donovan, I. A. Technical errors in gastric emptying measurements, 268
Hardoff, R. see Front, D.
Hardy, M. A.
see Fawwaz, R. A.
see Johnson, P. M.
Harley, N. H. see Blum, M.
Harolds, J. A.
see Grove, R. B.
see Powers, T. A.
Harp, G. D. see Larson, S. M.
Harper, P. V., Fox, W., Charleston, D. B., Rutkowsky, G., Stark, V., Ryan, J. W., Brunsden, B. S., Goodman, J., Chua, K. G. and Resnekov, L. Single photon longitudinal tomography with a 7-pinhole collimator, 644*
Harper, P. V.
see Atkins, F. B.
see Brunsden, B. S.
see Lathrop, K. A.
see Ryan, J.
see Zalutsky, M.
Harris, C. C. see Beck, J. W.
Harrison, K. S. see Camargo, E. E.
Harrison, M. J. see Potchen, E. J.
Hart, H. E. and Greenwald, E. B. Scintillation proximity assay of antigen-antibody binding kinetics, 1062
Harvey, E., Loberg, M., Ryan, J. W., Sikorski, S., Faith, W. and Cooper, M. Hepatic clearance of Tc-99m HIDA, 310
Harvey, E. see Spicer, J. A.
Harwig, J. F. see Vallabhajosula, S. R.
Hashimoto, S. see Kubo, A.
Hattner, R. S., Vincente, F. and Hull, A. Skeletal abnormalities following renal transplantation, 646*
Hattner, R. S. see Hull, A.
Hauer, D. see Shepard, J. W.
Haven, G. T. see Hansell, J. R.
Hay, I. D. see Brown, M. L.
Hayashi, T. see Wasnich, R.
Hayden, P. W., Larson, S. M. and Lakshminarayanan, S. Atropine clearance from human plasma, 366
Hayden, P. W., Rudd, T. G. and Shurtleff, D. B. Radionuclide evaluation of CSF shunt malfunction, 621*
Hayes, R. L., Rafter, J. J. and Byrd, B. L. Mechanism of Ga-67 uptake, 672*
Hayes, R. L., Szymendera, J. J. and Byrd, B. L. Effect of food intake on Ga-67 citrate distribution, 938

Hayes, R. L.
see Brown, D. H.
see Digenis, G. A.
see Hübner, K. F.
see Washburn, L. C.
Hays, M. T. Kinetics of the human thyroid trap, 219
Hays, M. T. Kinetics of the human thyroid trap, 944
Hayt, D. B., Blatt, C. J., Goldman, S. M. and Moses, D. C. Hypervascular presentation of multiple myeloma of the skull, 125
Head, R. see Ehrhardt, G. J.
Heading, R. C. see Tothill, P.
Heaf, P. J. D. see Short, M. D.
Healey, G. see Chisholm, P. M.
Hecht, H. S., Hopkins, J. M. Blumfield, D. E., Wong, M. and Rose, J. G. Reverse Tl-201 redistribution, 650*
Heckman, J. R. see Doherty, P. W.
Heffelinger, M. J. see Waxman, A. D.
Hegge, F. N. Femoral head activity in Perthes' disease, 170
Heiman, D. F. see Katzenellenbogen, J. A.
Heindel, C. C. see Partain, C. L.
Heindel, N. D.
see Burns, H. D.
see Markoe, A. M.
Heise, C. M. Parameters of free T_4 by kinetic reaction rate technique, 627*
Heise, C. M. see Reece, P. O.
Heitzman, E. R. see Grossman, Z. D.
Helfant, R. H. see Bodenheimer, M. M.
Heller, S. see Blaufox, M. D.
Helliwill, P. S. I-131 Hippuran renograms in orthostatic hypertension, 461
Hellman, C., Carpenter, J., Garner, T., Johnson, W. D. and Schmidt, D. H. Reversible left ventricular dysfunction, 662*
Hellman, D. see Hilts, S. V.
Helms, P. see Gordon, I.
Henkin, R. see O'Connell, J.
Henkin, R. E. and Plos, W. J. Book review; *Manual of Nuclear Medicine Procedures,* 586
Henkin, R. E. Book review; *Correlations in Diagnostic Imaging,* 1320
Henkin, R. E. see Chang, W.
Henry, R. E. Book review; *Radioimmunoassay and Related Techniques,* 1003
Henry, R. G. see Bloss, R. S.
Herman, D. C. see Paik, C. H.
Hermann, G. A. see Bodenheimer, M. M.
Herner, A. see Perlstein, M.
Hershman, J. M. see Tamagna, E. I.
Heyman, S. Toxicity and safety factors in lung perfusion studies with particles, 1098
Heyman, S., Kirkpatrick, J. A., Winter, H. S. and Treves, S. Gastroesophageal reflux and pulmonary aspiration in children, 680*
Heyman, S. and Treves, S. Adrenal hemorrhage in the newborn, 521
Heyman, S. see Collier, B. D.
Hickey, D. C.
see Datz, F. L.
see Lewis, S. E.
Higgins, C. S. see Ter-Pogossian, M. M.
Higgins, S. B. see O'Connor, J. L.
Hill, J.
see Alter, W. A.
see Grissom, M.
Hill, M. see Ryan, J. W.
Hill, T. C.
see Holman, B. L.
see Zimmerman, R. E.
Hillis, L. D. see Lewis, S. E.
Hilson, A. J. W. see Wainwright, R. J.
Hilts, S. V., Hellman, D., Anderson, J., Woolfenden, J., Van Antwerp, J. and Patton, D. Serial TSH determination in therapy of thyroid carcinoma, 928
Himelstein, E. S. see Kagan, A.
Hine, G. J. see Adams, R.
Hines, H. H. see Glass, E. C.
Hirsch, M. see Staniloff, H.
Hisada, K. see Aburano, T.
Hnatowich, D., Clancy, B., Kulprathipanja, S. and O'Connell, T. A new liposome with improved biodistribution, 680*
Ho, L. see Cahill, P.
Ho, S. L. see Carter, J.
Hoan, N. N., Majewski, S., Charpak, G. and Policarpo, A. J. P. L. Gaseous detector for low energy imaging, 335
Höck, A. see Vyska, K.
Hoffer, P. B., Miller-Catchpole, R. and Turner, D. A. Lactoferrin in tumor tissue, 424
Hoffer, P. B., Samuel, A., Bushberg, J. T. and Thakur, M. L. Effect of desferoxamine on Ga-67 citrate biodistribution and tumor uptake, 248
Hoffer, P. B. see Johnstone, D. E.
Hoffman, E. J., Phelps, M. E., Huang, S. C. and Kuhl, D. E. Effect of accidental coincidences in positron computed tomography, 634*
Hoffman, E. J.
see Huang, S. C.
see Phelps, M. E.
see Schelbert, H. R.
see Wisenberg, G.
Holdorf, D. see Waxman, A. D.
Hollenbeck, J. see Taylor, A.
Holliday, R. L. see Driedger, A. A.
Hollifield, J. W. see Price, R. R.
Holloway, S. see Hübner, K. F.
Holman, B. L., Hill, T. C., Wynne, J., Lovett, R. D., Zimmerman, R. E. and Smith, E. M. Single photon transaxial computed tomography of the heart, 736
Holman, B. L. and Wynne, J. When should we use Tl-201, 1206
Holman, B. L., Wynne, J., Idoine, J., Zielonka, J. and Neill, J. Non-invasive index of regional left ventricular dyskinesis, 661*
Holman, B. L., Wynne, J., Idoine, J., Zielonka, J. and Neill, J. The paradox image of left ventricular dyskinesis, 1237
Holman, B. L., Wynne, J., Neill, J. and Idoine, J. Regional asynchrony in coronary artery disease, 667*
Holman, B. L., Zimmerman, R. E., Bifolck, L. V. and Neirinckx, R. D. Anger camera imaging with Ta-178, 538
Holman, B. L.
see Neirinckx, R. D.
see Wynne, J.
Holmes, R. see Ahmad, M.
Holmes, R. A. see Troutner, D. E.
Homcy, C. see Strauss, H. W.
Honda, T. see Markoe, A. M.
Hood, J. T. see Ter-Pergossian, M. M.
Hoogland, D. R.
see Forstrom, L.
see Williams, L. E.
Hooper, H. R., Scrimger, J. W. and Lentle, B. C. Correction for out-of-focal plane blurring, 1194
Hopkins, G. B. see Kan, M. K.
Hopkins, J. M. see Hecht, H. S.
Horn, N. L., Bennett, L. R. and Marciano, D. In-111 chloride scanning in aplastic anemia, 603*
Horton, M. R. see Bunow, B.
Hotte, C. E. and Ice, R. D. In vitro stability of I-131 *o*-iodohippurate, 441
Hotte, C. E., Vecchione, J. J., Ledig, C. B., Valeri, C. R., Callow, A. D. and Kahn, P. C. Dosimetry of In-111 oxine labeled platelets, 685*
Hourani, M. see Ashkar, F. S.
Houser, T. see Fouad, F. M.
Housholder, D. F. see Alderson, P. O.
Hricak, H., Marks, D. S. and Eyler, E. R. Ventilatory abnormalities induced by pulmonary embolism, 638*
Hsu, T. H. see Lipson, A.
Huang, C. C., Friedman, A.M., Dinerstein, R. and Kulmala, H. Preparation of carrier free Br-75 and Br-77 bromocriptine, 683*
Huang, P. J. see Pierson, R. N.
Huang, S. C., Hoffman, E. J., Phelps, M. E. and Kuhl, D. E. Sampling requirements of emission computed tomography scanners, 609*
Huang, S. C., Schelbert, H. R., Phelps, M. E., Hoffman, E. J., Selin, C. J. and Kuhl, D. E. Single pass extraction of N-13 ammonia by myocardium, 648*
Huang, S. C.
see Hoffman, E. J.
see Phelps, M. E.
see Robinson, G. D.
see Schelbert, H. R.
Hübner, K. F., Andrews, G. A., Buonocore, E., Hayes, R. L., Washburn, L. C., Collmann, I. R. and Gibbs, W. D. C-11 amino acids for pancreas scanning and tomography, 507
Hübner, K. F., Buonocore, E., Gibbs, W. D., Holloway, S. and Byrd, B. L. Retroperitoneal tumor differentiation by positron tomography, 631*
Huesman, R. H.
see Budinger, T. F.

see Gullberg, G. T.
Hughes, S. P. F. see Lavender, J. P.
Hui, J. C. K., Atkins, H. L., Som, P., Ku, T. H., Fairchild, R. G., Giwa, L. O. and Richards, P. Mn-52m positron transaxial tomography in myocardial infarct, 648*
Hull, A., Hattner, R. S., and Vincente, F. Evaluation of avascular necrosis of the femoral head in renal transplant recipients, 646*
Hull, A. see Hattner, R. S.
Hungerford, G. D. see Leman, R. B.
Hunt, J. L. see Lewis, S. E.
Hunt, T. see Okerlund, M. D.
Hunter, W. W. see Deutchman, A. H.
Huq, S. S. see Chervu, L. R.
Hurley, J. see Cahill, P.
Hurst, C. see Reese, L.
Hyde, J. E. see Bacharach, S. L.
Hyland, J. R.
see Deutchman, A. H.
see Steidley, J. W.
Hyodo, K. see Fukuchi, M.

Ice, R. D.
see Basmadjian, G. D.
see Hotte, C. E.
Idoine, J.
see Holman, B. L.
see Wynne, J.
Iio, M. Nuclear medicine in the People's Republic of China, 453
Iio, M.
see Clorius, J. H.
see Coupal, J. J.
see Kitani, K.
Iloreta, F. see Blaufox, M. D.
Ingwall, J. see Goldman, M. R.
Ishibashi, K. see Ito, M.
Ishii, Y.
see Suzuki, T.
see Yonekura, Y.
Isikoff, M. see Ryan, J. W.
Ithakissios, D. S. and Hapke, B. Radioiodinated DNA for tumor imaging, 785
Ito, M., Ishibashi, K., Ohsawa, R. and Nagataki, S. Thyroid stimulating hormone radioimmunoassay, 615*

Jackson, G. Percentage uptake of therapeutic I-131 dose by thyroid, 366
Jackson, G. L. Shielding for Xe-127 ventilation studies, 171
Jackson, G. L. and MacIntyre, F. Accumulation of radioiodine in staff members, 995
Jacobstein, J. G. Air monitoring of Xe-133, 159
Jacobstein, J. G. Xe-127 or Xe-133 for ventilation studies, 460
Jain, V. K. see Eikman, E. A.
James, R. C. see Perry, J. R.
Janicki, P. see Partain, C. L.
Janowitz, W. R., Read, M., Fester, A. and Gilson, A. J. Quantification of left ventricular regurgitant fraction, 668*
Janowitz, W. R. see Zusmer, N. R.
Jarritt, P. H., Ell, P. J., Myers, M. J., Brown, N. J. G. and Deacon, J. M. Transverse-section brain imager for single gamma emitters, 319
Jarritt, P. H. see Ell, P. J.
Javaheri, S. see Ahluwalia, B.
Jengo, J. A., Conant, R., Freeman, R., Brizendine, M. and Mena, I. Effects of isometric and dynamic exercise on ejection fraction and segmental wall motion, 668*
Jensen, D. P. see Vogel, R. A.
Jette, D. see Billinghurst, M. W.
Jhingran, S. G.
see Abrenio, J. K.
see Joseph, U.
Jiang, V. W. see Berridge, M.
Johnson, P. C.
see Abrenio, J. K.
see Joseph, U.
see LeBlanc, A. D.
Johnson, P. M., Fawwaz, R. A., Hardy, M. A. and Nowygrad, R. Sequential Ga-67 imaging in renal allograft rejection, 630*
Johnson, P. M.
see Fawwaz, R. A.
see Keim, H. J.
see Wang, T. S. T.
Johnson, W. D. see Hellman, C.
Johnston, G. S.
see Bacharach, S. L.
see Blei, C. L.
see Ryan, J. W.
Johnston, R. E. Moiré patterns in gamma camera images, 1100
Johnstone, D. E., Wackers, F. J. Th., Berger, H. J., Hoffer, P. B., Kelley, M. J., Gottschalk, A. and Zaret, B. L. Effect of patient positioning on left lateral T1-201 myocardial images, 183
Johnstone, D. E. see Berger, H. J.
Jonckheer, M. see Deconinck, F.
Jones, A. E. see Blei, C. L.
Jones, A. G., Davison, A., Trop, H. S., DePamphilis, B. V., Orvig, C. and Davis, M. A. Oxotechnetium complexes, 641*
Jones, A. G.
see Davison, A.
see Orvig, C.
Jones, J. P., Price, R. R. and Rollo, F. D. Edge-finding algorithm for gated cardiac images, 643*
Jones, J. P.
see Price, R. R.
see Touya, J. J.
Jones, P. F. see Baumgartner, A. M.
Jones, R. H.
see McEwan, P.
see Newman, G. E.
Jones, S. C., Reivich, M. and Greenberg, J. H. Cerebral blood flow with $C^{15}O_2$ inhalation, 606*
Jones W. see Daly, M. J.
Jones, W. B. see Grove, R. B.
Josa, M. see Dewanjee, M. K.
Joseph, U., Jhingran, S. G. and Johnson, P. C. Ga-67 imaging in Crohn's disease, 903
Joy, M. L. G. see Renaud, L.
Judy, P. F. see Zimmerman, R. E.
Julian, P. see Waxman, A. D.
Juttner, H. U. see Waxman, A. D.

Kadir, S. see Powers, T. A.
Kadota, K., Matsumori, A., Kambara, H. and Kawai, C. Tc-99m Sn-pyrophosphate uptake in viral myopericarditis, 1047
Kadota, K. see Yonekura, Y.
Kagan, A., Fried, W., Ernst, J., Thomson, S., and Himelstein, E. S. I-123 ADH for in vivo vasopressin receptor assay, 657*
Kahan, B. D. see Bloss, R. S.
Kahl, F. R. see Kelly, R. J.
Kahn, P. C. see Hotte, C. E.
Kaiser, R. see Slutsky, R.
Kaizer, H. A. see Yang, S. L.
Kambara, H.
see Kadota, K.
see Yonekura, Y.
Kamkar, M. see Lindsay, J.
Kan, M. K. Scintillation camera simulator for remote-data acquisition testing, 1087
Kan, M. K. and Hopkins, G. B. Measurement of liver volume by emission computed tomography, 514
Kanai, S. see Kitani, K.
Kaplan, W. D., Davis, M. A. and Rose, C. Comparison of two Tc-99m agents for lymphoscintigraphy, 933
Kaplan, W. D., Ensminger, W. D., Smith, E. H., D'Orsi, C. J. and Levin, D. C. Intra-arterial hepatic infusion of Tc-99m MAA, 675*
Kaplan, W. D., Whitmore, W. F. and Gittes, R. F. Tc-99m antimony sulfide colloid visualization of prostatic lymphatic drainage, 645*
Karaffa, S. see Folland, E. D.
Kariyone, S. see Uchida, T.
Karliner, J. see Slutsky, R.
Karran, S. J., Eagles, C. J., Fleming, J. S. and Ackery, D. M. Tc-99m S colloid measurement of liver perfusion in rats, 26
Karube, Y. see Kono, A.
Kasecamp, W. R. see Lipson, A.
Kass, E. see Ash, J. M.
Kato, M. Distribution of Tc-99m Sn-pyridoxylideneisoleucine, 1189
Kato, M. In vivo Tc-99m RBC labeling with stannous pyridoxylideneaminates, 1071
Katus, H. A. see Khaw, B. A.
Katz, R. D., Alderson, P. O., Tochman, M. S., Buchanan, J. W. and Wagner, H. N. Ventilation-perfusion imaging in early detection of lung cancer, 612*
Katz, R. D., Rosenshein, N. B., Alderson, P. O. and Wagner, H. N. Abdominal-mediastinal lymphoscintigraphy in ovarian carcinoma, 646*
Katzenellenbogen, J. A., Heiman, D. F., Goswami, R., Allison, K. J., Carlson, K. E. and Payne, D. W. Halogenated estrogen analogs for breast tumor imaging, 671*

Kawaguchi, S. see Kitani, K.
Kawai, C.
see Kadota, K.
see Yonekura, Y.
Kaye, M. P. see Dewanjee, M. K.
Kazemi, H. see Ahluwalia, B.
Kazner, E. see Buell, U.
Keim, H. J., Johnson, P. M., Vaughan, E. D., Beg, K., Follett, D. A., Freeman, L. M. and Laragh, J. H. Computer-assisted static/dynamic renal imaging, 11
Kellershohn, C. see Syrota, A.
Kelley, M. J. see Johnstone, D. E.
Kelley, J. F. see Triplett, R. G.
Kelly, P. J. see Gorten, R. J.
Kelly, R. J., Chilton, H., Hackshaw, B. T., Ball, J. D., Watson, N. E., Kahl, F. R. and Cowan, R. J. Comparison of Tc-99m pyrophosphate and methylene diphosphonate in myocardial infarction, 402
Kennamer, R. Hemangioma of liver treated by irradiation, 901
Kennedy, A. C. see Rosenspire, K.
Kennedy, J. W.
see Caldwell, J. H.
see Sorensen, S. G.
Kereiakes, J. G. see Thomas, S. R.
Kertchner, J. A., Guilarte, T. R., Chen, M. F., Rider, A. A. and McIntyre, P. A. Radiometric microbiologic assay for niacin, 419
Ketring, A. see Troutner, D. E.
Keyes, J. W.
see Koral, K. F.
see Rogers, W. L.
Keyes, W. I. see Carril, J. M.
Khan, R. A. A. see Lavender, J. P.
Khaw, B. A., Fallon, J. T., Strauss, W., Gold, H. K., Katus, H. A., Essington, B. and Haber, E. In-111 DTPA-antimyosin-Fab fragment for myocardial infarct imaging, 605*
Khedkar, N., Arnold, J. S., Milo, T., Barnes, W. E. and Gergans, G. Digital comparison of Tc-99m HMDP, 655*
Khedkar, N. see Arnold, J. S.
Khentigan, A., Rudd, T. G., Bennett, L. R., Weber, P. M., Coleman, R. E., Pavel, D. G. and Conway, J. J. I-123 iodohippurate renography, 619*
Khentigan, A., Rudd, T. G., Liff, E., Weber, P. M. and dos Remedios, L. V. Tc-99m DMSA renal imaging, 619*
Khentigan, A. see Conway, J. J.
Kido, A. see Fukuchi, M.
Kim, E. E. Book review; *Normal Radiologic Patterns and Variances of the Human Skeleton,* 273
Kim, E. E., DeLand, F. H. and Maruyama, Y. Brain and lung imaging in mycosis fungoides, 240
Kim, E. E.
see Coupal, J. J.
see DeLand, F. H.
see Domstad, P.
Kim, J. H. see Silberstein, E. B.
King, M. A., Casarett, G. W. and Weber, D. A. Histopathologic and physiologic changes in irradiated bone, 1142
Kingston, E. see Krishnamurthy, G. T.
Kirch, D. L., Vogel, R. A., LeFree, M. T. and Steele, P. P. Current status of seven pinhole tomography, 643*
Kirchner, P. T. Book review; *Medical Examination Review Book, Volume 25; Nuclear Medicine, 1269 Multiple Choice Questions and Reference Explanatory Answers,* 273
Kirchner, P. T.
see Armstrong, C. J.
see Bidani, N.
see Brunsden, B. S.
see McAfee, J. G.
see Rezai-Zadeh, K.
see Ryan, J.
Kirkpatrick, J. A. see Heyman, S.
Kirschner, A. S. see Basmadjian, G. P.
Kirshenbaum, H. D., Okada, R. D., Kushner, F. G., Gewirtz, H., Strauss, H. W., Boucher, C. A. and Pohost, G. M. Global left ventricular function in Tl-201 exercise scintigrams, 687*
Kirshenbaum, H. D.
see Boucher, C. A.
see Kushner, F. G.
see Okada, R. D.
Kishore, R. Radiation decomposition of Tc-99m agents, 999
Kishore, R. and Flesh, L. H. Acute cardiopulmonary toxicity of microspheres, 899
Kitani, K., Kawaguchi, S., Iio, M., Sasaki, Y., Kanai, S. and Someya, K. Effect of sulfobromophthalein on Tc-99m HIDA and -pyridoxylideneisoleucine dynamics, 642*
Klatte, E. C. see Siddiqui, A. R.
Klausmeier, W. H. see Pozderac, R. V.
Kleinmann, R. E., Abreau, C., Brock, P. and Braverman, L. E. Radioimmunoassay of serum free thyroxine, 627*
Kleinmann, R. E., Vagenakis, A. G., Abreau, C. and Braverman, L. E. Neck abscess masquerading as acute suppurative thyroiditis, 1051
Klingensmith, G. J. see Klingensmith, W. C.
Klingensmith, W. C., Fritzberg, A. R. and Koep, L. J. Tc-99m diethyl-IDA and I-131 rose bengal studies in liver transplant, 314
Klingensmith, W. C., Fritzberg, A. R., Spitzer, V. and Koep, L. J. Tc-99m diethyl-IDA and PIPIDA for hepatobiliary evaluation, 686*
Klingensmith, W. C., Klingensmith, G. J. and Tollefsen, S. Effect of growth hormone and T_4 therapy on metaphyseal bone image, 678*
Klingensmith, W. C.
see Fritzberg, A. R.
see Shanahan, W. M. S.
Klos, D. see Fernandez-Pol, J. A.
Kloster, G. see Tisljar, U.
Kmet, J. P., Gerber, F. H. and Raflo, C. P. Red blood cell survival after stannous pyrophosphate administration, 294
Knight, L. C.
see Frick, M. P.
see Welch, M. J.
Knobelman, R. A. see Freedman, G. S.
Knoll, G. F. see Koral, K. F.
Knospe, W. see Fordham, E.
Knust, E. J., Kupfernagel, Ch. and Stöcklin, G. Long chain F-18 fatty acids for heart and liver studies, 1170
Koehler, S. A. see Williams, L. E.
Koep, L. J. see Klingensmith, W. C.
Kolber, A. B. see Blum, M.
Komaiko, M. see Waxman, A. D.
Kono, A., Maeda, T., Karube, Y., Shiokawa, H. and Matsushima, Y. Tc-99m glutamic acid-3-hydroxy-4-formalpyridine complex for hepatobiliary system, 39
Konstam, M. A., Strauss, H. W., Alpert, N. M., Miller, S. W., Murphy, R. X., Greene, R. E. and McKusick, K. A. Estimation of pulmonary arterial pressure, 923
Kopiwoda, S. Y.
see Castronovo, F. P.
see Strauss, H. W.
Koral, K. F., Freitas, J. E., Rogers, W. L. and Keyes, J. W. Thyroid scintigraphy with time-coded aperture, 345
Koral, K. F., Rogers, W. L., Keyes, J. W., Thrall, J. H., Knoll, G. F., Bennett, M. C. and Strange, D. R. Effect of camera linearity correction on N-pinhole tomography, 644*
Koral, K. F. see Rogers, W. L.
Kostick, J. A. see Bigler, R. E.
Kostuk, W. J. see Chamberlain, M. J.
Kotrappa, P., Raghunath, B., Subrahmanyam, P. S. S., Soni, P. S. and Raikar, U. R. Dry aerosol delivery system, 1000
Kousaka, T. see Torizuka, K.
Kovaleski, B. see Stanton, T.
Krishnamurthy, G. T., Bobba, V. R., Kingston, E., Brown, P. and Eklem, M. Motor function of the gallbladder, 632*
Krohn, K. A. see DeNardo, S. J.
Kronenberg, M. W., Ettinger, U. R., Wilson, G. A., Schenk, E. A. and Cohen, J. Radiotracer and biochemical determinations of experimental myocardial infarct weight, 224
Kronenberg, M. W.
see O'Connor, J. L.
see Steckley, R. A.
Kronenwetter, C. M. and Yeh, E. L. Distortion of bar phantom image, 1316
Krupski, W. see Datz, F. L.
Ku, T. H., Stang, L. G. and Prach, T. Generator production of Mn-52m, 682*
Ku, T. H.
see Fordham, E.
see Hui, J. C. K.
Kubo, A., Takagi, Y., Ando, Y. and Hashimoto, S. Analysis of diffuse Ga-67 lung uptake, 674*
Kuhl, D. E.
see Hoffman, E. J.

see Huang, S. C.
see Phelps, M. E.
Kulmala, H. see Huang, C. C.
Kulprathipanja, S. see Hnatowich, D.
Kun, L. see Sty, J.
Kuntz, D. see Maziere, B.
Kuperus, J. see Lyons, K. P.
Kupfernagel, Ch. see Knust, E. J.
Kushner, F. G., Okada, R. D., Kirshenbaum, H. D., Boucher, C. A., Strauss, H. W. and Pohost, G. M. Stress induced pulmonary Tl-201 uptake in coronary disease, 649*
Kushner, F. G.
see Boucher, C. A.
see Kirshenbaum, H. D.
see Okada, R. D.
Kyriakakos, A. see Maayan, M. L.

Lakshminarayanan, S. see Hayden, P. W.
Lands, E. see Brunsden, B. S.
Langan, J. K., Wagner, H. N. and Buchanan, J. W. Design concepts of a nuclear medicine department, 1093
Lantieri, R. L.
see Baumert, J. E.
see Doherty, P. W.
Lao, R. S. see Sy, W. M.
Lapidus, S. see Metal, I.
Laragh, J. H. see Keim, H. J.
Larson, S. M., Grunbaum, Z., Rasey, J. S., Nelson, N. J., Allen, D. R., Harp, G. D. and Williams, D. L. Transferrin binding component of EMT-6 sarcoma, 672*
Larson, S. M., Rasey, J. S., Allen, D. R. and Grunbaum, Z. Transferrin mediated uptake of Ga-67 by EMT-6 sarcoma, 843
Larson, S. M., Rasey, J. S., Allen, D. R. and Nelson, N. J. Transferrin-mediated uptake of Ga-67 by EMT-6 sarcoma, 837
Larson, S. M.
see Hayden, P. W.
see Srivastava, S. C.
Laskey, W. K. see Bianco, J. A.
LaTegola, M. R. see Davison, A.
Lathrop, K. A., Tsui, B. M. W. and Harper, P. V. Model for GI transport of Tc in the mouse, 606*
Lathrop, K. A. see Tsui, B. M. W.
Laughlin, J. S.
see Bigler, R. E.
see Gelbard, A. S.
LaVallee, C. A. see Freedman, G. S.
Lavender, J. P. and Armstrong, J. D. Ventilation/perfusion scans in collapse and consolidation, 638*
Lavender, J. P., Khan, R. A. A. and Hughes, S. P. F. Blood flow and tracer uptake in bone, 413
Lawrence, J. H. Early experiences in nuclear medicine, 561
Leaf, A. see Bingham, J. B.
Leask, J. see Boucher, C. A.
LeBlanc, A. D., Evans, H. J., Johnson, P. C. and Timpe, G. Measurement of Xe-133 air contamination, 981
Ledig, C. B. see Hotte, C. E.
Lee, C. Y., Lee, S. L. and Loken, M. K. Ovarian imaging with radioiodinated chorionic gonadotropin, 941
Lee, H. see Alderson, P. O.
Lee, P. C. see Stoub, E. W.
Lee, S. L. see Lee, C. Y.
Lee, T. see Wong, D. W.
LeFree, M. T. see Kirch, D. L.
Leman, R. B., Gooneratne, N. S., Hungerford, G. D. and Williams, A. V. Pontine glioma diagnosis, 462
Lentle, B. C. see Hooper, H. R.
Leonard, J. C., Allen, E. W., Goin, J. and Smith, C. W. Renal cortical imaging for mass lesions, 1018
Leonard, J. C. see Basmadjian, G. P.
Leonard, J. M. Rudd, T. G., Burgess, E. C. and Monda, G. A. I-131 iodocholesterol concentration in adenoma of the testis, 307
Lepoudre, R. see Deconinck, F.
Levin, D. C. see Kaplin, W. D.
Levin, S. G. Using statistics in nuclear medicine, 550
Levine, G. A. see Tamagna, E. I.
Levine, J. H. see Gordon, L.
Levine, S. see Waxman, A. D.
Levinson, E. D., Baldwin, R. D. and Spencer, R. P. Renal sinus lipomatosis, 1105
Levinson, E. D. see Spencer, R. P.
Levy, J. see Pastakia, B.
Levy, L. M. see Moskowitz, G. W.
Lew, R. A. see Sober, A. J.
LeWinter, M. see Verba, J. W.
Lewis, B. see Samuels, L. D.
Lewis, C. L. Ventilation studies and the perfusion lung scan, 268
Lewis, G. K. see Groch, M. W.
Lewis, J. C. see Chilton, H.
Lewis, J. T., Neff, R. A., Nishiyama, H. and Bahr, G. H. Photon energy effects on field uniformity tests, 363
Lewis, S. E., Dehmer, G. J., Falkoff, M., Hillis, L. D. and Willerson, J. T. Non-geometric method for determination of left ventricular volume, 661*
Lewis, S. E., Hunt, J. L., Baxter, C., Hickey, D. C. and Parkey, R. W. Tc-99m pyrophosphate muscle imaging in acute electrical burns, 646*
Lewis, S. E. see Datz, F. L.
Lieberman, L. M., Wessels, B., Gatley, S. J., Wiley, A. L., Nickles, R. J. and Young, D. F-18 fluorouracil imaging, 645*
Lieberman, L. M. see Pastakia, B.
Lief, L. see Slutsky, R.
Liff, E. see Khentigan, A.
Limbacher, J. see Partain, C. L.
Lindsay, J., Kamkar, M. and Nolan, N. G. Handgrip vs bicycle exercise for stress radionuclide ventriculography, 669*
Line, B. R. see Bunow, B.
Links, J. M. see Alderson, P. O.
Lippincott, W. see Markoe, A. M.
Lipson, A., Nickoloff, E. L., Hsu, T. H., Kasecamp, W. R., Drew, H. M., Shakir, R. and Wagner, H. N. Age-dependent changes in thyroid function tests in adults, 1124
Lipsyck, H. see Bardfeld, P. A.
Littlefield, J. see Malmud, L. S.
Liu, R. S. see Yeh, S. H.
Llaurado, J. G., Smith, G. A., Madden, J. A. and Meade, R. C. Partition of Tl-201 in isolated rat myocardial after rest and exercise, 1136
Lo, H. H. see Sober, A. J.
Lo, K. see Brady, T. J.
Loberg, M. see Harvey, E.
Loberg, M. D., Corder, E. H., Fields, A. T. and Callery, P. S. Membrane transport of Tc-99m radiopharmaceuticals in brain, 1181
Loberg, M. D. see Porter, D. W.
Logan, K. see Ahmad, M.
Logic, J. R.
see Cowley, M. J.
see Goldenberg, D. J.
Logsdon, D. F. Book review; *Health Implications of Nuclear Power Production*, 1004
Loken, M. K.
see Forstrom, L.
see Frick, M. P.
see Lee, C. Y.
see Williams, L. E.
Lopes-Virella, M. F. see Gordon, L.
Lopez, E. M. see Maayan, M. L.
Lorimer, A. R. see McKillop, J. H.
Lovett, R. D.
see Holman, B. L.
see Zimmerman, R. E.
Luck, S. R. see Conway, J. J.
Luke, R. G. see Preston, D. F.
Lukes, S. see Nishiyama, H.
Lull, R. J. see Dye, S. F.
Lumia, F. J. see Germon, P. A.
Lund, R. S. see Williams, L. E.
Lushbaugh, C. C. and Washburn, L. C. FDA IND approval for Zn-DTPA, 73
Luthmann, R. W. see Mauderli, W.
Lutz, R. J. Models for in vivo drug distribution, 614*
Lyons, K. P., Olson, H., Aronow, W., Kuperus, J., Collins, R. and Evans, R. Tc-99m pyrophosphate scintigraphy in acute myocardial infarction, 660*

Maayan, M. L., Volpert, E. M., Fine, E. J., Lopez, E. M., Eisenberg, J., Solomon, N. A. and Kyriakakos, A. Effect of TSH on Tl-201 thyroid uptake, 678*
MacDonald, A. C. see Manyari, D. E.
MacDonald, A. F. see Carril, J. M.
MacDonald, N. S. see Spolter, L.
MacGregor, R. R. see Som, P.
Machulla, H. J. see Vyska, K.
MacIntyre, F. see Jackson, G. L.
MacIntyre, W. J. see Fouad, F. M.
Mack, G. A. see Eikman, E. A.
MacKenzie, R. see Prato, F. S.
Maddahi, J., Berman, D. S., Freeman, M., Elkayam, U., Staniloff, H., Pantaleo, N., Forrester, J., Swan, H. J. C. and Waxman, A. D. Right and left ventricular responses

to exercise, 625*
Maddahi, J., Berman, D. S., Matsuoka, D., Charuzi, Y., Gray, R., Pantaleo, N., Swan, H. J. C., Forrester, J. and Waxman, A. D. Right ventricular ejection fraction at rest and during exercise, 625*
Maddahi, J., Berman, D. S., Matsuoka, D., Forrester, J., Swan, H. J. C. and Waxman, A. D. Right ventricular ejection fraction by multi-gated equilibrium scintigraphy, 666*
Maddahi, J.
see Berman, D. S.
see Elkayam, U.
see Shah, P. K.
Madden, J. A.
see Eikman, E. A.
see Llaurado, J. G.
Maeda, T. see Kono, A.
Maisey, M. N. see Wainwright, R. J.
Majd, M., Altman, R. P. and Reba, R. C. Hepatobiliary scintigraphy with Tc-99m PIPIDA in pediatrics, 680*
Majewski, S. see Hoan, N. N.
Makey, D. G. see Bianco, J. A.
Makler, P. T.
see Charkes, N. D.
see Malmud, L. S.
see Stelzer, F. A.
Malech, H. L. see Zakhireh, B.
Mallard, J. R. see Carril, J. M.
Malmud, L. S., Fisher, R. S., Stelzer, F. A., Menin, R., Makler, P. T. and Applegate, G. Quantitative gastro-cholecystoscintigraphy, 632*
Malmud, L. S., Littlefield, J., Reilley, J., Stern, H., Rosenberg, R. and Fisher, R. S. Alginic acid compound in reduction of gastroesophageal reflux, 1023
Malmud, L. S.
see Charkes, N. D.
see Fisher, R. S.
see Stelzer, F. A.
Manaka, R. C. see Wolf, W.
Manspeaker, H. see Burns, H. D.
Mantle, J. A. see Cowley, M. J.
Manyari, D. E., Cradduck, T. D., Melendez, L. J., Driedger, A. A. and MacDonald, A. C. Effect of nitroglycerine on left ventricular function, 639*
Maranhao, V. see Germon, P. A.
Marciano, D. see Horn, N. L.
Marcus, M. L. see Verani, M. S.
Margulis, A. R. Federation of American Societies of Radiological Science, 1318
Markoe, A. M., Risch, V. R., Heindel, N. D., Emrich, J., Lippincott, W., Honda, T. and Brady, L. W. Pharmacokinetics of S-35 thioglucose for pancreas tumor, 753
Marks, D. S. see Hricak, H.
Marshall, R.
see Schelbert, H. R.
see Wisenberg, G.
Marshall, R. C., Nash, W. W., Shine, K. E., Phelps, M. E., Ricchiuti, N. and Whitehorn, I. Myocardial glucose metabolism during supply-demand imbalance, 648*
Martindale, A. A. see Turner, J. H.
Maruyama, Y. see Kim, E. E.
Marzilli, L. G., Worley, P. and Burns, H. D. Electrophoretic method for determining ligands, 871
Marzilli, L. G.
see Burns, H. D.
see Dannals, R. F.
Mathias, C. J. and Welch, M. J. Labeling mechanism of In-111 in platelets, 659*
Mathur, P. see Chamberlain, M. J.
Mathur, V. S. see Burdine, J. A.
Matin, P. Bone scans of fractures, 1227
Matin, P., Glass, E. C., Villarica, J. and Carretta, R. F. Peripheral radionuclide angiography, 652*
Matsuda, S. see Uchida, T.
Matsumori, A. see Kadota, K.
Matsuoka, D. see Maddahi, J.
Matsushima, Y. see Kono, A.
Maturo, V. see Zusmer, N. R.
Mauderli, W., Luthmann, R. W., Fitzgerald, L. T., Urie, M. M., Williams, C. M., Tosswill, C. H. and Entine, G. Computerized rotating laminar camera, 341
Maxon, H. R.
see Chen, I. W.
see Thomas, S. R.
Mayfield, R. K. see Gordon, L.
Mazaitis, J. K. see Eckelman, W. C.
Maziere, B., Kuntz, D., Comar, D. and Ryckewaert, A. Bone Ca by neutron activation of the hand, 85
Maziérè, M. see Syrota, A.
McAfee, J. G., Gagne, G. M., Atkins, H. L., Kirchner, P. T., Reba, R. B., Blaufox, M. D. and Smith, E. M. Biological distribution and excretion of Tc-99m and In-111 DTPA, 1273
McAfee, J. G.
see Bassano, D. A.
see Collier, B. D.
see Grossman, Z. D.
see Wistow, B. W.
McAuley, R. J. see Dye, S. F.
McCombs, R. K., Singhi, V. and Olson, W. H. Positive Ga-67 citrate scan in retroperitoneal fibrosis, 238
McConnell, B. G. see Bloss, R. S.
McConnell, R. W. see Bloss, R. S.
McCready, V. R.
see Clorius, J. H.
see Coupal, J. J.
see Domstad, P.
McCullough, J. see Forstrom, L.
McDonald, G. B. see Sailer, J. F.
McDonald, J. M. see Gelbard, A. S.
McDougall, I. R. see Doherty, P. W.
McElvany, K. D. and Welch, M. J. Preparation of radiobrominated proteins, 663*
McEwan, P., Newman, G. E., Portwood, J., Port, S., Upton, M. T., Cobb, F. R. and Jones, R. H. Rest and exercise radionuclide angiocardiography in coronary artery disease, 687*
McGovern, R. see Cahill, P.
McIntyre, P. A.
see Chen, M. F.
see Guilarte, T. R.
see Kertchner, J. A.
see Scheffel, U.
McKenzie, C. C. see Fazio, F.
McKillop, J. H., Murray, R. G., Turner, J. G., Bessent, R. G., Lorimer, A. R. and Greig, W. R. Extent of coronary disease from Tl-201 images, 715
McKillop, J. H.
see Bessent, R. G.
see Fogelman, I.
McKusick, K. A.
see Bingham, J. B.
see Boucher, C. A.
see DeLuca, S.
see Konstam, M. A.
see Sober, A. J.
see Wernikoff, R. E.
see Winzelberg, G. G.
McLaughlin, R. C. see Bray, S. T.
McLaughlin, R. E. see Williamson, B. R. J.
McLeod, R. A. see Bruschwein, D. A.
McLoughlin, G. P. see Tothill, P.
McTaggert, M. P. see Mincey, E. K.
Meade, R. C.
see Llaurado, J. G.
see Yeh, E-L.
Meinken, G. E. see Srivastava, S. C.
Melendez, L. J. see Manyari, D. E.
Melnikoff, L. see Blum, M.
Melton, R. E. see Grove, R. B.
Mena, I., Bishop, H., Nelson, T. and Bennett, L. R. Cardiac transit at rest in coronary patients, 670*
Mena, I. see Jengo, J. A.
Mendenhall, K. G.
see Alderson, P. O.
see Triplett, R. G.
Mendiondo, O. Book review; *Gynecologic Oncology*, 175
Menin, R.
see Malmud, L. S.
see Stelzer, F. A.
Merchant, L. and Nickoloff, E. L. Five methods for free T_4, 627*
Merchant, L. see Perlstein, M.
Merrick, M. V. see Boyd, G. S.
Metal, I. and Lapidus, S. Properties of a rotating parallel slit collimator, 610*
Metz, C. E., Atkins, F. B. and Beck, R. N. Geometric response of a parallel hole camera collimator, 610,* 635*
Mihas, A. A. see Goldenberg, D. J.
Miller, D. W.
see Deutchman, A. H.
see Steidley, J. W.
Miller, I. D., Freeman, M. J. and Shaw, S. M. Lactoperoxidase/hydrogen peroxide system for protein iodination, 616*
Miller, R. see Burns, H. D.
Miller, S. W. see Konstam, M. A.
Miller-Catchpole, R. see Hoffer, P. B.
Milo, T.
see Arnold, J. S.

see Khedkar, N.
Mincey, E. K. and McTaggert, M. P. Single tube radioimmunoassay of thyroxine, 615*
Miniati, M. see Fazio, F.
Mintzis, M. M. see Sober, A. J.
Mishkin, F. Book review; *Data Supplement/Computerized Tomography in Clinical Medicine*, 1108
Mishkin, F. see Wong, D. W.
Miyamae, T., Fujioka, M., Tsubago, Y., Tonariya, Y., Dohi, Y., Akashi, Y. and Watanabe, H. Detection of an arteriovenous fistula between the internal iliac vessels, 36
Moffat, J. see Driedger, A. A.
Mojdehi, G. E. see Wang, T. S. T.
Molinski, V. J. see Thornton, A. K.
Monda, G. A. see Leonard, J. M.
Monroe, L. A. see Procianoy, R. S.
Moodie, D. S. see Pastakia, B.
Moon, T. E. see Woolfenden, J. M.
Moore, H. V. see Covitz, W.
Moore, M. L. see Murphy, P. H.
Moore, R. H. see Bingham, J. B.
Moossa, A.
see Ryan, J.
see Zalutsky, M.
Morita, R. see Torizuka, K.
Morita, T. see Fukuchi, M.
Morley, T. R., Short, M. D. and Dowsett, D. J. Femoral head activity in Perthes' disease, 170
Morley, T. R., Short, M. D. and Dowsett, D. J. Femoral head activity in Perthes' disease, 459
Morris, C. R. see Gard, M. F.
Morse, T. S. see Sfakianakis, G. N.
Moser, K. M. see Shepard, J. W.
Moses, D. C. see Hayt, D. B.
Moskowitz, G. W. and Levy, L. M. Automatic reservoir for serial pipetting, 262
Moss, C. M. see Rudavsky, A. Z.
Most, A. S. see Gewirtz, H.
Motazedi, A. see Alderson, P. O.
Motsinger, S. F. see Chilton, H.
Mould, R. F. Analog-circuit motion correction for liver imaging, 802
Mould, R. F. Nuclear imaging and probability levels, 364
Moyer, B. R. see Budinger, T. F.
Muehllehner, G. Effect of crystal thickness on scintillation camera performance, 992
Muehllehner, G. see Stoub, E. W.
Mukai, T. see Yonekura, Y.
Mullani, N. A., and Eichling, J. O. Single slice via multiple slice positron tomographs, 799
Mullani, N. A. see Ter-Pogossian, M. M.
Murphy, P. H. Book review; *Intermediate Physics for Medicine and Biology*, 368
Murphy, P. H., Thompson, W. L., Moore, M. L. and Burdine, J. A. System for radionuclide computed tomography, 102
Murphy, P. H. see Burdine, J. A.
Murphy, R. X. see Konstam, M. A.
Murray, D. see Faraj, B. A.
Murray, I. P. see Slutsky, R.
Murray, R. G. see McKillop, J. H.
Muz, J., Dindogru, A., Figiel, S. J. and Vaitkevicus, V. K. Arterial liver perfusion scintigraphy, 622*
Myers, M. J. see Jarrit, P. H.
Myers, R. W., Bails, R. P. and Drasin, E. Correlative role of echocardiography and radionuclide angiocardiography, 651*
Myers, W. G. Historian's note, 560, 575
Myers, W. G. The Anger scintillation camera comes of age, 565

Nadeau, J. H. see Price, R. R.
Nagai, K. see Fukuchi, M.
Nagataki, S. see Ito, M.
Nakajima, K. see Torizuka, K.
Naperstak, E. see Samuels, L. D.
Nardini, M. see Fazio, F.
Nash, W. W. see Marshall, R. C.
Nass, H. W. New I-123 nuclear decay data, 1216
Neff, R. A. see Lewis, J. T.
Neill, J.
see Holman, B. L.
see Wynne, J.
Neirinckx, R. D. and Davis, M. A. Ga-68 column chromatography generators, 1075
Neirinckx, R. D. and Davis, M. A. Ga-68 generator, 681*
Neirinckx, R. D., Holman, B. L., Davis, M. A. and Zimmerman, R. E. Ta-178 agents for lung and liver imaging, 1176
Neirinckx, R. D. see Holman, B. L.
Nelp, W. B. see Chesnut, C. H.
Nelson, M. see Arnold, J. S.
Nelson, N. J. see Larson, S. M.
Nelson, T. see Mena, I.
Němec, J., Röhling, S., Zamrazil, V. and Pohunková, D. Diagnostic and thyroablative I-131 distribution, 92
Němec, J., Röhling, S., Zamrazil, V. and Pohunková, D. Scanning dose and detection of thyroid metastases, 1100
Nemoto, T. see Uchida, T.
Newcomer, K. see Chapman, D.
Newman, G. E., Rerych, S. K., Upton, M. T., Sabiston, D. C. and Jones, R. H. Rest and exercise radionuclide angiocardiography in coronary disease, 649*
Newman, G. E. see McEwan, P.
Nichols, A. B., Cochavi, S., Hales, C. A., Beller, G. A. and Strauss, H. W. Serial imaging with inhaled $C^{15}O_2$ in pulmonary embolism, 281
Nickles, R. J. A dynamic phantom for radionuclide cardiology, 547
Nickles, R. J.
see Halama, J. R.
see Lieberman, L. M.
Nickoloff, E. L.
see Lipson, A.
see Merchant, L.
see Perlstein, M.
Nir, I. see Front, D.
Nishiyama, H., Adolph, R., Gabel, M., Lukes, S. and Williams, C. Effects of coronary blood flow on Tl-201 uptake, 650*
Nishiyama, H., Adolph, R., Lukes, S., Gabel, M., Blue, J. and Sodd, V. Blood flow and myocardial uptake of Tl-201 and Tc-99m pyrophosphate, 650*
Nishiyama, H. see Lewis, J. T.
Nixon, D. see Faraj, B. A.
Nolan, W. G. see Lindsay, J.
Nowak, D. see Verba, J.
Nowygrad, R.
see Fawwaz, R. A.
see Johnson, P. M.
Nunn, A. D. Affinity chromatography of serum protein-radiopharmaceutical interactions, 682*

O'Brien, C. see Owunwanne, A.
O'Brien, H. A.
see Bingham, J. B.
see Budinger, T. F.
see Yano, Y.
O'Connell, J., Henkin, R., Robinson, J., and Gunnar, R. Ga-67 myocardial scintigraphy in cardiomyopathy, 604*
O'Connell, T. see Hnatowich, D.
O'Connor, J. L., Kronenberg, M. W., Higgins, S. B., Pederson, R. W. and Rhea, T. C. Count-based border definition for radionuclide ventriculography, 642*
Ohsawa, R. see Ito, M.
Okada, R. D., Kirshenbaum, H. D., Kushner, F. G., Dinsmore, R. E., Strauss, H. W., Boucher, C. A. and Pohost, G. M. Observer variance in left ventricular regional wall motion studies, 661*
Okada, R. D., Pohost, G. M., Kirshenbaum, H. D., Kushner, F. G., Boucher, C. A. and Strauss, H. W. Exercise induced changes in regional pulmonary blood pool activity, 626*
Okada, R. D.
see Bingham, J. B.
see Boucher, C. A.
see Kirshenbaum, H. D.
see Kushner, F. G.
Okerlund, M. D., Sommers, J., Sakmar, T., Galante, M., Hunt, T. and Clark, O. "Cold" thyroid nodules following childhood neck irradiation, 678*
Okulski, T. A. see Eikman, E. A.
Olson, H. see Lyons, K. P.
Olson, W. H. see McCombs, R. K.
Olsthoorn, Q. P. W. see Turner, J. H.
Oluwole, S. see Fawwaz, R. A.
O'Mara, R. E., Chanamolu, V. B. and Wilson, G. A. Effects of pretreatment on bone uptake of $Na^{32}P$ and P-32 pyrophosphate, 684*
O'Mara, R. E. see Owunwanne, A.
Onoue, K. see Fukuchi, M.
Oppenheim, B. E. and Appledorn, C. R. A new method for functional renal imaging, 657*
Oppenheim, B. E. see Appledorn, C. R.
O'Rourke, O. see Sorensen, S. G.

Orr, S. C. see Grove, R. B.
Ortega, C. J. see Tsui, B. M. W.
Ortiz, V. N. see Sfakianakis, G. N.
Orvig, C., Jones, A. G., Davison, A., Trop, H. S., DePamphilis, B. V. and Davis, M. A. Tc complex preparation with different reducing agents, 653*
Orvig, C.
see Davison, A.
see Jones, A. G.
Orzan, F. see Burdine, J. A.
Oseas, R. S. see Siddiqui, A. R.
Osman, S. see Chisholm, P. M.
Oster, Z. H.
see Som, P.
see Tzen, K. Y.
Ostertag, H. see Clorius, J. H.
Ostrow, H. G., Allen, S. L., Bacharach, S. L., Green, M.V. and Borer, J. S. A gated probe system for real-time pressure-volume loops, 610*
Owunwanne, A., Durakovic, A., Schenk, E. A. and O'Mara, R. E. Radioactive calcium uptake by isoproterenol damaged heart, 650*
Owunwanne, A., O'Mara, R. E. and O'Brien, C. Interactions of Tc-99m phosphates and serum proteins, 653*

Paik, C. H., Herman, D. C., Eckelman, W. C. and Reba, R. C. Pharmacokinetics of conjugated In-111 chelate-proteins, 656*
Panagoitis, N. M. see Verma, R. C.
Pande, S. G. see Srivastava, S. C.
Pang, S. C. and Genna, S. The effect of Compton scattering on transmission axial tomography, 608*
Pang, S. C. see Genna, S.
Pantaleo, N. see Maddahi, J.
Pappagianopoulos, P. see Ahluwalia, B.
Parab, P. B. see Patel, M. C.
Parisi, A. F. see Folland, E. D.
Park, C. H. see Galkin, B. M.
Park, H., Wheat, J., Siddiqui, A. R., Burt, R., Robb, J. and Wellman, H. N. Three phase bone scan in diabetic foot, 602*
Park, H. M., Zieverink, S. E. and Ransburg, R. C. Marine-Lenhart syndrome, 624*
Parker, G. A. see Vieras, F.
Parkey, R. W.
see Datz, F. L.
see Lewis, S. E.
Partain, C. L., Guinto, F. C., Scatliff, J. H., Limbacher, J., Janicki, P. and Heindel, C. C. Brain scan, transmission computed tomography and angiography in cerebral venous angioma, 1166
Partain, C. L. see Bray, S. T.
Pastakia, B., Lieberman, L. M., Levy, J., Moodie, D. S. and Polcyn, R. E. Quantification of superior vena cava-right pulmonary artery shunting, 670*
Patel, G. C. see Colombetti, L. G.
Patel, M. C., Parab, P. B., Samuel, A. M. and Ganatra, R. D. In vitro Tc-99m red blood cell labeling, 877
Patel, S. see Tetalman, M.
Patil, A. see Germon, P. A.
Patton, D. see Hilts, S. V.
Patton, J. A. and Rollo, F. D. Evaluation of imaging systems using Tl-201 and the performance index, 635*
Patton, J. A.
see Pickens, D.
see Powers, T. A.
see Touya, J. J.
Pauwels, E. K. J. see de Graaf, P.
Pauwels, S., Piret, L., Schoutens, A., Vandermoten, G. and Beckers, C. Tc-99*m* diethyl IDA scintigraphy in jaundice, 685*
Pavel, D. G. see Khentigan, A.
Pavia, D. see Short, M. D.
Payne, D. W. see Katzenellenbogen, J. A.
Pearce, P. C. see Ell, P. J.
Pearse, D. see Pickens, D.
Pearson, A. J. see Sober, A. J.
Pederson, R. W.
see Grove, R. B.
see O'Connor, J. L.
Perlstein, M., Herner, A., Rock, R., Nickoloff, E. L., Almaraz, B., Merchant, L. and Chan, D. W. Drug interference and protein matrix effects on serum free T_4, 627*
Perillo, R. P. see Ahmad, M.
Perry, J. R. and James, R. C. Interpolative background correction for cardiac blood pool studies, 643*
Persson, B. R. R. see Strand, S-E.
Peters, L. J. Book review; *Radiobiology for the Radiotherapist*, 583
Peterson, K. E.
see Pfisterer, M. E.
see Slutsky, R.
Pfisterer, M. E., Battler, A., Swanson, S. M., Slutsky, R., Froelicher, V. and Ashburn, W. L. Reproducibility of ejection fraction determinations, 491
Pfisterer, M. E., Ricci, D. R., Schuler, G., Swanson, S. S., Gordon, D. G., Peterson, K. E. and Ashburn, W. L. LVEF at rest and peak exercise by short-time equilibrium studies, 484
Pfisterer, M. E. see Slutsky, R.
Phaosawadsi, K. see Fisher, R. S.
Phelps, M. E., Hoffman, E. J. and Huang, S-C. Single slice vs multiple slice positron tomography, 800
Phelps, M. E., Huang, S. C., Hoffman, E. J. and Kuhl, D. E. C-11 carboxyhemoglobin tomography for cerebral blood volume, 328
Phelps, M. E., Huang, S. C., Kuhl, D. E., Selin, C. and Hoffman, E. J. $^{13}NH_3$ as a cerebral blood tracer, 611*
Phelps, M. E., Huang, S. C., Schelbert, H. R., Hoffman, E. J. and Kuhl, D. E. Models and tomography for cerebral and myocardial glucose metabolism, 605*
Phelps, M. E.
see Hoffman, E. J.
see Huang, S. C.
see Marshall, R. C.
see Robinson, G. D.
see Schelbert, H. R.
see Wisenberg, G.
Phillips, J.
see Alter, W. A.
see Grissom, M.
Piccone, J. M. see Sagar, V. V.
Pichler, M. see Shah, P. K.
Pickens, D., Patton, J. A., Pearse, D., Price, R. R. and Brill, A. B. Simultaneous multiplane deconvolution in focal plane tomography, 666*
Piepsz, A. see Vandevivere, J.
Pierrez, J. and Bertrand, A. Fixation of gallium, 456
Piers, D. A. see Beekhuis, H.
Pierson, R. N., Huang, P. J., Tansey, W. A. and Friedman, M. I. Right ventricular ejection fraction methods, 666*
Piltingsrud, H. V. Low temperature scintillation properties of bismuth germanate, 1279
Pinsky, S. M.
see Colombetti, L. G.
see Ryo, U. Y.
Pirchner, F. Book review; *Lungen Diagnostik mit Radionukliden-Physiologie, Pathophysiologie, Klinik*, 583
Piret, L. see Pauwels, S.
Pitt, B. see Brady, T. J.
Pitt, M. J. see Woolfenden, J. M.
Plos, W. J. see Henkin, R. E.
Plummer, D. see Syrota, A.
Plunkett, J. M. see Powers, T. A.
Pohost, G. M.
see Bingham, J. B.
see Boucher, C. A.
see Cochavi, S.
see Goldman, M. R.
see Kirshenbaum, H. D.
see Kushner, F. G.
see Okada, R. D.
see Zir, L. M.
Pohunková, D. see Němec, J.
Polcyn, R. E. see Pastakia, B.
Policarpo, A. J. P. L. see Hoan, N. N.
Pollak, R. H. see Stolzenberg, J.
Pond, M. see Burow, R. D.
Ponto, R. A.
see Frick, M. P.
see Williams, L. E.
Popescu, H. I. see Reichelt, H. G.
Port, S. see McEwan, P.
Porter, D. W., Loberg, M. D., Eacho, P. I. and Weiner, M. Comparison of hepatobiliary radiopharmaceuticals, 642*
Portwood, J. see McEwan, P.
Possa, M. see Fazio, F.
Potchen, E. J. and Harrison, M. J. Book review; *Medical Malpractice Law*, 907
Potsaid, M. S. see Sober, A. J.
Powers, T. A., Grove, R. B., Bowen, R. D., Plunkett, J. M., Kadir, S., Harolds, J. A., Patton, J. A. and Stone, W. J. Radionuclide measurement of absolute differential GFR, 630*

Powers, T. A. see Grove, R. B.
Pozderac, R. V., Weinhold, P. A., Counsell, R. E., Castonguay, A., Klausmeier, W. H. and Skinner, R. W. S. Radiobrominated steroid analogs for prostate imaging, 683*
Prach, T. see Ku, T. H.
Prager, P. Book review; *Radiologie*, 368
Prato, F. S. and MacKenzie, R. *Performing* a ventilation study after the perfusion lung scan, 578
Prato, F. S. see Reese, L.
Pratt, T. A. see *Fazio, F.*
Preisman, R. see Halpern, S. E.
Preston, D. F. and Luke, R. G. *Teaching* editorial; radionuclide evaluation of renal transplants, 1095
Preston, D. F. see Spicer, J. A.
Price, D. see Seder, J.
Price, R. R., Born, M. L., Jones, J. P., Touya, J. J., Grove, R. B., Nadeau, J. H., Branch, R. A., Rhamy, R. H., Hollifield, J. W., Brill, A. B. and Rollo, F. D. Differential renal function determined by three radionuclide methods and catheterization, 631*
Price, R. R.
see Jones, J. P.
see Pickens, D.
see Touya, J. J.
Primus, F. J. see DeLand, F. H.
Prince, J. R. Definition of equilibrium in serial radioactive decay, 162
Prince, M. J. see Balachandran, S.
Procianoy, R. S., Monroe, L. A., Garcia-Prats, J. A., Rudolph, A. J. and Burdine, J. A. Thyroid screening in the premature infant, 615*
Profant, M. see Vyska, K.
Profant, R. T. see Deutchmann, A. H.
Prokop, E. K. Ultrasound and Tc-99m PIPIDA and S colloid scanning in jaundice, 600*
Pujara, S. S. and Russell, C. D. Evaluation of peritoneo-venous shunt, 72
Purdom, R. C. see Thomas, S. R.
Pur-Shariari, A. A. see Ahmad, M.

Quaife, M. A., Boschult, P., Baltaxe, H. A. and Dzindzio, B. Tc-99m pyrophosphate distribution in malignant pericardial effusion, 392

Rackley, C. E. see Cowley, M. J.
Raflo, C. P. see Kmet, J. P.
Rafter, J. J.
see Brown, D. H.
see Hayes, R. L.
Raghunath, B. see Kotrappa, P.
Rahimtoola, S. see Seder, J.
Raikar, U. R. see Kotrappa, P.
Rainwater, J. O. see Vogel, R. A.
Ramanna, L. see Tanasescu, D. E.
Ramu, N. see Samuels, L. D.
Ransberg, R. C. see Park, H. M.
Rao, G. M., Guruprakash, G. H. and Bhaskar, G. Ga-67 localization in aspergilloma, 900
Raper, D. A. see Wainwright, R. J.
Raptou, E. see Clorius, J. H.
Rasey, J. S.
see Larson, S. M.
see Srivastava, S. C.
Ravikrishnan, K. P. see Sarkar, S. D.
Rayudu, G. see Fordham, E.
Read, M. see Janowitz, W. R.
Reba, R. C. Poster presentations at a scientific meeting, 582
Reba, R. C.
see Eckelman, W. C.
see Gibson, R. E.
see Majd, M.
see McAfee, J. G.
see Paik, C. H.
Reece, P. O. and Heise, C. M. Human gastrin radioimmunoassay, 617*
Reemtsma, K. see Fawwaz, R. A.
Reese, L., Prato, F. S., Tevaarwerk, G. J. M. and Hurst, C. Cord blood thyroxine and thyrotropin screening, 616*
Reese, L. and Uksik, P. Serum myoglobin radioimmunoassay screening for acute myocardial infarct, 664*
Rehani, M. M. Container geometry for better sensitivity in radiometric assays, 1090
Reichelt, H. G. and Popescu, H. I. Liver uptake and retention in assessment of hepatobiliary agents, 171
Reid, B. D. see Driedger, A. A.
Reid, P. R. see Camargo, E. E.
Reilley, J.
see Charkes, N. D.
see Fisher, R. S.
see Malmud, L. S.
see Stelzer, F. A.
Reiman, R. E. see Gelbard, A. S.
Rein, A. see Atlan, H.
Reisinger, W. E. Safe handling of radioiodine, 363
Reisinger, W. E. Thyroid contamination from airborne I-131, 362
Reivich, M.
see Alavi, A.
see Jones, S. C.
Rempel, S. see Billinghurst, M. W.
Renaud, L., Joy, M. L. G., and Gilday, D. L. Fourier multiaperture emission tomography, 986
Rerych, S. K. see Newman, G. E.
Reske, S. N., Vyska, K. and Feinendegen, L. E. Kinetics of phagocytosis and proteolytic metabolism in liver macrophages, 606*
Resnekov, L. see Harper, P. V.
Rezai-Zadeh, K., Kirchner, P. T., DeMeester, T. R., Golomb, H. and Cooper, M. Ga-67 scanning in clinical staging of cancer, 644*
Rhamy, R. H. see Price, R. R.
Rhea, T. C.
see O'Connor, J. L.
see Steckley, R. A.
Rhodes, B. A. see Study, K. T.
Ricchiuti, N. see Marshall, R. C.
Ricci, D. R. see Pfisterer, M. E.
Richards, P.
see Fordham, E.
see Hui, J. C. K.
see Schachner, E. R.
see Srivastava, S. C.
Richmond, P. H. see Waxman, A. D.
Rider, A. A. see Kertchner, J. A.
Ring, E. see Alavi, A.
Rintelman, W. see Alavi, A.
Risch, V. see Burns, H. D.
Risch, V. R. see Markoe, A. M.
Ritchie, J. L., Albro, P. C., Caldwell, J. H., Trobaugh, G. B., and Hamilton, G. W. T1-201 redistribution and rest myocardial images, 477
Ritchie, J. L.
see Caldwell, J. H.
see Sorensen, S. G.
Ritman, E. L. see Singh, M.
Ritzl, F. see Tisljar, U.
Robb, J. see Park, H.
Robbins, E. B. see Chervu, L. R.
Robbins, P. J. and Williams, C. C. Low tagging yields of Tc-99m DTPA kits, 653*
Robinson, G. D., Phelps, M. E. and Huang, S. C. Pharmacokinetics of F-18 fluorodeoxymannose and fluorodeoxyglucose, 672*
Robinson, G. D.
see Schelbert, H. R.
see Wisenberg, G.
Robinson, J. see O'Connell, J.
Robinson, R. G. see Spicer, J. A.
Rock, R. see Perlstein, M.
Rod, J. L. see Atlan, H.
Rogers, W. J. see Cowley, M. J.
Rogers, W. L., Koral, K. F., Keyes, J. W. and Thrall, J. H. Tomographic gated blood pool imaging, 628*
Rogers, W. L.
see Brady, T. J.
see Koral, K. F.
Röhling, S. see Němec, J.
Roland, J-M. A. see Chipps, B. E.
Rollo, F. D.
see Jones, J. P.
see Patton, J. A.
see Price, R. R.
see Steckley, R. A.
see Touya, J. J.
Root, R. K. see Zakhireh, B.
Rose, C. see Kaplan, W. D.
Rose, J. G. see Hecht, H. S.
Rosen, G. see Gelbard, A. S.
Rosenberg, R.
see Malmud, L. S.
see Spencer, R. P.
Rosenquist, A. see Alavi, A.
Rosenshein, N. B. see Katz, R. D.
Rosenspire, K., Blau, M., and Green, F. A. Local distribution of $^{99m}TcO_4^-$ and pyrophosphate in joints, 673*
Rosenspire, K., Blau, M., Kennedy, A. C., Green, F. A. and Steinbach, J. Increased

bone uptake in rheumatoid arthritis, 673*
Rosenstein, B. L. see Chipps, B. E.
Roskopf, M. L. see Grossman, Z. D.
Roth, J. see Wachslicht-Rodbard, H.
Royal, H. D., Brown, P. H. and Claunch, B. C. Effects of crystal thickness on Anger camera performance, 977
Royal, H. D. see Brown, P. H.
Rubinstein, K. see Clorius, J. H.
Rudavsky, A. Z., Strauch, B., Daniller, A. and Moss, C. M. Isotope angiography of reimplanted digits, 674*
Rudd, T. G., Allen, D. R. and Smith, F. D. Comparison of Tc-99m MDP and HEDP, 821
Rudd, T. G.
see Blumhagen, J. D.
see Daly, M. J.
see Hayden, P. W.
see Khentigan, A.
see Leonard, J. M.
Rudolph, A. J. see Procianoy, R. S.
Rue, C. see Wisenberg, G.
Rumble, W. F. Ingestion of Tc-99m in breast milk, 799
Russell, C. D. and Cash, A. G. Complexes of Tc with pyrophosphate, etidronate and medronate, 532
Russell, C. D.
see Goldenberg, D. J.
see Pujara, S. S.
Russell, R. O. see Cowley, M. J.
Rutkowski, G. see Harper, P. V.
Ryan, J., Zalutsky, M., Kirchner, P. T., Moossa, A., Harper, P. V. and Cooper, M. C-11 tryptophan single photon tomography of the pancreas, 632*
Ryan, J. W., Hill, M., Isikoff, M., and Johnston, G. S. Ultrasound and Tc-99m HIDA studies in jaundice diagnosis, 600*
Ryan, J. W.
see Bidani, N.
see Harper, P. V.
see Harvey, E.
Ryckewaert, A. see Maziérè, B.
Ryerson, T. W. and Spies, S. M. Plasma integral method of renal clearance measurement, 630*
Ryo, U. Y., Vaidya, P., Schneider, A. and Pinsky, S. M. Histopathology of discrepant Tc-99m and I-123 thyroid scan lesions, 678*
Rzeszotarski, W. J. see Eckelman, W. C.

Sabiston, D. C. see Newman, G. E.
Sacker, D. F.
see Schachner, E. R.
see Som, P.
Saecker, G. see Forstrom, L.
Sagar, V. V., Piccone, J. M. and Charkes, N. D. Bone uptake of Tc-99m MDP as a function of blood flow, 1257
Sagel, J. see Gordon, L.
Sagerman, R. H. see Wistow, B. W.
Sailer, J. F. and McDonald, G. B. Radionuclide angiography in suspected false aneurysms, 808
Sakimura, I. see Siegel, M. E.
Sakmar, T. see Okerlund, M. D.
Salassa, R. M. see Wahner, H. W.
Salomon, J. see Atlan, H.
Samols, E. Book review; *Radioimmunoassay and Related Procedures in Medicine,* 1218
Samuel, A. see Hoffer, P. B.
Samuel, A. M. see Patel, M. C.
Samuels, L. D. Soft-tissue tumor uptake of bone agents, 674*
Samuels, L. D., Godfrey, S. and Warshaw, B. Xe-133 ventilation-perfusion lung scans in pediatrics, 638*
Samuels, L. D., Lewis, B., Weiss, A. and Naperstak, E. Monitoring rubidimycin therapy with pyrophosphate and MUGA heart scans, 651*
Samuels, L. D. and Ramu, N. Differential diagnosis of abdominal tumors in children, 679*
Samuels, L. D. see Atlan, H.
Sandock, K. see Ahmad, M.
Sands, M. J. see Berger, H. J.
Sarkar, S. D., Ravikrishnan, K. P., Woodbury, D. H., Carson, J. J. and Daley, K. Ga-67 citrate scanning in extrapulmonary tuberculosis, 833
Sarper, R. see Tarcan, Y.
Sasaki, Y. see Kitani, K.
Sayres, M. see Wynne, J.
Scanlon, G. T. see Sty, J. R.
Scatliff, J. H. see Partain, C. L.
Schachner, E. R., Gil, C., Atkins, H. L., Som, P., Srivastava, S. G., Sacker, D. F. and Richards, P. Ru-HIDA for delayed biliary tract studies, 682*
Schadt, W. see Sherbini, S.
Schafer, A. W. see Burow, R. D.
Schechter, E. see Venkatesh, N.
Scheffel, U., Tsan, M-F. and McIntyre, P. A. Labeling human platelets with In-111 hydroxyquinoline, 524
Scheffel, U. see Tsan, M-F.
Schelbert, H. R., Gould, L., Wisenberg, G., Marshall, R., Phelps, M. E. and Hoffman, E. J. $^{13}NH_3$ positron computerized tomography in coronary disease, 604*
Schelbert, H. R., Phelps, M. E., Robinson, G. D., Huang, S. C., Hoffman, E. J. and Selin, C. $^{13}NH_3$ measurements of myocardial blood flow, 603*
Schelbert, H. R.
see Huang, S. C.
see Phelps, M. E.
see Wisenberg, G.
Schenk, E. A.
see Kronenberg, M. W.
see Owunwanne, A.
Schicht, I. M. see de Graaf, P.
Schlafke, A. T. see Watson, E. E.
Schlosser, P. A.
see Deutchman, A. H.
see Steidley, J. W.
Schmidt, D. H. see Hellman, C.
Schmidt, K. see Tetalman, M.
Schneider, A. see Ryo, U. Y.
Schoutens, A. see Pauwels, S.
Schreyer, M. see Stanton, T.
Schuler, G. see Pfisterer, M. E.
Schumitzky, A. see Wolf, W.
Scott, R. see Atkins, F. B.
Scrimger, J. W. see Hooper, H. R.
Secker-Walker, R. and Ho, J. E. Regional lung function in asbestos workers, 621*
Seder, J., Rahimtoola, S., Botvinick, E., Goldstone, J., Effeney, D. J. and Price, D. Tl-201 leg imaging in peripheral arterial disease, 634*
Selin, C.
see Huang, S. C.
see Phelps, M. E.
see Schelbert, H. R.
see Wisenberg, G.
Sellers, B. B. see Covitz, W.
Serafini, A. see Ashkar, F. S.
Sfakianakis, G. N., Haase, G. M., Ortiz, V. N. and Morse, T. S. Bone scanning in early recognition of child abuse, 675*
Sfakianakis, G. N., Sotos, J. and Vasquez, S. Adrenal imaging in pediatric congenital adrenal hyperplasia, 622*
Sgroi, V. see Shepard, J. W.
Shaber, G. S. see Galkin, B. M.
Shabetai, R. see Verba, J. W.
Shafer, R. B. and Bianco, J. A. Book review; *Nuclear Cardiology: Clinical Applications,* 1107
Shafer, R. B. and Bianco, J. A. Teaching editorial; hepatic Xe activity in ventilation scans, 450
Shafer, R. B., Eckfeldt, J. H., and Elson, M. K. Radioimmunoassay for serum prostatic acid phosphatase, 664*
Shafer, R. B. see Bianco, J. A.
Shah, P. K., Berman, D. S., Pichler, M., Shellock, F., Maddahi, J., Waxman, A. D. and Swan, H. J. C. Nitroprusside effect on ventricular performances in acute infarction, 640*
Shakir, R. see Lipson, A.
Shanahan, W. M. S., Klingensmith, W. C. and Weil, R. Perfusion and clearance in Tc-99m DTPA studies for acute tubular necrosis, 629*
Shapiro, L. see Uszler, J. M.
Shaw, S. M. see Miller, I. D.
Shaw, M. S. see Williams, L. E.
Shea, W. H. see Zir, L. M.
Shearer, D. R. and Wong, R. Distortion of bar phantom images, 1315
Shearer, D. R. see Gewirtz, H.
Shellock, F. see Shah, P. K.
Shelnutt, R. see Covitz, W.
Shepard, J. W., Hauer, D., Sgroi, V. and Moser, K. M. Isoproterenol effects on perfusion distribution in embolism, 950
Sherbini, S., Schadt, W., Thomas, M., Alavijeh, H. S. and Tripathi, A. Computer code for calculation of radiation dose from syringes, 882
Shine, K. E. see Marshall, R. C.

Shiokawa, H. see Kono, A.
Shiue, C-Y. see Som, P.
Short, M. D., Dowsett, D. J., Heaf, P. J. D., Pavia, D. and Thomson, M. L. Comparison of Tc-99m aerosol and Kr-81m for lung function assessment, 194
Short, M. D. see Morley, T. R.
Shuler, S. E. see Witherspoon, L. R.
Shurtleff, D. B. see Hayden, P. W.
Sibbald, W. J. see Driedger, A. A.
Siddiqui, A. R. Ingestion of Tc-99m in breast milk, 799
Siddiqui, A. R., Bruns, D. J., Wellman, H. N. and Klatte, E. C. Diagnosis of thromboembolism disease, 639*
Siddiqui, A. R., Oseas, R. S., Wellman, H. N., Doerr, D. R. and Baehner, R. L. Tc-99m S colloid bone marrow scanning in pediatric oncology, 379
Siddiqui, A. R. and Tight, R. R. Ga-67 citrate kinetics in subcutaneous polyethylene chambers in rabbits, 660*
Siddiqui, A. R.
see Park, H.
see Thirunavukkarasu, S.
Siegel, B. A. see Welch, M. J.
Siegel, M. E., Stewart, C. A., Sakimura, I., Wagner, W. and Bessman, A. Tl-201 determination of ischemic ulcer perfusion, 634*
Siemsen, J. K. see Waxman, A. D.
Sikorski, S. see Harvey, E.
Silberstein, E. B., and Bove, K. E. Visualization of alcohol-induced rhabdomyolysis, 127
Silberstein, E. B. and Kim, J. H. Radionuclide and computerized tomographic brain imaging, 600*
Simmons, G. Book review; *Computer Methods-The Fundamentals of Digital Nuclear Medicine*, 907
Simmons, G. Book review; *SI for the Health Professions*, 465
Simmons, G. Book review; *SI Units in Medicine: An Introduction to the International System of Units with Conversion Tables and Normal Ranges*, 465
Simmons, G.
see Coupal, J. J.
see Domstad, P.
Simon, J. see Troutner, D. E.
Simpkin, D. J. see Halama, J. R.
Singer, F. see Waxman, A. D.
Singh, A. see Grossman, Z. D.
Singh, H. and Causer, D. A. Tl-201 myocardial studies in aortocoronary saphenous bypass surgery, 576
Singh, M., Berggren, M. J., Gustafson, D. E., Dewanjee, M. K., Bahn, R. C. and Ritman, E. L. Tc-99m pyrophosphate computed tomography in canine acute myocardial infarction, 50
Singhi, V. see McCombs, R. K.
Sisson, J. C. see Freitas, J. E.
Skinner, R. W. S. see Pozderac, R. V.
Slutsky, R., Battler, A., Gordon, D., Walaski, S., Verba, J., Lief, L., Peterson, K. E., Murray, I. P. and Ashburn, W. L. Simplified calculation of left ventricular volume, 669*
Slutsky, R., Gordon, D. G., Karliner, J., Kaiser, R., Battler, A. and Peterson, K. E. Left ventricular function assessment by first-pass radioangiography, 626*
Slutsky, R., Karliner, J., Battler, A., Pfisterer, M. E. and Ashburn, W. L. Reproducibility of ejection fraction and left ventricular volume by gated equilibrium method, 669*
Slutsky, R. see Pfisterer, M. E.
Smith, A. J. see Sy, W. M.
Smith, A. L. see Glass, E. C.
Smith, C. W. see Leonard, J. C.
Smith, E. H. see Kaplan, W. D.
Smith, E. M.
see Holman, B. L.
see McAfee, J. G.
Smith, F. D. see Rudd, T. G.
Smith, G. A. see Llaurado, J. G.
Smith, R. B., Coupal, J. J., DeLand, F. H. and Triplett, J. W. Pharmacokinetics of hepatobiliary imaging agents in rats, 45
Smoak, W. M. see Zusmer, N. R.
Sobel, B. E. Assessing the current needs of cardiology, 599*
Sober, A. J., Mintzis, M. M., Lew, R. A., Lo, H. H., Whalen, C., McKusick, K. A., Potsaid, M. S., Vialotti, C. and Pearson, B. Increased spleen uptake of radiocolloids in malignant melanoma, 1232
Sodd, V. see Nishiyama, H.
Sohn, M. see Davison, A.
Solomon, N. A.
see Maayan, M. L.
see Steigman, J.
Som, P., Atkins, H. L., Bandyopadhyay, D., Fowler, J. S., MacGregor, R. R., Oster, Z. H., Sacker, D. F., Shiue, C-Y. and Wolf, A. P. Early detection of neoplasms with F-18 sugar analog, 662*
Som, P.
see Atkins, H. L.
see Hui, J. C. K.
see Schachner, E. R.
see Srivastava, S. C.
Someya, K. see Kitani, K.
Sommers, J. see Okerlund, M. D.
Soni, P. S. see Kotrappa, P.
Sonnemaker, R. E., Daniels, D. L., Craig, W. E., Floyd, J. L. and Bode, R. F. Serum myoglobin determination, 120
Sonnemaker, R. E., DePuey, E. G., Floyd, J. L., Thompson, W. L. and Burdine, J. A. Left ventricular function in coronary artery disease, 667*
Sorensen, S. G., Caldwell, J. H., Ritchie, J. L., Hamilton, G. W. and Kennedy, J. W. Intervention radionuclide angiography, 625*
Sorensen, S. G., Groves, B., O'Rourke, O. and Chaudhuri, T. Quantitation of valvular regurgitation by gated equilibrium radioangiography, 626*
Sorenson, J. A. Book review; *Internal Radiation Dose in Diagnostic Nuclear Medicine*, 812
Sorenson, J. A. Stable I measurement by Ce-139 absorption-edge transmission, 1286
Sotos, J. see Sfakianakis, G. N.
Souverijn, J. H. M. see de Graaf, P.
Sowton, E. see Wainwright, R. J.
Spehl, M. see Vandevivere, J.
Spencer, J. T. see Thornton, A. K.
Spencer, R. P. Imaging biochemical systems in vivo, 364
Spencer, R. P., Levinson, E. D., Baldwin, R. D., Sziklas, J. J., Witek, J. T. and Rosenberg, R. Bone scan abnormalities in "shin splints," 1271
Spencer, R. P.
see Dhawan, V. M.
see Levinson, E. D.
see Sripada, P. K.
Sperling, M. see Chen, I. W.
Spicer, J. A., Preston, D. F., Baranczuk, R. J., Harvey, E., Guffey, M. M., Bradshaw, D. L. and Robinson, R. G. Biodistribution of Br-77 estrone, 761
Spies, S. M. see Ryerson, T. W.
Spinelli, F. see Fazio, F.
Spitzer, V. see Klingensmith, W. C.
Spolter, L., Cohen, M. B., Chang, C. C. and MacDonald, N. S. Enzymatic synthesis of C-11 acetyl carnitine, 662*
Spremulli, E. see DeLand, F. H.
Sripada, P. K., Spencer, R. P., Vitkauskas, G. and Becker, E. L. Binding of N-formyl-selenomethionine-methionine to neutrophils, 681*
Srivastava, S. C., Richards, P., Meinken, G. E., Pande, S. G., Som, P., Atkins, H. L., Larson, S. M., Grunbaum, Z. and Rasey, J. S. Radiolabeled Ru-compounds for tumor localizing, 684*
Srivastava, S. C. see Schachner, E. R.
Staab, E. V. Book review; *Atlas of the Human Brain and the Orbit for Computed Tomography*, 908
Stacciarini, W. see Faraj, B. A.
Stang, L. G. see Ku, T. H.
Staniloff, H., Diamond, G., Hirsch, M., Berman, D. S., Charuzi, Y., Freeman, M., Elkayam, U., Vas, R., Waxman, A. D. and Forrester, J. Sequential Bayesian analysis for detection of coronary artery disease, 651*
Staniloff, H.
see Berman, D. S.
see Elkayam, U.
see Maddahi, J.
see Tanasescu, D. E.
Stanton, T., Bohlman, W., Schreyer, M., Vanags, K., Kovaleski, B. and Franco, J. Scintigraphically guided ultrasonography of intra-abdominal abscess, 601*
Stark, V. see Harper, P. V.
Steckley, R. A., Kronenberg, M. W., Born, M. L., Rhea, T. C., Bateman, J. M., Rollo, F. D. and Friesinger, G. C. Automated and visual methods for regional wall motion analysis, 641*

Steele, P. P. see Kirch, D. L.
Steffen, S. M. see DeNardo, S. J.
Steidley, J. W., Miller, D. W., Schlosser, P. A., Deutchman, A. H. and Hyland, J. R. Quantitative comparison of solid state and scintillation cameras, 635*
Steidley, J. W. see Deutchman, A. H.
Steigman, J., Chin, E. V. and Solomon, N. A. Tc-99m reduction by electrolysis and Sn(II), 766
Steinbach, J. see Rosenspire, K.
Steinbach, J. J. and Donoghue, G. D. Toxic diffuse goiter treatment with I-131 and antithyroid drugs, 624*
Steinbach, J. J., Donoghue, G. D. and Goldman, J. K. Toxic diffuse goiter treatment with I-131 and antithyroid drugs, 1263
Steiner, R. E. see Fazio, F.
Stelzer, F. A., Malmud, L. S., Fisher, R. S., Tolin, R. D., Menin, R., Makler, P. T. and Reilley, J. Quantitative gastro-cholecystoscintigraphy, 621*
Stelzer, F. A.
see Fisher, R. S.
see Malmud, L. S.
Stern, H. see Malmud, L. S.
Stern, M. see Zusmer, N. R.
Sterrett, R. see Cahill, P.
Stewart, C. A. see Siegel, M. E.
Stibolt, T. B. and Bradley-Moore, P. R. Renal functional mapping to detect segmental arterial lesions, 657*
Stöcklin, G.
see Knust, E. J.
see Tisljar, U.
see Vyska, K.
Stolzenberg, J. and Pollak, R. H. Anomolous Tl-201 myocardial stress uptake, 900
Stone, W. J. see Powers, T. A.
Stoub, E. W., Colsher, J. G., Lee, P. C. and Muehllehner, G. Spatial distortion correction for gamma cameras, 608*
Strand, S-E. and Persson, B. R. R. Quantitative lymphoscintigraphy I, 1038
Strange, D. R. see Koral, K. F.
Strashun, A. and Chayes, Z. Migratory osteolysis, 129
Strauch, B. see Rudavsky, A. Z.
Strauss, H. W. Book review; *Thallium-201 Myocardial Imaging*, 273
Strauss, H. W. Teaching editorial; diagnosis of heart disease, 165
Strauss, H. W., Homcy, C., and Kopiwoda, S. Y. Imaging for competitive binding assessment of beta receptor occupancy, 681*
Strauss, H. W.
see Bingham, J. B.
see Boucher, C. A.
see Castronovo, F. P.
see Cochavi, S.
see DeLuca, S.
see Goodman, M. M.
see Kirshenbaum, H. D.
see Konstam, M. A.
see Kushner, F. G.
see Nichols, A. B.
see Okada, R. D.
see Wernikoff, R. E.
see Winzelberg, G. G.
see Zir, L. M.
Strauss, W. see Khaw, B. A.
Strelow, D. A. see Clements, I. P.
Study, K. T., Breslow, K. and Rhodes, B. A. Acceptance testing of Tl-201, 684*
Sty, J., Kun, L. and Thorp, S. Scintigraphy in acute lymphatic cell leukemia, 1101
Sty, J. R., Babbitt, D. P. and Boedecker, R. A. Bone imaging radiation induced cartilaginous exostosis, 580
Sty, J. R., Boedecker, R. A. and Babbitt, D. P. Skull scintigraphy in infantile hypophosphatasia, 305
Sty, J. R., Boedecker, R. A., Scanlon, G. T. and Babbitt, D. P. "Dermal backflow" in lymphatic obstruction, 905
Subramanian, G. see Collier, B. D.
Subrahmanyam, P. S. S. see Kotrappa, P.
Sullivan, M. J. see Gewirtz, H.
Sullivan, T. see Ahmad, M.
Summer, W. R. see Alderson, P. O.
Sun, T. T. see Washburn, L. C.
Sung, D. I. see Fawwaz, R. A.
Sunwoo, Y. C. see Ahmad, M.
Suzuki, R. see Waxman, A. D.
Suzuki, T., Ishii, Y., Hamanaka, D., Yamamoto, K. and Torizuka, K. Uneveness of ventilation in chronic obstructive pulmonary disease, 620*
Swan, H. J. C.
see Berman, D. S.
see Elkayam, U.
see Maddahi, J.
see Shah, P. K.
Swanson, D. P., Wirth, N. E. and Gross, M. D. Altered biodistribution of I-131 iodomethylnorcholesterol, 805
Swanson, D. P.
see Carey, J. E.
see Freitas, J. E.
see Gross, M. D.
see Thrall, J. H.
see Wieland, D. M.
see Wu, J. L.
Swanson, M. A., Chatterjee, S., and DeNardo, S. J. I-123 fibrinogen scintigraphy in allograft rejection diagnosis, 619*
Swanson, M. A. see DeNardo, S. J.
Swanson, S. M. see Pfisterer, M. E.
Swanson, S. S. see Pfisterer, M. E.
Sy, W. M., Smith, A. J. and Lao, R. S. Bone images after parathyroidectomy, 674*
Syrota, A., Comar, D., Cerf, M., Plummer, D., Maziérè, M. and Kellershohn, C. C-11 methionine computed tomography of the pancreas, 778
Sziklas, J. J. Femoral head activity in Perthes' disease, 458
Sziklas, J. J.
see Dhawan, V. M.
see Spencer, R. P.
Szymendera, J. J. see Hayes, R. L.

Tachibana, K. see Fukuchi, M.
Takagi, Y. see Kubo, A.
Takeda, S. Fixation of gallium, 457
Tamagna, E. I., Levine, G. A. and Hershman, J. M. Thyroid hormone levels after I-131 therapy, 387
Tanaka, T. see Wong, D. W.
Tanasescu, D. E., Berman, D. S., Staniloff, H., Brachman, M. B., Ramanna, L. and Waxman, A. D. Changes in Tl-201 myocardial defects during Tl-201 redistribution, 688*
Tanasescu, D. E., Wolfstein, R. S., Brachman, M. B. and Waxman, A. D. Early and delayed Tc-99m glucoheptonate brain images, 287
Tanasescu, D. E.
see Berman, D. S.
see Brachman, M. B.
see Waxman, A. D.
Tansey, W. A. see Pierson, R. N.
Tapia, L. see Cahill, P.
Taplin, G. V. and Elam, D. Smaller lung particles for safer perfusion examinations, 613*
Tarazi, R. C. see Fouad, F. M.
Tarcan, Y., Faraj, B. A., Camp, V. M., Sarper, R., Fajman, W., Cantrell, J. B. and Galambos, J. Pharmacokinetics of C-14 aminopyrine breath test in liver disease, 686*
Tarcan, Y. see Faraj, B. A.
Taroli, E. J. see Bingham, J. B.
Tatum, J. L. see Beck, J. W.
Taube, R. A. see Davis, M. A.
Taylor, A., Hollenbeck, J. and Hagan, P. L. DMSA scanning; an index of relative renal plasma flow, 630*
Taylor, A. see Verba, J. W.
Teates, C. D.
see Bray, S. T.
see Williamson, B. R. J.
Ter-Pogossian, M. M., Mullani, N. A., Higgins, C. S., Hood, J. T. and Caston, N. J. Performance of PETT V, 628*
Terpstra, I. see Bakker, A.
Tetalman, M., Fordham, E., Ali, A., Chiles, J., Patel, S., Schmidt, K. and Turner, D. A. Hypertrophic pulmonary osteoarthropathy, 602*
Tevaarwerk, G. J. M. see Reese, L.
Tewson, T. J. and Welch, M. J. Synthesis of carrier free F-18 aromatic compounds, 671*
Tewson, T. J. and Welch, M. J. Synthesis of carrier free F-18 fluoroethanol, 663*
Thakur, M. L.
see Armas, R. R.
see Hoffer, P. B.
see Zakhireh, B.
Thane, T. T. see Conway, J. J.
Thirunavukkarasu, S., Siddiqui, A. R., Wyllie, R., Eigen, H., Franken, E. A., Wellman, H. N., Grosfield, J. L. and Fitzgerald, J. F. Detection of gastroesophageal reflux and pulmonary aspiration in children, 637*
Thomas, F. D.

see Grossman, Z. D.
see Wistow, B. W.
Thomas, M. see Sherbini, S.
Thomas, S. R., Gelfand, M. J., Kereiakes, J. G., Burns, G. S., Purdom, R. C. and Maxon, H. R. Dosimetry considerations for Ga-67 citrate scanning in children, 637*
Thompson, M. A. see Yeh, E-L.
Thompson, W. L.
see Murphy, P. H.
see Sonnemaker, R. E.
see Short, M. D.
Thomson, S. see Kagan, A.
Thornton, A. K., Molinski, V. J. and Spencer, J. T. Radiolytic production of peroxides in Tc-99m solutions, 653*
Thorp, S. see Sty, J.
Thrall, J. H., and Swanson, D. P. Comparison of Tc-99m HSA and in vivo labeled Tc-99m RBC's for cardiac studies, 1210
Thrall, J. H.
see Brady, T. J.
see Carey, J. E.
see Freitas, J. E.
see Koral, K. F.
see Rogers, W. L.
Tight, R. R. see Siddiqui, A. R.
Timpe, G. see LeBlanc, A. D.
Tisljar, U., Kloster, G., Ritzl, F. and Stöcklin, G. Radioiodinated L-α-methyltyrosine uptake by mouse pancreas, 973
Tochman, M. S. see Katz, R. D.
Tofe, A. J., Bevan, J. A., Fawzi, M. B., Whitehouse, H. S. and Francis, M. D. Gentisic acid stabilizer for bone agents, 654*
Tofe, A. J.
see Conway, J. J.
see Francis, M. D.
Tolin, R. S.
see Fisher, R. S.
see Stelzer, F. A.
Tollefsen, S. see Klingensmith, W. C.
Tonami, N. see Aburano, T.
Tonariya, Y. see Miyamae, T.
Torizuka, K., Morita, R., Yoshii, M., Nakajima, K. and Kousaka, T. Serum ferritin levels as malignancy indicators, 617*
Torizuka, K.
see Suzuki, T.
see Yonekura, Y.
Tosswill, C. H. see Mauderli, W.
Tothill, P., McLoughlin, G. P. and Heading, R. C. Technical errors in gastric emptying measurement, 269
Touya, J. J., Price, R. R., Patton, J. A., Erickson, P., Jones, J. P. and Rollo, F. D. Gated regional spirometry, 620*
Touya, J. J. see Price, R. R.
Tow, D. E. see Folland, E. D.
Trageser, T. C. see Dannals, R. F.
Trapani, J. S. see Witherspoon, L. R.
Trelford, J. D. see DeNardo, S. J.
Tremann, J. see Daly, M. J.
Treves, S.
see Collier, B. D.
see Heyman, S.
Tripathi, A. see Sherbini, S.
Triplett, J. W. see Smith, R. B.
Triplett, R. G., Kelly, J. F., Mendenhall, K. G. and Vieras, F. Early quantitative imaging of mandibular bone grafts, 297
Trobaugh, G. B. see Ritchie, J. L.
Trop, H. S.
see Davison, A.
see Jones, A. G.
see Orvig, C.
Troutner, D. E., Volkert, W. A., Simon, J., Ketring, A. and Holmes, R. A. Complexes of Tc-99m with cyclam, 641*
Truman, A. T. see Covitz, W.
Tsai, S. H. see Williams, L. E.
Tsan, M-F. and Scheffel, U. Ga-67 accumulation in inflammatory lesions, 173
Tsan, M. F.
see Scheffel, U.
see Tzen, K. Y.
Tsubago, Y. see Miyamae, T.
Tsui, B. M. W., Chen, C-T., Yasillo, N. J., Ortega, C. J., Charleston, D. B. and Lathrop, K. A. A conjugate whole-body scanner for quantitative organ distribution studies, 628*
Tsui, B. M. W. see Lathrop, K. A.
Turner, D. A.
see Hoffer, P. B.
see Tetalman, M.
Turner, J. G.
see Bessent, R. G.
see Fogelman, I.
see McKillop, J. H.
Turner, J. H., Martindale, A. A. and Olsthoorn, Q. P. W. Post-fracture femoral head vascularity assessment, 673*
Twardock, A. R. see DeNardo, S. J.
Tzen, K. Y., Oster, Z. H., Wagner, H. N. and Tsan, M. F. Enhanced capillary permeability and iron binding protein roles in Ga-67 accumulation, 660*
Tzivoni, D. see Atlan, H.

Uchida, T., Nemoto, T., Yui, T., Matsuda, S. and Kariyone, S. Tc-99m study of leukocyte migratory patterns, 1197
Uksik, P. see Reese, L.
Undrill, P. E. see Carril, J. M.
Upton, M. T.
see McEwan, P.
see Newman, G. E.
Urie, M. M. see Mauderli, W.
Uszler, J. M., Effros, R. M. and Shapiro, L. Altered clearance of inhaled small solutes from the lungs, 613*

Vagenakis, A. G. see Kleinmann, R. E.
Vaidya, P. see Ryo, U. Y.
Vaitkevicus, V. K. see Mua, J.
Valeri, C. R. see Hotte, C. E.
Vallabhajosula, S. R., Harwig, J. F. and Wolf, W. Mechanism of tumor localization of gallium, 655*
Vanags, K. see Stanton, T.
Van Antwerp, J. see Hilts, S. V.
van Aswegen, A. see Chipps, B. E.
Van Dam, B. E. see Dye, S. F.
Vandermoten, G. see Pauwels, S.
Vandevivere, J., Spehl, M., Dab, I., Baran, D. and Piepsz, A. Detection of bronchiectasis in children, 638*
van Luyk, W. H. J. see Beekhuis, H.
Vannier, M. see Beihn, R.
Vartsky, D., Ellis, K. J. and Cohn, S. H. In vivo body N by neutron capture analysis, 1158
Vas, R. see Staniloff, H.
Vasquez, S. see Sfakianakis, G. N.
Vaughan, E. D. see Keim, H. J.
Vecchione, J. J. see Hotte, C. E.
Venkatesh, N., Wilson, M. F., Schechter, E. and Allen, E. W. Comparison of Tl-201 imaging with Q-ST and R-wave changes in coronary disease, 661*
Verani, M. S. and Marcus, M. L. Tl-201 myocardial studies in aortocoronary saphenous bypass surgery, 576
Verba, J., Bornstein, I., Almasi, J., Goliash, T., Eisner, R. and Nowak, D. 3D Fourier filtering in nuclear cardiac studies, 658*
Verba, J. see Slutsky, R.
Verba, J. W., Bornstein, I., Alazraki, N. P., Taylor, A., Bhargava, V., Shabetai, R. and LeWinter, M. Computer program for behavior of all four cardiac chambers, 665*
Verba, J. W., Bornstein, I., Alazraki, N. P., Taylor, A., Bhargava, V., Shabetai, R. and LeWinter, M. Onset and progression of mechanical systole, 625*
Verma, R. C., Chang, B., Webber, M. M. and Buffkin, D. C. Anti-beta-hCG-antibody for tumor localization, 656*
Verma, R. C. and Panagoitis, N. M. I-131 therapy for hyperthyroidism, 624*
Verma, R. C., Webber, M. M. and Eisenman, J. I. Tourniquet pressure and venous flow in the legs, 639*
Verma, R. C.
see Buffkin, D. C.
see Webber, M. M.
Vialotti, C. see Sober, A. J.
Vicher, T. see Wasnich, R.
Vieras, F., Barron, E. L. and Parker, G. A. Tc-99m S colloid uptake in experimental deep vein thrombosis, 633*
Vieras, F., Fraser, L. M. and Bridgeman, J. R. Xe-133 ventilation studies in subjects on artificial ventilation, 613*
Vieras, F.
see Alderson, P. O.
see Alter, W. A.
see Eckelman, W. C.
see Gibson, R. E.
see Grissom, M.
see Triplett, R. G.
Villarica, J. see Matin, P.
Vincente, F.
see Hattner, R. S.
see Hull, A.
Vitkauskas, G. see Sripada, P. K.
Vlietstra, R. E. see Clements, I. P.

Vogel, R. A., Kirch, D. L., LeFree, M. T., Rainwater, J. O., Jensen, D. P. and Steele, P. P. Gated blood pool tomography with a wide-field camera, 643*
Vogel, R. A. see Kirch, D. L.
Volf, V. Book review; *Biological Effects of Ra-224. Benefit and Risks of Therapeutic Application,* 175
Volkert, W. A. see Troutner, D. E.
Volpert, E. M. see Maayan, M. L.
Vomero, J. J. see Gelbard, A. S.
Von Behren, P. L. see Groch, M. W.
Voukydis, P. C. see Zir, L. M.
Vyska, K., Höck, A., Freundlieb, C., Profant, M., Feinendegen, L. E., Machulla, H. J. and Stöcklin, G. Myocardial imaging and fatty acid metabolism using I-123 heptadecanoic acid, 650*
Vyska, K. see Reske, S. N.

Wachslicht-Rodbard, H. and Roth, J. In vivo measurement of whole-body insulin receptor, 605*
Wackers, F. J. Th. see Johnstone, D. E.
Wagner, H. N. Time for FASORS? 581
Wagner, H. N.
see Alderson, P. O.
see Boonyaprapa, S.
see Bourguignon, M. H.
see Buchanan, J. W.
see Burns, H. D.
see Camargo, E. E.
see Chipps, B. E.
see Dannals, R. F.
see D'Antonio, R.
see Katz, R. D.
see Langan, J. K.
see Lipson, A.
see Tzen, K. Y.
see Yang, S. L.
Wagner, S. J. and Welch, M. J. Ga-68 labeling of albumin and albumin microspheres, 428
Wagner, W. see Siegel, M. E.
Wahner, H. W., Brown, M. L. and Dickson, E. R. Ga accumulation in the stomach, 577
Wahner, H. W., Carpenter, P. C., Salassa, R. M. and Duick, D. S. Gonadal tumor scanning with I-131 iodomethylnorcholesterol, 677*
Wahner, H. W. and Goldstein, N. P. Cu-64 kinetics in Wilson's disease, 679*
Wahner, H. W. see Brown, M. L.
Wainwright, R. J., Raper, D. A., Hilson, A. J. W., Sowton, E., and Maisey, M. N. Multiple gated Tc-99m cardiac imaging during the cold pressor test, 640*
Walaski, S. see Slutsky, R.
Waltman, A. C. see Winzelberg, G. G.
Walton, J. A. see Brady, T. J.
Wang, T. S. T., Mojdehi, G. E., Fawwaz, R. A. and Johnson, P. M. Chemical structure and bone localization of Tc-99m diphosphonic acids, 1066
Warbick-Cerone, A. Colloidal particle size determination by gel filtration, 1098
Warner, G. G. see Coffey, J. L.
Warshaw, B. see Samuels, L. D.
Warshaw, D. see Atlan, H.
Washburn, L. C., Sun, T. T., Byrd, B. L., Hayes, R. L. and Butler, T. A. Aminócyclobutane-^{11}C-carboxylic acid for tumor, 1055
Washburn, L. C., Sun, T. T., Byrd, B. L., Hayes, R. L. and Butler, T. A. Carboxyl-^{11}C-tryptophan for pancreas imaging, 857
Washburn, L. C.
see Digenis, G. A.
see Hübner, K. F.
see Lushbaugh, C. C.
Wasnich, R., Glober, G., Hayashi, T., Vicher, T. and Yeh, F. Computer quantitation of spleen-to-liver ratios in hepatocellular disease, 149
Watanabe, H. see Miyamae, T.
Watson, D. C. see Alderson, P. O.
Watson, E. E. Book review; *Radiation Shielding and Dosimetry,* 1219
Watson, E. E. and Coffey, J. L. Radiation dose from Tl-201 contaminants, 607*
Watson, E. E., Coffey, J. L., Schlafke, A. T. and Cloutier, R. J. A computer base of bibliographic entries on radiopharmaceuticals, 607*
Watson, N. E. see Kelly, R. J.
Waxman, A. D., Julian, P., Komaiko, M., Brachman, M. B., Tanasescu, D. E., Wolfstein, R. S. and Berman, D. S. Ga-67 uptake by hilar and mediastinal structures, 645*
Waxman, A. D., Richmond, R. H., Juttner, H. U., Siemsen, J. K., Heffelinger, M. J. and Fink, E. J. Gallium uptake in primary liver cell carcinoma, 632*
Waxman, A. D., Siemsen, J. K., Levine, S., Holdorf, D., Suzuki, R., Singer, F. and Bateman, J. Ga-67 imaging in multiple myeloma, 647*
Waxman, A. D.
see Berman, D. S.
see Brachman, M. B.
see Chapman, D.
see Elkayam, U.
see Maddahi, J.
see Shah, P. K.
see Staniloff, H.
see Tanasescu, D. E.
Webber, M. M., Chang, B., Buffkin, D. C. and Verma, R. C. In-111 platelets or iodinated fibrinogen for deep venous thrombosis detection, 459
Webber, M. M.
see Buffkin, D. C.
see Verma, R. C.
Weber, D. see Clorius, J. H.
Weber, D. A. see King, M. A.
Weber, P. M. see Khentigan, A.
Weiblen, B. see Forstrom, L.
Weil, R. see Shanahan, W. M. S.
Weiner, M. see Porter, D. W.
Weinhold, P. A. see Pozderac, R. V.
Weiss, A.
see Atlan, H.
see Samuels, L. D.
Weiss, G. H. see Bunow, B.
Weiss, J. F. see Bradley, W. P.
Weiss, S. C. see Conway, J. J.
Weissman, H. S., Frank, M. S. and Freeman, L. M. Post-operative Tc-99m HIDA cholescintigraphy, 686*
Weissman, H. S., Frank, M. S., and Freeman, L. M. Tc-99m HIDA cholescintigraphy, 679*
Welch, D. M., Baker, W. J., Beightol, R. W. and Coleman, R. E. In-111 leukocytes in suspected inflammatory process, 659*
Welch, M. J., Knight, L. C. and Siegel, B. A. In-111 platelets for deep venous thrombosis detection, 460
Welch, M. J.
see Berridge, M.
see Ehrhardt, G. J.
see Mathias, C. J.
see McElvany, K. D.
see Tewson, T. J.
see Wagner, S. J.
Wellman, H. N.
see Appledorn, C. R.
see Park, H.
see Siddiqui, A. R.
see Thirunavukkarasu, S.
Wernikoff, R. E., McKusick, K. A., and Strauss, H. W. Exchange of photon count for blur reduction, 658*
Wesner, D. A. see Digenis, G. A.
Wessels, B. see Lieberman, L. M.
Westendorf, B. A. see Billinghurst, M. W.
Whalen, C. see Sober, A. J.
Wheat, J. see Park, H.
Wheeler, J. C. see Eikman, E. A.
Whipple, J. M. see Chen, M. F.
Whitehead, F. R. Optimization of gray scale for photoscanners, 996
Whitehorn, I. see Marshall, R. C.
Whitehouse, H. S. see Tofe, A. J.
Whitmore, W. F. see Kaplan, W. D.
Whitney, W. P. see Fritzberg, A. R.
Wickland, T. see Zalutsky, M.
Wicks, R. and Blau, M. Effect of spatial distortion on Anger camera field uniformity correction, 252
Wieland, D. M., Swanson, D. P., Brown, L. E., and Beierwaltes, W. H. I-131 antiadrenergic agent imaging of adrenal medulla, 155
Wieland, D. M. see Wu, J. L.
Wiener, J. D. Hypothyroidism after radioiodine treatment, 267
Wiley, A. L. see Lieberman, L. M.
Wilkinson, R. H. and Gaede, J. T. Concentration of Tc-99m methylene diphosphonate in liver metastases, 303
Willerson, J. T.
see Datz, F. L.
see Lewis, S. E.
Williams, A. V. see Leman, R. B.
Williams, C. see Nishiyama, H.
Williams, C. C. see Robbins, P. J.
Williams, C. M. see Mauderli, W.

Williams, D. L. Numerical deconvolution of quantitative data analyses, 568
Williams, D. L. see Larson, S. M.
Williams, J. W. see Eikman, E. A.
Williams, L. E., Koehler, S. A., Shaw, M. S., Tsai, S. H. and Lund, R. S. Gate synchronization in equilibrium cardiac imaging, 807
Williams, L. E., Loken, M. K., Forstrom, L. A., Ponto, R. A. and Frick, M. P. Effect of cardiac rate on radionuclide left-ventricular dV/dT, 997
Williams, L. E., Loken, M. K. and Frick, M. P. Psychophysical gray scale for photoscan transparencies, 1215
Williams, L. E., Loken, M. K., Ponto, R. A. and Frick, M. P. Photon energy effects on field uniformity tests, 363
Williams, L. E., Ponto, R. A., Forstrom, L. A., Loken, M. K. and Hoogland, D. R. Human dosimetry of Tc-99m PIPIDA, 607*
Williamson, B. R. J., McLaughlin, R. E., Teates, C. D., Bray, S. T. and Croft, B. Y. Bone scanning in painful total hip prosthesis, 602*
Williamson, B. R. J. see Bray, S. T.
Wilson, G. A.
see Kronenberg, M. W.
see O'Mara, R. E.
Wilson, M. A. Multiple chemodectomas, 904
Wilson, M. F. see Venkatesh, N.
Winston, M. A. Echography compared with radiotracer scanning for parathyroid adenoma, 270
Winter, H. S. see Heyman, S.
Winzelberg, G. G., McKusick, K. A., Strauss, H. W., Waltman, A. C. and Greenfield, A. J. In vivo labeled, Tc-99m RBC evaluation of gastrointestinal bleeding, 1080
Winzelberg, G. G., McKusick, K. A., Strauss, H. W., Waltman, A. C. and Greenfield, A. J. Tc-99m in vivo labeled RBC evaluation of gastrointestinal bleeding, 631*
Winzelberg, G. G. see DeLuca, S.
Wirth, N. E. see Swanson, D. P.
Wisenberg, G., Marshall, R., Schelbert, H. R. and Rue, C. Oral propanolol effect on left ventricular function, 639*
Wisenberg, G., Schelbert, H. R., Robinson, G. D., Selin, C. J., Hoffman, E. J. and Phelps, M. E. Regional myocardial blood flow quantitation, 648*
Wisenberg, G. see Schelbert, H. R.
Wistow, B. W., McAfee, J. G., Sagerman, R. H., Thomas, F. D. and Grossman, Z. D. Renal uptake of Tc-99m MDP after radiation therapy, 32
Witek, J. T. see Spencer, R. P.
Witenhafer, S. R. see Eikman, E. A.
Witherspoon, L. R. Methods for the estimation of free thyroxine, 626*
Witherspoon, L. R., Shuler, S. E., Garcia, M. M., and Zollinger, L. A. Serum myoglobin as a marker for acute myocardial infarction, 115
Witherspoon, L. R. and Trapani, J. S. Forensic radioimmunoassay, 796
Wolf, A. P.
see Alavi, A.
see Som, P.
Wolf, W., Manaka, R. C., Young, D. and Schumitzky, A. Mathematical models of radiopharmacokinetics, 614*
Wolf, W. see Vallabhajosula, S. R.
Wolfangel, R. G. Accumulation of radioiodine in staff members, 995
Wolfstein, R. S. Radionuclide angiography of kidneys in superior vena caval obstruction, 1106
Wolfstein, R. S.
see Brachman, M. B.
see Tanasescu, D. E.
see Waxman, A. D.
Wong, D. W., Tanaka, T., Mishkin, F. and Lee, T. In vitro assessment of Tc-99m bovine thrombin and streptokinase activated human plasmin, 967
Wong, M. see Hecht, H. S.
Wong, R. see Shearer, D. R.
Woodbury, D. H. see Sarkar, S. D.
Woods, M. J. Nuclear medicine and radionuclide metrology ICRM life sciences working group, 998
Woolfenden, J. see Hilts, S. V.
Woolfenden, J. M., Pitt, M. J., Durie, B. G. M. and Moon, T. E. Bone scanning in multiple myeloma, 647*
Worley, P. see Marzilli, L. G.
Wu, J. see Zalutsky, M.
Wu, J. L., Wieland, D. M., Brown, L. E., Swanson, D. P., and Beierwaltes, W. H. Adrenal imaging with I-131 iodobenzylguanidine, 681*
Wu, L. C. see Yeh, S. H.
Wyllie, R. see Thirunavukkarasu, S.
Wynne, J., Birnholz, J. C., Holman, B. L., Finberg, H. and Alpert, J. S. Radionuclide and ultrasound assessment of regional asynergy in acute myocardial infarction, 600*
Wynne, J., Sayres, M., Idoine, J., Alpert, J. S., Neill, J. and Holman, B. L. Global and regional function in acute myocardial infarction, 667*
Wynne, J. see Holman, B. L.

Yamamoto, K.
see Suzuki, T.
see Yonekura, Y.
Yang, S. see Chipps, B. E.
Yang, S. L., Alderson, P. O., Kaizer, H. A. and Wagner, H. N. Serial Ga-67 citrate imaging in children with neoplastic disease, 210
Yano, Y., Budinger, T. F., Chiang, G., O'Brien, H. A. and Grant, P. M. Rb-82 generators charged with high levels of Sr-82 and Sr-85, 961
Yano, Y., Budinger, T. F., O'Brien, H. A. and Grant, P. M. Alumina column Rb-82 generators, 684*
Yano, Y. see Budinger, T. F.
Yasillo, N. J. see Tsui, B. M. W.
Yeh, E-L. Distortion of bar phantom image by collimator, 260
Yeh, E-L, Chiang, L-C. and Meade, R. C. Tc-99m DTPA studies of urinary extravasation with ureteral obstruction, 236
Yeh, E-L., Thompson, M. A. and Meade, R. C. Accumulation of Tc-99m diphosphonate in pericardial effusion, 1102
Yeh, E. L. see Kronenwetter, C. M.
Yeh, F. see Wasnich, R.
Yeh, S. D. J. see Dhawan, V.
Yeh, S. H., Liu, R. S. and Wu, L. C. Mean transit time following temporal-middle cerebral artery anastomosis, 611*
Yocum, K. M. see Deutchman, A. H.
Yonekura, Y., Ishii, Y., Torizuka, K., Yamamoto, K., Mukai, T., Kadota, K., Kambara, H. and Kawai, C. Quantitative fractional myocardial Tl-201 uptake, 688*
Yoshii, M. see Torizuka, K.
Young, B. see Handmaker, H.
Young, D.
see Lieberman, L. M.
see Wolf, W.
Young, R. L. Hypothyroidism after radioiodine treatment, 267
Young, W. see Dye, S. F.
Yui, T. see Uchida, T.

Zakhireh, B., Thakur, M. L., Malech, H. L., Cohen, M. S., Gottschalk, A. and Root, R. K. In-111 human polymorphonuclear leukocytes, 741
Zalutsky, M., Wu, J., Wickland, T., Harper, P. V. and Moossa, A. Synthesis and purification of C-11 tryptophan, 663*
Zalutsky, M. see Ryan, J.
Zamrazil, V. see Němec, J.
Zander, J. D. see Eikman, E. A.
Zaret, B. L. see Johnstone, D. E.
Zelt, J. see Clorius, J. H.
Zens, A. L. see Grossman, Z. D.
Zielonka, J. see Holman, B. L.
Zieverink, S. E. see Park, H. M.
Zimmerman, R. E., Judy, P. F., Hill, T. C. and Lovett, R. D. Performance of an emission tomographic brain scanner, 628*
Zimmerman, R. E.
see Holman, B. L.
see Neirinckx, R. D.
Zir, L. M., Strauss, H. W., Gewirtz, H., Shea, W. H., Forwand, S. A., Voukydis, P. C. and Pohost, G. M. Tl-201 redistribution in cases of acute myocardial infarction, 649*
Zollinger, L. A. see Witherspoon, L. R.
Zusmer, N. R., Maturo, V., Stern, M., Smoak, W. M., Janowitz, W. R. and Gilson, A. J. Sonography and scintigraphy in hepatobiliary disease, 600*

1979 SUBJECT INDEX

Asterisk indicates abstract

Abdomen
see also *Abscess; specific organ*
adrenal hemorrhage diagnosis, 521
anatomy, book review, 1319
cystic lesions, ultrasound, 179*
Ga-67 citrate imaging, starch granulomatous disease, 902
lymph node imaging, Tc-99m S colloid, 646*
mass, inferior vena cava elevation, ultrasound, 1113*
peritoneo-venous shunt evaluation, Tc-99m S colloid, HSA, 72
phantom, emission computed tomography, 102, 108
retroperitoneal fibrosis, Ga-67 citrate scan, ultrasound, 238
trauma, ultrasound, 1324*
tuberculous peritonitis, Ga-67 citrate scanning, 1111*
ultrasound, pediatrics, book review, 175

Abscess
abdominal, computerized axial tomography, 469*
abdominal, on hepatobiliary studies, 679*
abdominal, ultrasonography, 370*, 469*, 601*
brain, radionuclide studies, CAT, 600*
Ga-67 citrate imaging, 215, 469*, 577, 601*
Ga-67 citrate uptake mechanism, 672*
gas-containing, ultrasound, 1113*
inflammation differentiation, Crohn's disease, 215
In-111 leukocyte scanning, 659*
neck, thyroid imaging, 1051
pelvic, ultrasound, 370*
pericholecystic, ultrasound, 911*
splenic, ultrasound, Ga-67, Tc-99m S imaging, 1221*

Absorption edge transmission
stable I determination, 1286

Adrenal glands
absorbed dose, I-131 NP-59, 60
aldosteronism, I-131 NP-59, 7, 897
Cushing's syndrome, imaging cost-effectiveness, 677*
dexamethasone suppression imaging, I-131 NP-59, 621*, 1131
false-negative images, I-131 NP-59, 677*
I-131 antiadrenergic agents, preparation, distribution, imaging, in dogs, 155
I-131 iodobenzylguanidine, preparation, imaging, in animals, 681*
imaging and tomography, I-131 NP-59, 609*
imaging, gonadal tumor uptake of I-131 NP-59, 677*
imaging, RES uptake of I-131 NP-59, 803, 805, 806
mass, inferior vena caval involvement, ultrasound, 77*
melanoma, uptake of I-131 tyrosine derivatives, in animals, 1221*

Aerosol
dry, delivery system, 1000
regional delivery, 272
Tc-99m polystyrene, compared to Kr-81m, 194
Tc-99m, ventilation in chronic obstructive pulmonary disease, 620*

Albumin
see *Gallium-68; Iodine-131; Technetium-99m albumin; Tantalum-178*

Allergy
dermatitis, I-131 fibrinogen imaging, 808
insulin, IgG and IgE antibody radioassay, 673*

Alpha-1-antitrypsin
deficiency, hepatobiliary imaging, 680*

Alpha-fetoprotein
effect on liver cell carcinoma uptake of Ga-67 citrate, 632*
radioimmunoassay, in liver cancer, 372*

Amino acids
see *Carbon-11; Carbon-14; Fluorine-18; Iodine-125*

Anatomy
see *Book review*

Aneurysm
Intracranial, ruptured, dynamic cerebral perfusion imaging, 611*

Antibiotics
radiometric serum test, 616*

Antibody
see also *Radioimmunoassay*
-antigen binding kinetics, H-3, 1062
IgG, IgE, radioassay, 673*
IgG, Tc-99m labeling, 652*
In-111 DTPA-antimosin FAB fragments, myocardial infarct imaging, in dogs, 605*
to human chorionic gonadotropin for tumor, preparation, culture uptake, 656*

Antigen
see also *Radioimmunoassay*
Hepatitis A, effect on liver cell carcinoma uptake of Ga-67 citrate, 632*

Artifacts
Compton scatter, emission transaxial tomography, 608*

Atropine
plasma, radioimmunoassay, 366

Autoradiography
tissue uptake parameters, Tc-99m, P-32 pyrophosphate, in rats, 76*

Background
activity algorithm, myocardial imaging, 1312
correction, heart studies, 643*
Se-75 selenomethionine retention, 365
smoothing, adaptive filter, 665*
subtraction, computer, 578

Bacteria
see also *Infection*

Lactobacillus casei, microbiologic assay, 178*
Lactobacillus plantarum, radiometric assay for niacin, 419
Mycobacterium lepraemurium, fatty acid metabolism, C-14, 1222*
M. tuberculosis, fatty acid metabolism, drug response, radiometric assay, 676*
radiometric assay of B_{12} and folate in food, 616*
radiometric assay, serum antibiotics, 616*

Bayesian analysis
*multiple cardiac tests, 651**
observer performance, 622*

Bioassay
cobalamin, pernicious anemia, 1007*
hormones, book review, 1210

Bladder
Tc-99m DTPA *tomography, 108*

Blood
anemias, bone marrow imaging, 603*, 675*
anemia, iron-deficiency, GI blood loss, Cr-51 RBC, 178*
anemia, pernicious, false-negative radiodilution assays, 1007*
beta-thromboglobulin radioimmunoassay, 664*
hepatitis-B-core antigen antibody radioimmunoassay, 467*, 676*
I-125 cobra venom, distribution, in mice, 655*
iron deficiency, effect on Ga-67 citrate distribution, tumor uptake, in rats, 243
leukemia, bone marrow imaging, 675*
leukemia, Ga-67 citrate bone uptake, 854
leukocytes see also; *Indium-111*
leukocytes, Tc-99m labeling, in vivo migration, 1197
neutrophil binding, N-formyl-selenomethionine-methionine, *681**
plasma, atropine clearance, 366
platelets, see also *Indium-111*
platelets, radiation damage from radiolabeling, 255
platelets, radiolabeled, *recovery separation, 685**
polycythemia, bone marrow imaging, 675*
proteins, Fe binding, Ga-67 citrate uptake, *in rabbits, 660**
red cell see also *Carbon-11; Chromium-51; Technetium-99m red blood cells*
red cell survival, effect of Sn(II) pyrophosphate, in rabbits, 294
serum protein-radiopharmaceutical *interactions, 652*, 682**
-to-cell tracer uptake, multicapillary model, 605*
venous volume changes, Tc-99m RBC imaging, 633*

Bone
agents, gentisic acid stabilized, 654*
anatomy, radiographic, book review, 273, 907
blood flow, diabetic foot, 602*
blood flow, effect on Sr-85 microspheres, Kr-81m and Tc-99m MDP uptake, in dogs, 413
blood flow, effect on Tc-99m MDP uptake, in dogs, 1257
blood flow, migratory osteolysis, 129
CAT, compared to imaging, 1006*, 1110*
density, I-125 photon absorption, 911*
emission computed tomography, Tc-99m pyrophosphate, 108
F-18 pharmacokinetic model, 614*, 1150
Ga-67 citrate uptake, leukemia, 854
irradiation effects, in rabbits, 1142
joint, arthritic, Tc-99m pyrophosphate uptake, in rabbits, 673*
mass, osteoporosis, neutron activation analysis, 85, 677*
metaphyseal radiation dose, Ga-67 citrate, in children, 637*
metastases, in breast cancer, 586*, 1220*, 1319
metastases, Sr-89 therapy, 371*
$Na^{32}P$, P-32 pyrophosphate uptake, hormone pretreatment effects, in rabbits, 684*
uptake, comparison of Tc-99m MDP, HEDP and HMDP, in rats, 655*
uptake mechanisms, 794
uptake, Tc-99m diphosphonic acids, effect of structure, in rats, *1066*

Bone scanning
*avascular necrosis of the femoral head, Tc-99m MDP, 646**
calvarial markings, 621*
cartilaginous exostosis, irradiation induced, 580
child abuse recognition, Tc-99m HEDP, 675*
compared to CAT, 1006*, 1110*
compared to radiography, in children, 1322*
comparison of radiopharmaceuticals, 98, 655*, 821, 893
complementary to bone marrow scanning, 602*
disc space infection, Tc-99m HEDP, in animals, 601*, 1006*
fractures, 647*, 1271
Ga-67 citrate, 75*, 644*, 647*
*gallbladder and bowel visualization, 622**
hip prosthesis, 75*, 602*
*hypertrophic pulmonary osteoarthropathy, 602**
in breast cancer, 586*, 1220*, 1321
in lung cancer, 1321
in thyroid cancer, 271, 999
*metabolic disease, 602**
metaphyseal uptake, effect of growth hormone, T_4 therapy, Tc-99m *MDP, in children, 678**
metastases, 98, 177*, 271, 275*, 644*, 664*, 893, 999, 1220*, 1321*
multi-detector germanium camera, in animals, 629*
multiple myeloma, 125, 647*
osteitis of clavicle, Tc-99m phosphate, 910*
osteodystrophy, 467*, 602*, 646*
osteomyelitis, Ga-67 citrate, Tc-99m MDP, in rabbits, 647*
osteoporosis, idiopathic regional migratory, 1268
Perthes' disease, 75, 170, 458, 459*
post-parathyroidectomy, Tc-99m pyrophosphate, 674*
*primary hyperparathyroidism, 602**
quantitative grafts, Tc-99m HEDP, in dogs, 297
quantitative, osteogenic sarcoma, N-13 glutamate, in child, 782
quantitative, Perthes' disease, 170
rhabdomyolysis, alcohol induced, Tc-99m HEDP, 127
rheumatoid arthritis, non-joint Tc-99m pyrophosphate uptake, *673**
Rhizopus osteomyelitis, Tc-99m pyrophosphate, 75*
serial, Tc-99m HEDP, 177, 275**
skull, in children, Tc-99m MDP, 305, 1322*
stomach uptake of Tc-99m MDP, 791
stress fractures, 1271
*Tc-99m hydroxy-methane-diphosphonate, 653**
temporomandibular joint disease, 603*
three phase, diabetic foot, Tc-99m MDP, 602*
Tl-201, 815*
tumor, differential diagnosis, in children, 75*, 679*, 1110*
tumor, F-18 fluorouracil, 645*
tumoral calcinosis, 675*
vertebra, specificity, Tc-99m MDP, 674*

Bone marrow
aplastic anemia, In-111 chloride imaging, 603*
hemopoietic vs reticuloendothelial imaging, Fe-59, Tc-99m S colloid, 675*
imaging, complementary to bone and Ga-67 citrate scans, 602*
pediatric oncology, Tc-99m S colloid imaging, 379
prostatic acid phosphatase enzyme assay, 1222*
prostatic acid phosphatase radioimmunoassay, 910*, 1222*
subcapital femoral neck fracture, Tc-99m Sb colloid imaging, 673*
uptake in I-131 iodomethylnorcholesterol adrenal imaging, 803, 805, 806

Book review
A Color Atlas of Sectional Anatomy; Chest, Abdomen and Pelvis, 1319

A User's Guide to Diagnostic Ultrasound, 1003
Atlas of Abdominal Ultrasonography in Children, 175
Atlas of Human Anatomy, 368
Atlas of Radiologic Anatomy, 74
Atlas of the Human Brain and the Orbit for Computed Tomography, 908
Atlas of Xeroradiographic Anatomy of Normal Skeletal Systems, 907
Biological Effects of Ra-224. Benefit and Risks of Therapeutical Application, 175
Cancer Therapy by Hyperthermia and Radiation, 1218
Clinical Nuclear Cardiology, 465
Computer Methods-The Fundamentals of Digital Nuclear Medicine, 907
Correlations in Diagnostic Imaging, 1320
Data Supplement/Computerized Tomography in Clinical Medicine, 1108
Gynecologic Oncology, 175
Health Implications of Nuclear Power Production, 1004
Intermediate Physics for Medicine and Biology, 368
Internal Radiation Dose in Diagnostic Nuclear Medicine, 812
Lungen Diagnostik mit Radionukliden-Physiologie, Pathophysiologie, Klinik, 583
Manual of Nuclear Medicine Procedures, 584
Medical Examination Review Book, Volume 25, Nuclear Medicine, 272
Medical Malpractice Law, 907
Normal Radiologic Patterns and Variances of the Human Skeleton, 273
Nuclear Cardiology: Clinical Applications, 1107
Nuclear Radiology (Second Series) Syllabus, 465
Obstetrical Diagnosis by Radiographic, Ultrasonic and Nuclear Methods, 74
Pulmonary Macrophage and Epithelial Cells, 74
Quality Control in Nuclear Medicine Radiopharmaceuticals, Instrumentation and In Vitro Assays, 811
Radiation Shielding and Dosimetry, 1219
Radioassay and Related Techniques, 1003
Radiobiology for the Radiotherapist, 583
Radioimmunoassay and Related Procedures in Medicine 1977, 1107, 1218
Radiological Atlas of Biliary and Pancreatic Disease, 1218
Radiological Protection, 1003
Radiologie, 368
Secondary Spread in Breast Cancer, 1319
SI for the Health Professions, 465
SI Units in Medicine; An Introduction to the International System of Units with Conversion Tables and Normal Ranges, 465
Textbook of Nuclear Medicine: Basic Science, 1108
Thallium-201 Myocardial Imaging, 273
Thyroid Cancer, 811

Brain
anatomy, book review, 908
C-11 tryptophan preparation, 663*
dopamine receptor, Br-75, Br-77 bromocriptine preparation, distribution, in rats, 683*
F-18 deoxyfluoromannose, preparation, metabolism, 672*
functional activity mapping, F-18 fluorodeoxyglucose, 612*
membrane transport, Tc-99m agents, 1181
$^{15}O_2$ and $H_2{}^{15}O$ steady state distribution, compartmental model, 606*
Tc-99m bis(2 mercaptoethyl)amine ligands, preparation, distribution, in mice, 654*
tumor vascularity, $^{99m}TcO_4^-$ uptake, 612*
uptake of C-14 methionine, phenylalanine, effect of L-dopa and reserpine, in rats, 76*

Brain, blood flow
cerebral vascular disease, radionuclide angiography, 1221*,
$C^{15}O_2$ inhalation, error propagation, 606*
mean transit time, $^{99m}TcO_4^-$, anastomosis, 611*
N-13 ammonia, in dogs, 611*
perinatal hypoxia/ischemia, $^{99m}TcO_4^-$, 1110*
regional, continuous Kr-81m, emission computed tomography, 611*
ruptured aneurysm studies, 611*
stroke diagnosis, Tc-99m, 76*
venous angioma, radionuclide imaging, CAT, angiography, 1166
compared to CAT scanning, 319, 462, 600*, 1166, 1320
early, Tc-99m glucoheptonate, 287
hematoma, 620*
infarct, 620*
leukodystrophy, $^{99m}TcO_4^-$, 909*
lymphocytic cell leukemia, Tc-99m glucoheptonate, 1101
metastatic lung cancer, 644*, 1321
multi-detector germanium camera, in animals, 629*
multiple myeloma of the skull, $^{99m}TcO_4^-$, 125
mycosis fungoides, Tc-99m DTPA, 240
perinatal hypoxia/ischemia, $^{99m}TcO_4^-$, 1110*
sclerosing panencephalitis, Tc-99m DTPA, 1217*
stroke diagnosis, Tc-99m, 76*
tumor, Ga-67 citrate, 75*, 644*
tumor, Tc-99m DTPA, 462, 620*
tumor, $^{99m}TcO_4^-$, 620*, 909*
24 hour, $^{99m}TcO_4^-$, DTPA, 620*

Brain tomography
blood volume, C-11 and Cr-51 RBC, 328
blood volume, regional, ^{11}CO inhalation, 370*
computerized axial, compared to radionuclide methods, 319, 462, 600*, 1166
computerized axial, glioma, 462
computerized axial, leukodystrophy, 909*
computerized axial, sclerosing panencephalitis, 1221*
computerized axial, venous angioma, 1166
emission computed, clinical evaluation, 1117
emission computed, Tc-99m, 108
emission, multi-detector tomoscanner, Tc-99m, 319
emission, system performance, 628*
F-18 fluorodeoxyglucose, in dogs, 606*
glucose metabolism rate, 605*
positron, C-11 carboxyhemoglobin, $^{15}O_2$, 628*
seven pinhole collimator, 643*

Breast
Br-77 estrone, biodistribution, in animals, 761
cancer, bone imaging, 1220*, 1321*
cancer, book review, 1319
cancer, lymph node imaging, 585*, 586*, 933, 1243
cancer metastatic to liver, 370*
cancer, pericardial effusion, 392
milk, Tc-99m secretion, 586*, 799
tumor, halogenated estrogen analog, binding affinity, 671*

Bromine-75
-bromocriptine, preparation, distribution, in rats, 683*

Bromine-77
-bromocriptine, preparation, distribution, in rats, 683*
-estrone, biodistribution, in animals, 761
protein labeling, myeloperoxidase method, 663*

Bromine-82
-steroid analogs for prostate, receptor binding, 683*

Cadmium-115m
-chloride, distribution in hepatoma-bearing rats, 276*

Calcium-45
damaged myocardium uptake, in rats, 650*

Calcium-47
damaged myocardium uptake, in rats, 650*

Camera
computerized rotating laminar, 341
digital, design, performance, 628*
germanium, compared to scintillation camera, 635*
germanium, multi-detector, 629*
positron see also *Tomography, positron*
positron, $C^{15}O_2$ inhalation imaging, 281
Camera, scintillation
collimator distortion of bar phantom image, 260, 1100, 1316
collimator, geometric response, 635*
compared to solid state cameras, 635*
crystal size comparison, 610*
crystal thickness effects, 977, 992
deadtime correction, 168
depth resolution quantitation, 636*
field uniformity, 363
field uniformity correction, effect of spatial distribution, 252
Fourier multiaperture emission tomography, 986
gray scale optimization, 57, 996, 997, 1215, 1216
history, 563
kidney clearance during renography, 630*
large-field-of-view, Ta-178 imaging, 538
large-field-of-view, tomography, 50, 102, 108
linearity, effect on multi-pinhole collimator tomography, 644*
mobile, remote control computer system, 178*
quality control, book review, 811
simulator, remote data acquisition testing, 1087
spatial distortion correction, 608*
synchronous dual camera recording, heart, 911*
Cancer
see also *specific organ; Tumor*
serum ferritin radioimmunoassay, 617*
Carbon-11
-acetyl carnitine for myocardial metabolism, preparation, 662*
-aminocyclobutane carboxylic acid for tumor, preparation, distribution, imaging, in animals, 1055
-carboxyhemaglobin, brain tomography, 628*
^{11}CO inhalation, regional cerebral blood volume, 370*
-D- and -L-phenylalanine, preparation, separation, distribution, in rats, 662*
-DL-carboxyl-tryptophan for pancreas, preparation, distribution, in animals, 857
-methionine, pancreas tomography, 778
-palmitate, heart studies, 599*
receptor binding radiopharmaceuticals, 350
-RBC, cerebral blood volume, emission tomography, 328
-trytophan, preparation, 663*
-trytophan, single photon pancreas tomography, 632*
-tyrotophan, -valine, -aminocyclobutanecarboxylic acid, retroperitoneal tumor imaging, 631*
-tryptophan, -valine, pancreas tomography, 507
Carbon-14
-aminocyclobutane carboxylic acid for tumor, preparation, distribution, in animals, 1055
-aminopyrine breath test, liver disease, 686*
assay of serum angiotensin converting enzyme, 1112*
-cholic acid, biliary dynamics, in rats, 684*
-fatty acids, *M. lepraemurium* metabolism, 1218
-fatty acid, *M. tuberculosis* metabolism, 676*
-gentisic acid, effect on bone uptake of Tc-99m phosphates, 654*
-hydroxy-, -non-hydroxy-diphosphonates, in vitro bone uptake, 655*
-malic acid, radiometric assay for niacin, 419
-methionine, -phenylalanine, brain uptake, effect of L-Dopa and reserpine, in rats, 76*
serum antibiotics assay, 616*
-taurocholic acid, hepatobiliary pharmacokinetics, in vitro, 642*
-valine, vitamin B_6 radiometric assay, 676*
vitamin B_{12} and folate in food, radiometric assay, 616*
Carcinoembryonic antigen
I-131, lymph node imaging, 645*, 1243
radioimmunoassay, double antibody, 1007*
synthesis, medullary thyroid carcinoma, 813*
Cerebrospinal fluid
see also *Cisternography*
shunt evaluation, $^{99m}TcO_4^-$, 621*
Cerium-139
source, absorption-edge transmission I determination, 1286
Cerium-141
-microspheres, coronary venous bypass graft evaluation, in dogs, 1111*
-microspheres, renal blood flow, in dogs, 619*
Cervix
masses, ultrasound, CAT evaluation, 815*
Chemotherapy
antineoplastic drug, effect on *Lactobacillus casei* and serum folate radioimmunoassay, 178*
desferoxamine effect on Ga-67 citrate distribution, tumor uptake, in mice, 248
doxorubicin cardiotoxicity, 910*
gastrointestinal cancer, 1006*
intra-arterial hepatic infusion patterns, Tc-99m MAA, 675*
rubidomycin toxicity monitoring, Tc-99m pyrophosphate heart studies, 651*
testes cancer, monitoring, 467*
5-FU, arterial liver perfusion, Tc-99m S colloid, 622*
China
nuclear medicine in People's Republic, 453
Chromatography
(Ge-68)-(Ga-68) generator, 681*, 1075
I-131 iodomethylnorcholesterol, 803, 805, 806
paper, gel, Tc-99m labeled enzymes, 967
serum protein-radiopharmaceutical interactions, 682*
Tc-99m agents, Sn vs electrolytic reduction, 766
Tc-99m MDP, 791
thin layer, paper, I-131 Hippuran, 441
thin layer, Tc-99m hydroxyformylpyridine, glutamic acid complex, 39
Tl-201, 684*
Chromium-51
electron dose reduction coefficient, 277*
radiation dose to labeled neutrophils, platelets, 255
-RBC, bone marrow irradiation effects, in rabbits, 1142
-RBC, cerebral blood volume, emission tomography, 328
-RBC, GI blood loss in iron-deficiency anemia, 178*
-RBC, splenic Fc-receptor function, 813*
-RBC, spleen function in plasma exchange treatment, 814*
Cisternography
acoustic neurinoma visualization, Tc-99m HSA, 275*
acute lymphocytic cell leukemia, Tc-99m DTPA, 1110
Cobalt-57
-bleomycin, distribution in hepatoma-bearing rats, 276*
crystal size effects, 610*
Collimator
bar phantom image distortion, 260, 1100, 1315, 1316
bifocal diverging, biplane heart imaging, 651*
parallel hole, geometric response, 610*, 635*
pinhole, compared to time-coded aperture, $^{99m}TcO_4^-$ thyroid imaging, 345
pinhole, quantitative bone imaging in Perthes' disease, 170
pinhole, Ta-178 imaging, 538
rotating laminar camera, 341
rotating parallel slit, 610*
scatter response function, 608*

7-pinhole, camera linearity effect on tomography, 644*
7-pinhole, optical back projection of images, 608*
7-pinhole, tomography, 643*, 644*
Compton scatter
effects, emission transaxial tomography, 608*
response function, collimated imaging, 608*
Computer
see also; *Data processing; Model*
abnormality rating systems, 364
analysis of hepatobiliary studies, 686*
automatic ROC curves, 609*
code, radiation dose from filled syringes, 882
ECG gated probe system, 610*
liver mass estimation from gamma camera images, 144
LVEF determination, 484
methods, book review, 907
portable, 666*
precision display techniques, 607*
program, four chamber behavior from gated cardiac data, 665*
program, quantitation of energy resolution improvement effects, 635*
radiopharmaceutical bibliography, 607*
remote control, 178*
remote data acquisition testing, 1087
-rotating laminar camera system, 341
Tl-201 myocardial perfusion analysis, 771
Z-axis modulation improvement, 789
Congenital
adrenal hyperplasia, I-131 iodomethylnorcholesterol imaging, 622*
lung anomalies, Xe-133 ventilation, perfusion, in children, 638*
Copper-62
regional myocardial blood flow, positron tomography, in dogs, 648*
Copper-64
kinetics, Wilson's disease, 679*, 1323*
Copyright
policy, editorial, 83
Cortisol
assays, precision, 617*
metabolic clearance rate, 587*
Creatinine phosphokinase
depletion, myocardial infarct quantitation, in dogs, 224
Crystal
bismuth germanate, properties, 1279
scintillation camera, size comparison, 610*
scintillation camera, thickness effects, 977, 992
Data processing
see also *Computer; Model*
attenuation compensation, single photon tomography, 658*
background activity algorithm Tl-201 myocardial imaging, 1294, 1312
background correction, 578, 643*
biexponential curve fitting algorithm, 614*
blur reduction vs photon count, 658*
border definition, 642*, 643*
calculation of image information, 609*
cardiac output, automated program, 1301
cardiac ventricular pressure from time-activity curve, 648*
collimator transfer function, 610*
deconvolution analysis, 502, 568
digital images, adaptive filter, 665*
Fourier multiaperture emission tomography, 986
Ga-67 citrate tumor imaging, 614*
gated regional spirometry, 620*
liver image inhomogeneity measurement, 665*
liver image motion correction, 733, 802, 803
liver image processing, 586*
mean transit time difference, cerebral anastomosis, 611*
myocardial asynchrony, regional, 667*
myocardial equilibrium studies, gate synchronization, 807
myocardial extrinsic motion analysis, 657*
myocardial studies, 3D Fourier filtering, 658*
myocardial, synchronous dual camera recordings, 911*
myocardial, visualization of mechanical systole, 625*
noise propagation, positron tomography, 609*
off-plane blurring correction, 1194
optical back projection of 7-pinhole collimator images, 608*
paradox image, left ventricular dyskinesis, 661*
radioactive decay, pocket calculator, 1317
remote control computer, 178*
renal functional imaging, 657*
renal functional mapping, 657*
scatter response function, 608*
scintillation camera spatial distortion correction, 608*
simultaneous multiplane deconvolution in focal plane tomography, 666*
spleen-to-liver colloid uptake ratio, 149
whole-body quantitative distribution scanning, 628*
ventilation-perfusion mismatch algorithm, 613*
Deadtime
correction, radionuclide angiocardiography, 168
scintillation camera, crystal size effects, 610*
Departmental operations
computerized radiopharmaceutical bibliography, 607*
cost-effectiveness, book review, 1320
department design, 1093
Detector
bismuth germanate properties, 1279
coded aperture, emission tomography, 986
crystal size comparison, 610*
crystal thickness effects, scintillation camera, 977, 992
multi-, germanium, 629*
one-dimensional, digital camera, 628*
proportional gas chamber, 335
semiconductor, rotating computerized laminar camera, 341
time-coded aperture, thyroid imaging, 345
Digoxin
assay, precision, 617*
radioimmunoassay, stat procedure, 664*
Display
gray scale optimization, 57, 996, 997, 1215, 1216
precision computer, 607*
DMSA see *Technetium-99m, DMSA*
L-dopa
effect on pancreas uptake of Se-75 selenomethionine, in animals, 543
urinary excretion in melanoma, RIA, 664*
Dopamine
urinary excretion in melanoma, RIA, 664*
Drug effects
abuse, radioimmunoassay of hair, 748, 796
antithyroid, I-131 therapy, toxic diffuse goiter, 624*
cholinergic, GI transit and clearance of Tc-99m S colloid, 685*
nitroglycerine, cardiac function, 639*, 666*
nitroprusside, cardiac function, 640*
pancreas uptake of Se-75 selenomethionine, in animals, 543
propanolol, cardiac function, 639*
serum free thyroxine, 627*
DTPA
see also *Indium-111; Indium-113m; Technetium-99m*
Zn-, Ca-, decorporation of actinides, 73
Electrophoresis
Tc valence, 871

Enzyme
assay, prostatic acid phosphatase, 664*, 909*, 1222*
myeloperoxidase, Br-77 protein labeling, 663*
-radioimmunoassay, L-dopa, dopamine, 3-O-methyldopamine, 664*
radiotracer classification, 364
serum angiotensin converting, assay, in sarcoidosis, 1112*
SGOT, LDH, CPK, perioperative myocardial infarct, 711
synthesis, C-11 acetyl carnitine, 662*
Tc-99m bovin thrombin and streptokinase-activated plasmin, preparation, 967
Estrogen
derivatives, receptor binding radiopharmaceuticals, 350
Extremities
electrical trauma, Tc-99m pyrophosphate muscle imaging, 646*, 1322*
foot, diabetes, three phase bone imaging, 602*
forearm, venous volume changes, Tc-99m RBC imaging, 633*
hand, neutron activation analysis, Ca in osteoporosis, 85
ischemic ulcer perfusion, Tl-201, 634*
legs, false-positive I-131 fibrinogen study, dermatitis, 808
legs, nuclear magnetic resonance, in rat, 178*
legs, Tc-99m heparin imaging, 652*
leg, Tl-201 perfusion imaging, 634*, 1005*
legs, transverse section perfusion imaging, $C^{15}O_2$ inhalation, 619*
legs, venous blood flow, tourniquet effects, Tc-99m MAA, 639*
reimplanted digits, $^{99m}TcO_4^-$ angiography, 674*
Tc-99m angiography, 652*
Tc-99m microsphere venography, 291
thrombophlebitis, I-123 fibrinogen imaging, radiopaque venography, 633*
Eye
glaucoma visualization, ultrasound, 277*
melanoma, hemangioma, P-32 uptake, 1322*
orbit anatomy, book review, 908
quantitative lacrimal scintigraphy, 586*
radiation protection, lenses, 898
Fatty acids see *Carbon-11; Carbon-14; Fluorine-18*
Federation of American Societies of Radiological Sciences, 581, 1318
Ferritin
serum, in malignancy, RIA, 617*
Fetus
see also *Pregnancy*
breathing, movement dynamics, ultrasound, 815*
death diagnosis, ultrasound, 372*
growth, ultrasound, 1323*, 1324*
kidney, ultrasound, radiography, 1008*
Fibrinogen see *Iodine-123; Iodine-125; Technetium-99m*
Flood field see *Camera, scintillation; Quality Control*
Fluorescence scanning
compared with absorption-edge transmission measurements, 1286
Fluorine-18
deoxyfluoromannose, preparation, metabolism, 672*
-fluorodeoxyglucose, head and heart tomography, in dogs, 606*
-fluorodeoxyglucose, mapping functional brain activity, 612*
-fluorodeoxyglucose, myocardial metabolic rate, in rabbits, 648*
-fluoroethanol, carrier free preparation, 663*
-fluorouracil, pharmacokinetic model, 614*
-fluorouracil, tumor imaging, 645*
-glucose analog, tumor uptake, imaging, in animals, 662*
-haloperidol, preparation, 671*
heart imaging, infarct, in dogs, 1013
kinetics, 5 compartment model, in rats, 1150
-long chain fatty acids for heart and liver, preparation, distribution, in animals, 1170
pharmacokinetics, model, 614*
Fluorine-19
nuclear magnetic resonance heart imaging, in dogs, 604*
Folate
assay, precision, 617*
in food, radiometric assay, 616*
FWHM see *Resolution*
Gallbladder see *Hepatobiliary System*
Gallium-67
binding glycoprotein, rat hepatoma, 682*
dermatomyositis imaging, 1323*
electron dose reduction coefficient, 277*
emission computed tomography, whole-body, 108
-liposomes, preparation, distribution, in mice, 680*
radiation dose to labeled neutrophils, platelets, 255
Gallium-67, citrate
abscess imaging, 469*, 577, 601*, 1221*
abscess-inflammation differentiation, 215
abscess uptake mechanism, 672*
aspergilloma uptake, in lung, 900
biodistribution, effects of fasting, irradiation, in rats, 938
bone scanning, complementary bone marrow scanning, 602*
bone scanning, osteomyelitis, in rabbits, 647*
bone uptake, leukemia, 854
EMT-6 sarcoma uptake, transferrin-mediated, 837, 843
extrapulmonary tuberculosis scanning, 833
heart imaging, cardiomyopathy, 604*
imaging, Crohn's disease, 213, 903
infection, kinetics, in rabbits, 660*
infection scanning, disc-space, 601*, 1006*
inflammatory bowel disease scanning, 1110*
inflammatory lesion uptake mechanism, 173
kidney transplant imaging, 207, 630*
liver uptake, subcellular, 456, 457
lung imaging, mycosis fungoides, 240
lung uptake, diffuse, 674*
mediastinal metastases evaluation, 814*
multiple chemodectoma imaging, 904
multiple myeloma imaging, 647*
neurofibromatosis scanning, 275*
radiation dosimetry, in children, 637*
retroperitoneal fibrosis tomographic scanning, 238
starch granulomatous disease, abdominal image, 902
subtraction scanning, Hodgkin's lymphoma, 1006*
tuberculous peritonitis scanning, 1111*
tumor imaging compared to CAT, 1110*
tumor imaging, lung cancer staging, 177*, 644*, 645*
tumor imaging, pharmacokinetic, 614*
tumor studies, pediatric, 75*, 210
tumor uptake, carrier effect, in rats, 656*
tumor uptake, desferoxamine effect, on mice, 248
tumor uptake, iron deficiency effect, in rats, 243
tumor uptake, lactoferrin content, 424
tumor uptake mechanism, 655*, 672*
tumor uptake parameters, liver cell carcinoma, 632*
tumor uptake, tumor pH effects, 655*
uptake, effect of capillary permeability, Fe binding proteins, in rabbits, 660*
Gallium-68
-albumin, -microspheres, preparation, 428
generators, 681*, 1075
-microspheres, preparation, distribution, in rats, 1112*
solvent extractor, 682*
Gastrin
I-123, distribution, metabolism, in rats, 813*
radioimmunoassay, 617*
Gastrointestinal tract
bleeding, Tc-99m RBC evaluation, 631*, 1080
bleeding, Tc-99m S colloid imaging, 632*
blood loss estimation, Cr-51 RBC, 178*

bowel, inflammation, Ga-67 citrate scanning, 1110*
bowel localization of bone agents, 622*
cancer, chemotherapy, 1006*
cancer, metastatic to liver, scanning, CEA RIA, 232
cancer, F-18 fluorouracil imaging, 645*
clearance, transit, cholinergic effects, Tc-99m S colloid imaging, 685*
Crohn's disease, Ga-67 citrate imaging, 213, 903
enterogastric reflux quantitation, 632*
gastric emptying, gallbladder emptying, dual In-111 DTPA, Tc-99m HIDA, 621*
gastric emptying, In-113m DTPA, Tc-99m, 268, 269
gastrin radioimmunoassay, 617*
gastroesophageal reflux, acid reflux test, 636*
gastroesophageal reflux, alginic acid compound effects, 1023
gastroesophageal reflux, dynamic Tc-99m S colloid imaging, in children, 636*, 637*
gastroesophageal reflux, pulmonary aspiration detection, Tc-99m S colloid, in children, 680*
imaging, Meckel's diverticulum, $^{99m}TcO_4^-$, 586*, 888
infarct, Tc-99m HEDP imaging, in children, 1006*
lesions, on Tc-99m HIDA hepatobiliary studies, 679*
stomach uptake, Ga-67 citrate, 577
stomach uptake, Tc-99m MDP bone imaging, 791
Tc-99m transport in mice, model, 606*

Generator
(Fe-52)-(Mn-52m), 682*
(Ge-68)-(Ga-68), 681*, 1075
(Sr-82)-(Rb-82), 684*

Germanium-68
Ga-68 generator, 681*, 1075
Ga-68 solvent extractor, 682*

Glucose
see also *Fluorine-18*
metabolism rate measurement, brain and heart, 605*

Gold-195
crystal size effects, 610*

Gold-198
colloid, lymph node imaging, 467*
colloid, lymph node uptake parameters, in rabbits, 1038
lymph drainage distribution, 814*

Gynecology
see also *Ovary; Pregnancy*
oncology, book review, 175

Heart
arrhythmia, left ventricular function monitoring, 669*
bundle branch block, 625*
C-11 acetyl carnitine preparation, 662*
calcification, Tc-99m pyrophosphate uptake, 178*
contusion, Tc-99m scanning, 371*
cooperative studies, 377
damaged myocardium, Ca-45, Ca-47, Tc-99m PPi uptake, in rats, 650*
disease, diagnosed from hepatobiliary studies, 679*
ECG gated probe system, 610*
F-18 deoxyfluoromannose, preparation, metabolism, 672*
F-18 fluorodeoxyglucose myocardial metabolism rate, in rabbits, 648*
F-18 long chain fatty acids, preparation, regional metabolism, in mice, 1170
fetal, motion, ultrasound, 1324*
Ga-68 microspheres uptake, in rats, 1112*
H-3 dihydroalprenolol uptake, in dogs, 683*
H-3 methylquinuclidinyl benzilate, preparation, distribution, in animals, 671*
H-3 muscarinic acetylcholine receptor antagonists, distribution, in animals, 865
intracardiac thrombi, I-123 fibrinogen detection, in dogs, 604*
iodinated acetylcholinesterase preparation, distribution, in mice, 671*
mechanical systole onset visualization, 625*
myopericarditis, Tc-99m pyrophosphate uptake, in mice, 1047
nuclear cardiology, book review, 465, 1107
nuclear magnetic resonance imaging, in dogs, 604*
pacemaker rate optimization, Tc-99m RBC, 660*
pericardial effusion, Tc-99m phosphate accumulation, 392, 1102
phantom, dynamic, 547, 610*
phantom, heterogeneous, 607*
regional asynchrony measurement, 667*
reversible left ventricular dysfunction, 662*
right ventricular response to exercise, in left ventricular abnormalities, 624*
single pass extraction of N-13 ammonia, in dogs, 648*
Tl-201 uptake, isolated rat tissue, rest and exercise effects, 1136
transplant, effect of Pd-109 hematoporphyrin therapy, in rats, 659*
ultrasound studies, 651*
ventricular pressure measurement, Tc-99m HSA, RBC, 648*
ventricular volume determination, 625*, 639*, 649*, 661*, 667*, 668*, 669*
volume, edge finding algorithm, 643*

Heart, blood flow
see also *Heart, LVEF; Heart, RVEF*
aneurysm, left ventricular, 720, 851
arrhythmia, 669*
cardiac transit index, 670*
coronary venous bypass graft evaluation, Ce-141 microspheres, in dogs, 1111*
deadtime correction, 168
effect of AVF between internal iliac vessels, Tc-99m RBC, 36
ejection fraction, isometric and dynamic exercise, 668*, 669*
ejection fraction, regional, $^{99m}TcO_4^-$ angiography, 724
ejection fraction, Tc-99m HSA ventriculography, 370*
first-third ejection fraction, 666*
four chamber global and regional, computer program, 665*
intra-pulmonary shunt quantification, Tc-99m MAA angiography, 670*
left-to-right shunt quantitation, deconvolution analysis, in dogs, 502
left ventricular function, first-pass studies, 666*
left ventricular peak ejection rate, filling rate, effect of frame rate, 189
left ventricular regurgitant fraction, first pass Tc-99m, HSA, 668*
left ventricular systolic ejection rate, Tc-99m RBA, 1, 997
N-13 ammonia, in dogs, 603*
output, atrial pacing, in ischemia, 668*
output, computer program, 1301
output, post-surgery function, Tc-99m HSA, in children, 661*
regional, positron tomography, Cu-62, in dogs, 648*
right-to-left shunt quantitation, 670*
right ventricular function, first pass equilibrium and list mode methods, Tc-99m RBC, 668*
rubidomycin toxicity monitoring, Tc-99m RBC, 651*
valvular regurgitation, 626*, 670*

Heart, coronary disease
Bayesian analysis of multiple testing, 651*
cardiac transit at rest, 670*
cold pressor test, 640*
comparison of radionuclide and contrast ventriculography, 640*, 641*, 651*
comparison of Tl-201 imaging to exercise ECG, 661*
comparison of Tl-201 rest and exercise, radionuclide ventriculography, 687*

drug effects, 1, 639*
extent, Tl-201 imaging, 715
first pass studies, 626*, 651*, 666*, 668*, 670*, 851
global ventricular function, 370*
isometric vs dynamic exercise studies, 668*, 669*
N-13 tomography, 604*
rest and exercise radioangiography, 484, 491, 649*, 724
left ventricular dV/dt, 1, 997
left ventricular exercise studies, 275*
left ventricular function, rest and exercise, 639*, 687*
left ventricular peak ejection rate, 189
left ventricular volume, 661*
LVEF, 1, 189, 484, 624*, 625*, 639*, 649*, 667*, 670*, 724
LVEF, early third, 667*
radionuclide ventriculography, effects of amount of exercise, 687*
right and left ventricular exercise studies, 624*, 625*
RVEF, 624*, 625*, 666*, 724
spasm, 900
Tl-201 exercise imaging, 649*, 688*, 715, 771
Tl-201 left ventricular function, 275*, 687*
Tl-201 redistribution, 477, 649*, 650*, 687*, 688*
Tl-201 rest imaging, 771, 1005*
Tl-201 studies, clinical role, 1201, 1206
volume, rest and exercise, 649*
wall motion, 626*, 640*, 649*, 661*, 668*, 669*, 670*, 724

Heart imaging
adaptive filter for digital image processing, 665*
aortocoronary saphenous bypass surgery evaluation, 576
blood pool background, 496, 1294, 1312
compared to radiographic techniques, 1237
comparison of Tc-99m HSA and in vivo labeled RBC, 1214
exercise, St-vector orientation, perfusion defects, Tl-201, 275*
Ga-67 citrate, inflammation, 604*
gating, 658*, 807
I-123 heptadecanoic acid, 650*
in coronary disease see *Heart, coronary disease*
in infarct see *Heart, infarct*
in vivo labeled Tc-99m RBC, 877, 1214, 1220*
motion analysis, extrinsic, 657*
motion reduction, photon count exchange, 658*
multi-gated blood pool, atrial pacing, in ischemia, Tc-99m RBC, 668*
muscular dystrophy, Tc-99m pyrophosphate, in children, 1321
N-13 ammonia, scatter fraction, 635*
N-13 glutamate, 663*
paradox, left ventricular dyskinesis, 661*, 1237
persistently positive, Tc-99m pyrophosphate, 895
portable computer, 666*
rubidomycin toxicity monitoring, Tc-99m pyrophosphate, 651*
Tl-201, absence of myocardial uptake, 900
Tl-201, book review, 273
Tl-201, clinical role, 1201, 1206
Tl-201, compared to Q-ST and R wave changes, 661*
Tl-201, computer analysis, 771
Tl-201, exercise, correlated with coronary arteriograms, maximal exercise test, 275*
Tl-201 exercise, lung uptake, 649*
Tl-201 fibrosis, 1103
Tl-201, ischemia, *1201*
Tl-201 redistribution, 477, 649*, 650*, 688*, 1201
Tl-201, rest and exercise, compared to radionuclide ventriculography, 687*
Tl-201, *left lateral views*, *183*
Tl-201, left ventricular hypertrophy, 585*
3D Fourier filtering, *658**

Heart, infarct
acute, emission-computed tomography, Tc-99m pyrophosphate, in dogs, 50
anterior, inferior and transmural, LVEF and wall motion, 177*
assessment, ultrasound and radionuclide ventriculography, 600*
diagnosis, teaching editorial, 165
equilibrium radionuclide angiography, 669*
false left ventricular aneurysm, first pass $^{99m}TcO_4^-$, 851
In-111 DTPA-antimosin FAB fragment imaging, in dogs, 605*
Mn-52m positron tomography, in dogs, 648*
mobile camera imaging, comparison of Tc-99m phosphates, 1220*
nontransmural, Tc-99m pyrophosphate imaging, 585*
perioperative, evaluation, 275*, 711
positron tomography, F-18, in dogs, 1013
quantitation, Tc-99m pyrophosphate accretion, CPK depletion, autopsy, in dogs, 224
quantitative radionuclide ventriculography, 666*
serum myoglobin radioimmunoassay, 115, 120, 165, 664*
Tc-99m MDP imaging, 402
Tc-99m pyrophosphate imaging, 402, 468*, 496, 660*, 711, 895, 1111*
uptake of Tl-201, Tc-99m pyrophosphate, blood flow effects, in dogs, 650*
Tl-201 imaging, 1201
Tl-201 redistribution, 649*
Tl-201 transaxial computed tomography, 736
ventricular performance, nitroprusside effect, 640*

Heart, LVEF
arrhythmia, 669*
background correction, 643*
bifocal diverging collimator, 651*
border definition, 642*, 643*
cold pressor test, Tc-99m MUGA, 640*
compared to left ventricular systolic ejection rate, 1, 997
comparison of ultrasound, radionuclide and contrast studies, 651*
cystic fibrosis, Tc-99m HSA, in children, 637*
drug effects, 1, 639*, 640*, 910*
effect on right ventricular performance, 642*
equilibrium radionuclide angiography, 484, 491, 626*, 666*, 669*, 807, 1220*
exercise, in coronary disease, 1, 624*, 625*, 639*
first-pass radionuclide angiography, 626*, 651*, 666*
framing rate effects, 189
in chronic pulmonary disease, gated radioangiography, 669*
infarct, 177*, 649*
in paradoxical pulses, 1005*
pacemaker rate optimization, Tc-99m RBC, 660*
regional, radionuclide and contrast studies, 1220*
rest and exercise, in coronary disease, 1, 624*, 625*, 626*, 639*, 649*
rest and exercise, in mitral valve prolapse, Tc-99m RBC, 640*
rest, coronary disease, 667*, 670*
reversible left dysfunction, 662*
tomographic, 628*

Heart, RVEF
effect of left ventricular performance, 624*
in chronic obstructive pulmonary disease, 276*, 669*
in coronary disease, 624*, 625*
in cystic fibrosis, in children, 637*
in paradoxical pulses, 1005*
method comparison, 666*
rapid multiple gated equilibrium, Tc-99m RBC, 666*
tomographic, 628*

Heart, tomography
C-11 palmitate, 599*
emission computed, Tl-201, Tc-99m RBC, pyrophosphate, 108

F-18 fluorodeoxyglucose, in dogs, 606*
F-18, infarct, in dogs, 1013
gated, feasibility, 628*
glucose metabolism rate, 605*
Mn-52m, in dogs, 648*
positron, coronary artery disease, N-13 ammonia, 604*
positron, Rb-82, 603*
radionuclide, clinical role, 1206
radionuclide, multiple gated, 644*
seven pinhole collimator, 643, 644**
synchronous, dual camera recording, 911*
transaxial emission computed, Tl-201, infarct, 736
Heart, wall motion
background correction, 643*
bifocal diverging collimator, 651*
cold pressor test, Tc-99m, 640*
comparison of ultrasound, radionuclide and contrast studies, 651*
coronary disease, 626*, 640*, 649*, 661*, 668*, 669*, 670*, 724
exercise, nitroglycerine effects, Tc-99m RBC, 666*
*gated equilibrium Tc-99m angiography, 1216**
infarct, 177*, 649*
*in mitral valve prolapse, Tc-99m RBC, 640**
isometric and dynamic exercise effects, 668*, 669*
*monitoring rubidomycin toxicity, 651**
nitroprusside effects, Tc-99m RBC, 640*
radionuclide and contrast ventriculography, 640*, 641*
rest and exercise, 626*, 640*, 649*, 661*
rest, cardiac transit index, in coronary disease, 670*
reversible left ventricular dysfunction, 662*
tomographic, 628*
Hepatobiliary system
bile acids, radioimmunoassay, 676*
comparison of Tc-99m diethyl-IDA, Tc-99m PIPIDA studies, 686*
complementary imaging and ultrasound, 600*
computer analysis of studies, 686*
*cystic duct patency, CCK, I-131 rose bengal, 686**
enterogastric reflux quantitation, 632*
*gallbladder, gastric emptying, dual In-111 DTPA, Tc-99m HIDA, 621**
gallbladder imaging, liver retention effects, 171
gallbladder motor function, Tc-99m HIDA imaging, 632*
gallbladder uptake of bone agents, 622*
imaging, Tc-99m PIPIDA, in children, 680*
in vitro model, radiopharmacokinetics, 642*
jaundice evaluation, Tc-99m PIPIDA, Tc-99m S colloid, 600*
jaundice, Tc-99m diethyl-IDA studies, 685*
neonatal jaundice, Tc-99m parabutyl-IDA, I-131 rose bengal studies, 637*
pharmacokinetics of Tc-99m pyridoxylidene glutamate, HIDA, I-131 rose bengal, in rats, 45
*post-operative studies, Tc-99m HIDA, 686**
radiation dosimetry, Tc-99m PIPIDA studies, 607*
radiography, book review, 1214
Ru-103 HIDA, Ru-97 HIDA studies, in animals, 682*
Se-75 cholic acid analogs, dynamics, in rats, 684*
studies, teaching editorial, 358
Tc-99m diethyl-IDA, I-131 rose bengal studies, liver transplant, 314
Tc-99m HIDA clearance, bilirubin effects, in dogs, 310
Tc-99m HIDA clearance, sulfobromophthalein effects, in rats, 468*
Tc-99m HIDA studies, non-biliary abnormalities, 679*
Tc-99m hydroxyformylpyrine, glutamic acid complex, preparation, evaluation, in rabbits, 39
Tc-99m pyridoxylideneglutamate imaging, 468*
Tc-99m (Sn)pyridoxylideneisoleucine, labeling and storage effects, 1189
transport mechanism, Tc-99m diethyl-IDA, in rats, 642*
transport mechanism, Tc-99m HIDA, pyridoxyldeneisoleucine, in rats, 642*
traumatic hemorrhage diagnosis, 1112*
ultrasound, cholecystography correlation, 179*
ultrasound, gallbladder wall thickness, 1112*
ultrasound, gallstones, 179*
*ultrasound, pericholecystic abscess, 911**
Hilum
*Ga-67 citrate uptake, lung cancer staging, 645**
History
Anger scintillation camera, 563
editorial, 475
nuclear medicine, 560, 561
Hormone
assays, book review, 1214
gastrin radioimmunoassay, 617*
growth, effect on pancreas uptake of Se-75 selenomethionine, in animals, 543
growth, therapy effect on metaphyseal uptake of Tc-99m MDP, in children, 678*
I-123 gastrin, distribution and metabolism, in rats, 813*
I-131 human chorionic gonadotropin, ovary imaging, in rats, 941
in breast cancer, book review, 1319
*pretreatment regimen, effect on P-32 bone uptake, in rabbits, 684**
Hydrogen-3
-cortisol, metabolic clearance rate, 587*
*-dihydroalprenolol, myocardial uptake, in dogs, 683**
-methylquinuclidinyl benzilate for heart, preparation, distribution, in animals, 671*
-muscarinic acetylcholine receptor antagonist for heart, distribution, in animals, 865
receptor binding radiopharmaceuticals, 350
scintillation-proximity assay, antigen-antibody binding kinetics, 1062
Hyperthermia
cancer therapy, book review, 1214
Hypothalamus
effect on pancreas uptake of Se-75 selenomethionine, in animals, 543
ICRM
life sciences working group, 998
Image processing see *Data processing*
Immunology
see also *Antibody; Antigen; Radioimmunoassay*
Pd-109 hematoporphyrin therapy in heart allograft, in rats, 659*
quantitation of passive cutaneous anaphylaxis, 587*
serum ferritin in malignancy, 617*
Indium-111
-chloride, bone marrow imaging, aplastic anemia, 603*
-conjugated chelate-protein, blood clearance, in rats, 656*
*-DTPA, alveolocapillary permeability in septic pulmonary edema, 612**
*-DTPA-antimosin FAB fragments, myocardial infarct imaging, in dogs, 605**
*-DTPA, gastric imaging, 621**
-DTPA, pharmacokinetics, in dogs, 1273
*electron dose reduction coefficient, 277**
-hydroxyquinoline, autologous platelet labeling, 524
*-leukocytes, whole-body scanning, inflammatory disease, 659**
-lymphocytes, recirculation, 169
-oxine, platelet labeling mechanism, 659*
-oxine-autologous platelets, radiation dosimetry, 685*
-oxine-liposomes, preparation, distribution, in mice, 434

-oxine, lymphocyte and tumor cell labeling, cell damage, 1308
-oxine-polymorphonuclear leukocytes, labeling effects, 741
-platelets, coronary artery bypass graft deposition, in dogs, 604*
-platelets, stability, 459, 460
radiation dose to labeled neutrophils, platelets, 255
serum incubated, inflammatory lesion uptake, in rabbits, 173

Indium-113m
-DTPA, gastric emptying, 268, 269
electron dose reduction coefficient, 277*

Infection
abdominal cystic lesions, ultrasound, 179*
aspergilloma, Ga-67 citrate image, 900
brain lesion, Tc-99m glucoheptonate imaging, 287
cyst, liver ultrasonography, 179*
disc-space, in animals, 601*, 1006*
hepatitis-B-core antigen antibody radioimmunoassay, 467*, 676*
hip prosthesis, bone scanning, 75*, 602*
myopericarditis, uptake of Tc-99m pyrophosphate, in mice, 1047
neck abscess, thyroid studies, 1051
osteomyelitis, Ga-67 citrate, Tc-99m MDP scanning, 647*
Rhizopus osteomyelitis, Tc-99m pyrophosphate scan, 75*
Staphylococcus aureus, radioimmunoassay, in rabbits, 813*
subcutaneous, Ga-67 citrate kinetics, in rabbits, 660*
tuberculosis, extrapulmonary, Ga-67 citrate scanning, 833, 1111*
viral, cell culture, transferrin receptors, 672*

Inflammation
ankylosis spondylitis, Ra-224 therapy, book review, 175
bowel, Ga-67 citrate scanning, 1110*
cardiomyopathy, Ga-67 citrate imaging, 604*
diagnosis, In-111 leukocyte scanning, 659*
Ga-67 citrate uptake mechanism, 173, 660*
muscle, Tc-99m pyrophosphate uptake, 469*
osteitis, Tc-99m phosphate bone scanning, 910*
pelvic peritoneum, ultrasound, 372*
sclerosing panencephalitis, Tc-99m DTPA imaging, CAT scanning, 1221*
submucosal, endobronchial lymph node imaging, 467*

In memoriam
Asa E. Seeds, M.D., 573, 575

Insulin
allergy, IgG and IgE antibody radioassay, 673*
assay, precision, 617*
radioimmunoassay kit evaluation, 813*
whole-body receptor compartment, in vivo measurement, 605*

Iodine
labeling parameters, 616*
stable, absorption-edge transmission determination, 1286

Iodine-123
-fibrinogen, intracardiac thrombi detection, in dogs, 604*
-fibrinogen, kidney transplant rejection diagnosis, 619*
-fibrinogen, thrombophlebitis imaging, 633*
-fibrinogen, tumor imaging, 645*
-gastrin, distribution, metabolism, in rats, 813*
-heptadecanoic acid, heart metabolism, imaging, 650*
-Hippuran, renal functional mapping, atrial lesions, in dogs, 657*
-Hippuran, renography, 619*, 657*
-methyltyrosine for pancreas, preparation, distribution, in mice, 973
nuclear decay data, 1212
parathyroid adenoma scan, 270
thyroid imaging, discrepant $^{99m}TcO_4^-$ images, 678*
-vasopressin, kidney uptake, in animals, 657*

Iodine-125
albumin, alveolocapillary permeability in septic pulmonary adema, 612*
-albumin, distribution in hepatoma-bearing rats, 276*
-albumin, first-pass and equilibrium characteristics, in dogs, 654*
-albumin, quantitation of passive cutaneous anaphylaxis, 587*
-antiadrenergic agents for adrenal medulla, distribution, in dogs, 155
-cobra venom, distribution, in mice, 655*
-fibrinogen, coronary artery bypass graft uptake, in dogs, 604*
-fibrinogen, deep vein thrombosis uptake, compared to Tc-99m plasmin, 633*
-fibrinogen, thrombophlebitis detection, false-positive, in allergy, 808
-Hippuran, renogram, chlorpromazine pretreatment, ischemia, in rabbits, 18
-hydroxybenzolpindolol, beta receptor occupancy, in animals, 681*
-insulin, whole-body insulin receptor measurement, 605*
-microspheres, renal blood flow, in dogs, 619*
-nucleic acids, preparation, distribution, tumor uptake, in animals, 785
photon absorptiometry, bone density, 911*
receptor binding radiopharmaceuticals, 350
serum myoglobin radioimmunoassay, 115, 120, 165
therapy, thyrotoxicosis, 815*
thyroid scanning, compared to $^{99m}TcO_4^-$, 909*
-thyroxine, microencapsulated anti-T_4, preparation, radioimmunoassay, 956
-transferrin, cell culture binding, effect of virus, 672*
-transferrin, tumor uptake mechanism, 672*
-tyrosine, autoirradiation, 616*

Iodine-131
airborne contamination, 362, 363, 995
-antiadrenergic agent, adrenal medulla imaging, in dogs, 155
-carcinoembryonic antigen, lymph node metastases imaging, 645*, 1243
distribution, diagnostic and thyroablative doses, 92, 1099, 1100
-Hippuran, in vitro stability, 441
-Hippuran, kidney studies see *Kidney*
-Hippuran, serum protein interactions, 682*
-human chorionic gonadotropin, ovary imaging, in rats, 941
-iodobenzylguanidine, preparation, adrenal imaging, in animals, 681*
-iodomethylnorcholesterol, adrenal imaging see *Adrenal gland*
-iodomethylnorcholesterol, gonadal tumor uptake, 307, 677*, 1322*
-iodomethylnorcholesterol, RES distributing impurity, 803, 805, 806
-MAA, lung perfusion, in dogs, 950
-methyltyrosine for pancreas, preparation, distribution, in mice, 973
-nucleic acids, preparation, distribution, tumor uptake, in animals, 785
perspiration excretion, 469*
-proinsulin, whole-body insulin receptor measurement, 605*
receptor binding radiopharmaceuticals, 350
-rose bengal see *Hepatobiliary system*
serum myoglobin radioimmunoassay, 371*
thyroid therapy see *Thyroid therapy*
-tyrosine derivatives, adrenal medulla and melanoma uptake, in animals, 1221*

Iridium-192
Compton scatter tomography, 911*

Iron
deficiency, effect on Ga-67 citrate distribution, tumor uptake, in rats, 243

Iron-52
bone marrow imaging, 675*
-Mn-52m generator, 682*

Joints
arthritis, Ra-224 therapy, book review, 175
arthritis, rheumatoid, Tc-99m pyrophosphate imaging and radiography, 467*
arthritis, Tc-99m pyrophosphate, $^{99m}TcO_4^-$ uptake, in rabbits, 673*
bone scanning in idiopathic regional migratory osteoporosis, 1268
femoral head, quantitative bone imaging, 170
hip prosthesis, bone scanning, 75, 602**
imaging, Perthes' disease, 75*, 170
knees, dynamic bone study, *migratory osteolysis, 129*
temperomandibular, disease diagnosis, 603*
Kidney
C-11 D- and L-phenylalanine, preparation, separation, distribution, in rats, 662*
chronic dialysis, pulmonary calcification, imaging, Tc-99m HEDP, 201
clearance measurement, simultaneous renography, 630*
differential function, Tc-99m DMSA, DTPA, I-131 Hippuran, ureteral catheterization, 631*
differential function, Tc-99m DMSA, in dogs, 63
disease, in hepatobiliary studies, 679*
emission computed tomography, Tc-99m, 108
extraction efficiency, Tc-99m agents, I-131 Hippuran, Hg-197 chlormerodrin, in dogs, 629*
failure, urinary renin radioimmunoassay, 77*
Ga-68 microspheres uptake, in rats, 1112*
GFR, determination, absorption-edge transmission in dogs, 1286
GFR, in acute tubular necrosis, Tc-99m DTPA, in rats, 630*
GFR measurement, iothalamate, Tc-99m DMSA, Tc-99m DTPA, in dogs, 630*
hippurate clearance, biexponential curve fitting algorithm, 614*
I-123 vasopressin uptake, in animals, 657*
ischemia, effect of chlorpromazine pretreatments, in rabbits, 18
orthostatic hypertension evaluation, 461, 462
osteodystrophy, bone scanning, 467*, 602*
Tc-99m cyclam clearance, in animals, 641*
Tc-99m tetradentate ligand clearance, in animals, 641*
uptake of Tc-99m MDP, post radiation therapy, 32
urolithiasis evaluation, 371*
Kidney, blood flow
acute tubular necrosis diagnosis, Tc-99m DTPA, 629*
acute tubular necrosis, Tl-201, Tc-99m DTPA, in rats, 630*
arterial lesions, functional mapping, I-123 Hippuran, in dogs, 657*
comparison of Tc-99m glucoheptonate, I-131 Hippuran, 623*
effective renal plasma flow, Tc-99m DMSA, 630*
osteodystrophy, chronic hemodialysis, Tc-99m pyrophosphate, 1321*
Rb-82, in dogs, 619*
renal sinus lipomatosis, Tc-99m DTPA perfusion study, 1105
screening test, $^{99m}TcO_4^-$, 11
superior vena caval obstruction, Tc-99m glucoheptonate, 1106
Tc-99m MDP angiography, 623*
Kidney imaging
adrenal hemorrhage, neonates, Tc-99m DTPA, 521
comparison of Tc-99m glucoheptonate, I-131 Hippuran, 623*
cortical, acute pyelonephritis, Tc-99m DMSA, glucoheptonate, 623*
diuretic, pediatric hydronephrosis, Tc-99m DTPA, 623*
functional, Tc-99m DTPA, I-123 Hippuran, I-131 Hippuran, 657*
lateral scans, 909*
mass lesions, Tc-99m gluceptate, compared to IVU, 1018
obstruction detection, Tc-99m DTPA, 623*
portable computer, 666*
renovascular hypertension screening, Hg-197 chlormerodrin, 11
Tc-99m DMSA evaluation, 76*, 619*
Tc-99m methylene diphosphonate, 623*
*tumor differential diagnosis, in children, 679**
urinary extravasation with ureteral obstruction, Tc-99m DTPA, 236
urolithiasis, I-131 Hippuran, 371*
Kidney, renogram
chlorpromazine pretreatment effects, warm ischemia, in rabbits, 18
cortical, obstructive disease, 620*
differential function, comparison of I-123 Hippuran, Tc-99m DMSA, 898
*I-123 Hippuran evaluation, 619**
simultaneous clearance measurement, 630*
*ultrasound depth correction, 1007**
Kidney, transplant
avascular necrosis of the femoral head, *Tc-99m MDP scanning*, 646*
evaluation, radionuclide, teaching editorial, 1095
evaluation, $^{99m}TcO_4^-$, I-131 Hippuran, 1029, 1095
*Ga-67 citrate uptake imaging, 207, 630**
rejection diagnosis, I-123 fibrinogen, 619*
rejection, differentiation from acute tubular necrosis, Tc-99m DTPA, 629*
rejection prediction, I-131 Hippuran, 629*
osteodystrophy, bone scanning, 646*
ultrasound, 372*
vascular steal diagnosis, Tc-99m DTPA, I-131 Hippuran, 1053
Kidney, ultrasound
agenesis, uterine anomalies, 587*
chronic atrophic pyelonephritis, 1008*
complementary to nuclear medicine, 815*
depth correction, renogram, 1007*
hydronephrosis, in pregnancy, 1222*
lymphoma, 470*
parenchymal gas, 1113*
polycystic disease, with CAT, 470*
solid mass evaluation, 1007*
transitional cell carcinoma, 1113*
volume, 77*
Kit
Tc-99m DTPA, yields, 653*
Krypton-81m
blood flow, bone uptake, in dogs, 413
continuous infusion, regional cerebral blood flow, 611*
lung ventilation, 194, 613*, 638*, 639*
Lead-203
electron dose reduction coefficient, 277*
Leukocytes see also *Indium-111*
Tc-99m labeling, in vivo migration, 1197
Line spread function see *Resolution*
Liposomes
Ga-67, preparation, distribution, in mice, 680*
Tc-99m DTPA-, In-111 oxine-, preparation, distribution, in mice, 434
Liquid scintillation counting
antigen-antibody binding kinetics, 1062
container geometry, 1090
Liver
arterial blood flow, in 5-FU therapy, 622*
blood flow, intra-splenic injection, Xe-133, in dogs, 1323*
cancer, alpha-fetoprotein radioimmunoassay, 372*
cancer, Ga-67 citrate uptake parameters, 632*
cancer, Y-90 resin sphere intra-arterial radiation therapy, 674*
cirrhosis, cortisol clearance rate, 587*
colloid clearance rate, 586*
Cu-64 kinetics, Wilson's disease, 679*
disease, bile acids, radioimmunoassay, 676*

disease, C-14 aminopyrine breath test, 686*
F-18 long chain fatty acids, preparation, regional metabolism, in mice, 1170
Ga-67 citrate, subcellular uptake, 456, 457
Ga-67 liposomes, preparation, distribution, in mice, 680*
hemangioma, recurrent irradiated, 901
hepatitis, reversible functional asplenia, 34
hepatoma, Ga-67 binding glycoprotein, 682*
hepatoma, Ga-67, Mn-54 uptake, carrier effect, in rats, 656*
I-125 cobra venom distribution, in mice, 655*
In-111 oxine-, Tc-99m DTPA-liposomes, preparation, distribution, in mice, 434
metastases detection, teaching editorial, 264
metastases, intra-arterial infusion patterns, Tc-99m MAA, 675*
perfusion, post-partial hepatectomy, Tc-99m S colloid, in rats, 26
phagocytosis, proteolysis, Tc-99m albumin microparticles, 606*
radiation dose, Ga-67 citrate, in children, 637*
retention in hepatobiliary studies, 171, 686*
steatosis, Xe-133 retention, 397, 450
Ta-178 agents, preparation, distribution, imaging, in animals, 1176
Tc-99m HIDA, intracellular binding sites, 655*
Tc-99m HIDA uptake, effect of sulfobromophthalein, in rats, 468*
-to-spleen ratio of colloid uptake, 149
tomography, emission computed, Tc-99m S colloid, 108
tomography, emission computed, transmission, hematoma, in dogs, 448
tomography, single-photon, liver volume, 514
transplant, hepatobiliary studies, Tc-99m diethyl-IDA, 314
ultrasound, complementary to radionuclide methods, 601*
uptake, I-131 iodomethylnorcholesterol in adrenal imaging, 803, 805, 806

Liver imaging
clinical value, 370*
complementary to ultrasound, 601*
computer processing evaluation, 586*
differential diagnosis of tumor, in children, 679*
hematoma, compared to emission and transmission computed tomography, in dogs, 448
in breast carcinoma, 370*
inhomogeneity measurement, 665*
jaundice, 600*
mass estimation, 144
metastases, 232, 303, 644*, 814*, 1321*
motion correction, 733, 802, 803
partial Budd-Chiari syndrome, 679*
Ta-178, in animals, 538, 1176
Tc-99m methylene disphonate, 303
tumor, compared to CAT, ultrasound, 1111*

Liver, ultrasound
abscess, hematoma, gas-containing, 1113*
differential diagnosis of shadowing, 816*
fetus, 1008*
metastases, 814*
normal appearance, 816*
primary cysts, 179*

Lung
arteriovenous fistula diagnosis, 76*
blood flow distribution, pulmonary arterial pressure analysis, Xe-133, in dogs, 923
cancer, Ga-67 citrate staging, 177*, 644*, 645*
cancer staging, 1321*
chronic disease, gated cardiac radioangiography, 669*
clearance, mucociliary, Tc-99m microsphere aerosol, 613*
clearance, $^{99m}TcO_4^-$, Tc-99m DTPA aerosols, 613*
dry aerosol delivery system, 1000
Ga-67 citrate, diffuse uptake, 674*
Ga-68 microspheres uptake, in rats, 1112*
I-125 hydroxybenzolpindolol for beta receptor blockade, 681*
intrapulmonary shunt quantification, Tc-99m MAA cardiac angiography, 670*
perfusion, particle toxicity, 1098, 1099
perfusion, pulmonary embolism, isoproteronol effects, in dogs, 950
perfusion, small particle, 613*
perfusion, Ta-178, in rabbits, 538
physiology, book review, 74
pleural effusion, Tc-99m pyrophosphate accumulation, 276*
pulmonary aspiration detection, Tc-99m S colloid, in children, 636*, 637*, 680*
right-to-left shunt quantitation, 670*
septic edema, alveolocapillary permeability, I-125 HSA, In-111 DTPA, 612*
Ta-178 agents, preparation, distribution, imaging, in animals, 1176
Tl-201 uptake, stress myocardial imaging, 649*
tomography, pulmonary artery occlusion, in dogs, 601*, 1251
tomography, emission computed, Tc-99m, 108
tomography, transmission, dynamic, Tc-99m source, 665*
ultrasound, 76*
volume, quantitative gated analysis, Xe-133, 620*

Lung imaging
aspergilloma, Ga-67 citrate, 900
book review, 583
F-18 fluorouracil, in cancer, 645*
gated, ungated and cinematic, pulmonary embolism, in dogs, 407
myocosis fungoides involvement, Ga-67 citrate, 240
pulmonary artery occlusion, Tc-99m MAA, in dogs, 601*, 1251
pulmonary embolism, thrombosis, 291
uremic calcification, Tc-99m HEDP, 201

Lung, ventilation
chronic obstructive disease, Tc-99m aerosol, 620*
$C^{15}O_2$ pulmonary embolism, 281
comparison of Kr-81m and Tc-99m polystyrene aerosol, 194
comparison of Xe-127 and Xe-133, 460, 461
comparison of Xe-133 washout, single breath imaging, 917
regional delivery of radioaerosol, 272
studies in artificial ventilation, Xe-133, 613*
Xe-133 liver retention, 397, 450

Lung, ventilation-perfusion
asbestos workers, Tc-99m MAA, Xe-133, 621*
bronchial carcinoma, pre- and post-radiation therapy, 638*
bronchiectasis detection, Kr-81m, Tc-99m microspheres, in children, 638*
collapse and consolidation, Kr-81m, Tc-99m, 638*
early cancer detection, Tc-99m microspheres, Xe-133, 612*
lobectomy candidacy, Xe-133, spirometry, 1222*
mismatch, automated thresholding algorithm, 613*
order of studies, 268, 270, 578
pediatrics, 638*, 639*
pneumothorax diagnosis, 468*
pulmonary embolism, 638*, 639*, 1005*
simultaneous venography, Tc-99m MAA, 639*
ventilatory clearance methods, Xe, 703

Lymph
drainage, colloids, 645*, 814*, 905
endobronchial node imaging, radiocolloids, 467*
glands, tumor, Ga-67 citrate studies, in children, 75*
lymphocutaneous fistula, Tc-99m S colloid, 275*
metastases, in breast cancer, book review, 1319
mycosis fungoides, 240
node imaging, abdominal, mediastinal, Tc-99m S colloid, 646*
node imaging, metastases, I-131 CEA, 645*, 1243

node imaging, para-aortic, Tc-99m Sn-PO_4, in dogs, 654*
node imaging, Tc-99m SbS colloid and Sn-phytate, 585*, 933
nodes, radiocolloid uptake parameters, in rabbits, 1038
obstruction, dermal backflow, Tc-99m S colloid, 905
Lymphocytes see *Indium-111*
Macroaggregated albumin see *Iodine-131; Tantalum-178; Technetium-99m, microspheres*
Manganese-52m
generator, 682*
positron tomography, myocardial infarct, in dogs, 648*
Maganese-54
tumor uptake, carrier effect, in rats, 656*
Mediastinum
Ga-67 citrate uptake, lung cancer staging, 644*, 645*, 814*
mass, goiter, I-131 scanning, 177*
lymph node, Tc-99m S colloid imaging, 646*
Meetings
Atlanta 1979, 595
Australia, 571
poster presentations, 582
Mercury-197
-chlormerodrin, kidney imaging, 11
-chlormerodrin, renal extraction efficiency, in dogs, 629*
radiation dose to labeled neutrophils, platelets, 255
Microspheres
see also *Iodine-125; Strontium-85; Technetium-99m, microspheres*
cardiopulmonary toxicity, 899, 1098, 1099
*small, safer lung perfusion, 613**
Ta-178, preparation, distribution, liver and lung imaging, in animals, *1176*
Model
*animal, subcutaneous infection, 660**
compartmental, F-18 pharmacokinetics, 614*, 1150
compartmental, steady state distribution of $^{15}O_2$ and $H_2{}^{15}O$, 606*
compartmental, Tc-99m pyridoxylidene glutamate, -HIDA pharmacokinetics, 45
GI transport of Tc-99m in mice, 606*
heart, heterogeneous phantom, 607*
in vitro, hepatobiliary kinetics, 642*
mathematical, liver image motion correction, 802, 803
mathematical, liver perfusion post-partial hepatectomy, colloid, in rats, 26
multicapillary, cellular tracer uptake, 605*
pharmacokinetic, F-18 fluorouracil, Pt-195m cis-platin, 614*
physiologic pharmacokinetic, 614*
receptor binding, 350
thyroid, $^{99m}TcO_4^-$ trap, 219
tomographic measurement of glucose metabolism rate, 605*
3 compartment, Tl-201 heart, rest and exercise, 1136
Muscle
dermatomyositis, Ga-67 imaging, 1323*
electrical damage, Tc-99m pyrophosphate imaging, 646*, 1322*
I-125 cobra venom distribution, in mice, 655*
inflammation, Tc-99m pyrophosphate imaging, 469*
nuclear magnetic resonance imaging, in rat, 178*
rhabdomyolysis, Tc-99m HEDP imaging, 127
Myoglobin
serum, radioimmunoassay, 115, 120, 165, 371*
Neutron activation analysis
bone mass, drug therapy in osteoporosis, 677*
Ca in bone, hand, in osteoporosis, 85
whole body, bidirectional scanning, 277*
Neutrophils
radiation dose from labels, 255
Nitrogen
total body, prompt gammas from neutron capture, 1158
Nitrogen-13
-ammonia, cerebral blood flow, in dogs, 611*
-ammonia, myocardial blood flow, in dogs, 603*
-ammonia, myocardial studies, scatter fraction, 635*
-ammonia, single-pass myocardial extraction, in dogs, 648*
-glutamate, myocardium, pancreas imaging, 663*
-glutamate, quantitative scanning, osteogenic sarcoma, in child, 782
Nuclear magnetic resonance
muscle tissue imaging, rat leg, 178*
myocardial imaging, F-19, in dogs, 604*
Georg Charles de Hevesy, 590
Nuclear parameters
I-123 decay data, 1212
radioactive decay calculation, 1217
radioactive decay, terminology, 162
radiopharmaceutical bibliography, 607*
Observer performance
adrenal imaging and I-131 iodomethylnorcholesterol tomography, 609*
automated ROC curves, 609*
Bayesian analysis, 622*
calculation of information transmitted by images, 609*
gray scale optimization, 57, 996, 997, 1211, 1212
rest and exercise left ventricular wall motion studies, 661*
Obstetrics
see also *Pregnancy*
diagnosis, book review, 74
Ovaries
adnexal thickening, ultrasound, 1324*
carcinoma, Tc-99m S colloid lymph node imaging, 646*
cyst, ultrasound, 372*
I-131 human chorionic gonadotropin imaging, in rats, 941
masses, ultrasound, CAT evaluation, 815*
polycystic syndrome, metabolic clearance rate of cortisol, 587*
tumor, I-131 iodomethylnorcholesterol uptake, 677* 1322*
tumor, ultrasound, 912*
Oxygen-15
$C^{15}O_2$ inhalation, cerebral blood flow, 606*
$C^{15}O_2$ inhalation imaging, pulmonary embolism, 281
$C^{15}O_2$ inhalation, transverse section perfusion imaging of legs, 619*
O_2 and H_2O, compartmental analysis of steady-state distribution, 606*
O_2, brain tomography, 628*
Palladium-109
-hematoporphyrin, therapy, heart allograft, in rats, 659*
Pancreas
C-11 DL-carboxyl-tryptophan preparation, distribution, in animals, 857
C-11 D and L-phenylalanine, preparation, distribution, in rats, 662*
C-11 tryptophan preparation, 663*
cyst, ultrasound, angiography, 469*
disease, bile acid radioimmunoassay, 676*
I-131 and I-123 labeled methyltyrosine, preparation, distribution, in mice, 973
imaging, prone position anterior projection, 910*
mass, on Tc-99m HIDA hepatobiliary studies, 679*
N-13 glutamate imaging, 663*
positron tomography, C-11 amino acids, 507, 778
radiography, book review, 1214
Se-75 selenomethionine uptake, hypothalamic factors effects, in animals, 543
single photon tomography, C-11 tryptophan, 632*
transplant, contrast angiography, Se-75 selenomethionine imaging,

1111*
tumor imaging, C-11 tryptophan, -valine, -aminocyclobutanecarboxylic acid, 631*
tumor, S-35 thioglucose, in hamsters, 753
ultrasound, disease states, 1222*
ultrasound, normal, 1222*
ultrasound, tail neoplasms, 77*
Parathyroid
adenoma, I-123 scan, ultrasound, 270
hyper-, primary, bone scanning, 602*
removal, post-surgery bone imaging, 674*
Pediatrics
abdominal tumor, differential diagnosis, 679*
abdominal ultrasonography, book review, 175
adrenal hemorrhage diagnosis, 521
bone scanning, 675*, 1322*
brain lesions in lymphocytic cell leukemia, 1101
bronchiectasis, lung perfusion-ventilation, Kr-81m, Tc-99m microspheres, 638*
child abuse recognition, bone imaging, 675*
congenital adrenal hyperplasia, I-131 iodomethylnorcholesterol imaging, 622*
cystic fibrosis, ventricular function, rest and exercise, Tc-99m HSA, 637*
fetus see *Fetus; Pregnancy*
Ga-67 citrate studies, tumor, 75*
gallbladder and bowel uptake of bone agents, 622*
gastroesophageal reflux, Tc-99m S colloid imaging, 636*, 637*, 680*
gastrointestinal tract infarct imaging, Tc-99m HEDP, 1006*
hepatobiliary imaging, Tc-99m PIPIDA, 680*
hydronephrosis, diuretic kidney imaging, 623*
hypophosphatasia, Tc-99m MDP skull imaging, 305
I-123 Hippuran renography, 619*
I-131 therapy for hyperthyroidism, long term follow-up, 847, 890
irradiation induced cartilaginous exostosis, 580
kidney uptake of Tc-99m MDP, post radiation therapy, 32
Legg-Perthes' disease, bone imaging, 170, 458, 459
leukemia, Ga-67 citrate bone uptake, 854
leukodystrophy, 909*
lung ventilation, perfusion, 638*, 639*
metaphyseal uptake of Tc-99m MDP, effect of growth hormone, T_4 therapy, 678*
muscular dystrophy, Tc-99m pyrophosphate heart imaging, 1321*
neonate, brain studies in hypoxia/ischemia, 1110*
neonate, cord blood thyroxine, thyrotropin RIA, 616*
neonate, jaundice evaluation, 637*, 680*
neonate, thyrotropin RIA, 615*
neoplastic disease, Ga-67 citrate serial imaging, 210
oncology, bone marrow imaging, Tc-99m S colloid, 379
osteogenic sarcoma, quantitative N-13 glutamate scanning, 782
post-surgery cardiac function, Tc-99m HSA, 661*
premature infant, thyroid scanning, 615*
pulmonary arteriovenous fistula diagnosis, 76*
pulmonary aspiration detection, Tc-99m S colloid, 636*, 637*, 680*
radiation dosimetry, Ga-67 citrate scanning, 637*
serum angiotensin converting enzyme levels, 1112*
splenic abscess, Tc-99m S colloid, Ga-67 citrate, ultrasound imaging, 1221*
Tc-99m ingestion, breast milk, 799
testes imaging, $^{99m}TcO_4^-$, 1221*
toxicity of particles for lung studies, 1098, 1099
tumor, computerized axial tomography, Ga-67 citrate, Tc-99m phosphate scanning, 1110*
Peripheral see *Extremities*
Phantom
bar, collimator image distortion, 260, 1100, 1315, 1316
depth resolution, 636*
heart, dynamic, 547, 610*
heterogeneous heart, 607*
Phosphorus-32
bone therapy, effect of hormone pretreatment, in rabbits, 684*
-pyrophosphate, tissue uptake parameters, in rats, 76*
radiation dose to labeled neutrophils, platelets, 255
uptake, choroidal hemangiomas and melanomas, 1322*
Placenta
ultrasonography, 470*, 587*, 1223*
Platelets
see *Blood; Indium-111*
Platinum-195m
-cis-platin, pharmacokinetic model, 614*
Plutonium-238
-Be source, total body N by neutron capture, 1158
Pregnancy
amniocentesis, ultrasound, 277*, 1324*
ectopic, ultrasonography, 588*
fetal death, ultrasound, 372*
*gestational age and birth weight prediction, ultrasound, 277**
hydronephrosis, ultrasound, 1222*
*myometrial contractions, ultrasound, 912**
placental ultrasonography, fetal pulmonic maturity, 1223*
*serum free T_4 radioimmunoassay, 627**
trophoblastic disease, ultrasound, 470*
Probe
gated, pressure-volume loops, 610*
Prostate
Br-82 steroid analogs, receptor binding, in animals, 683*
*cancer, lymphatic drainage, Tc-99m SbS colloid, 645**
cancer, metastatic to bone, Tc-99m HEDP scanning, 177*, 275*
cancer, prostatic acid phosphatase assays, 664, 909*, 910*, 1222**
Proteins
see also *Carbon-11; Carbon-14; Indium-111*
autoirradiation, 616*
Br-77, myeloperoxidase labeling method, 663*
iodination parameters, 616*
serum, Tc-99m phosphates interaction, 652*
Quality control
see also *Chromatography*
autoirradiation induced decomposition, 138, 441, 616*, 999
bar phantom image distortion, 260, 1100, 1315, 1316
book review, 811
colloid particle size determination, gel filtration, 133, 1098
counter sensitivity, radioimmunoassay, 276*
evaluation of radioimmunoassay kits and control sera, 813*
I-131 Hippuran, in vitro stability, 441
I-131 iodomethylnorcholesterol, RES distributing impurity, 803, 805, 806
remote data acquisition testing, 1087
scintillation camera, crystal thickness effects, 977, 992
scintillation, field uniformity, 363
serum myoglobin radioimmunoassay, 120
Tc-99m DTPA kits, 652*
Tc-99m MDP stability, 791
Tc-99m (Sn)pyridoxylideneisoleucine, 1189
Tl-201, 684*
Radiation damage
autoirradiation, radiopharmaceuticals, 138, 441, 616*, 999
cartilaginous exostosis, 580
childhood neck irradiation, thyroid imaging, 678*
In-111 oxine leukocyte labeling, 741
In-111 oxine lymphocyte and tumor cell labeling, 1308
Radiation dosimetry

adrenals, I-131 iodomethylnorcholesterol, 60
book review, 812, 1320
C-11 amino acids for pancreas, 507
$C^{15}O_2$ inhalation, 606*
computer code for dose from syringes, 882
dose to labeled neutrophils and platelets, 255
electron dose reduction coefficients, 277*
Ga-67 citrate scanning in children, 637*
heterogeneous heart phantom, 607*
ICRM Life Sciences working group, 998
In-111 oxine-autologous platelets, in baboons, 685*
neutron activation analysis, hand, 85
Ra-224 therapy, book review, 175
radiopharmaceutical bibliography, computer, 607*
Ru-82, 603*
Se-75 selenomethionine retention, 365
Tc-99m in breast milk, 799
Tc-99m PIPIDA, 607*
Tl-201 contaminants, 607*

Radiation safety
air monitoring of Xe-133, 159, 981
book review, 1003, 1004, 1219
photochromic and glass lenses, 898
syringe shield modification, 1101
Xe-127 shielding, 171
volatile I-131, 362, 363, 995

Radiation therapy
bone changes, in rabbits, 1142
bronchial carcinoma, monitoring, 638*
cancer, book review, 1218
effect on bone marrow, in children, 379
effect on Ga-67 citrate distribution, in fasting rats, 938
hemangioma, recurrent, 901
in breast cancer, book review, 1319
lung cancer response, Ga-67 citrate monitoring, 177*
post-, kidney uptake of Tc-99m MDP, 32
radiobiology, book review, 583

Radioassay
see also *Immunoradiometric assay; Radioimmunoassay; Radiometric assay*
IgG, IgE antibodies, 673*
vitamin B_{12}, effect of oral ascorbic acid, 371*

Radiography
angiograms, iliac vessel AVF, 36
angiography, cerebral venous angioma, 1166
biliary, pancreatic, book review, 1218
bone, compared to CAT, 1006*
bone, compared to Tc-99m imaging, 602*, 1006*, 1220*, 1322*
book review, 74, 273, 368
fetal liver studies, 1008*
LVEF, compared to nuclear methods, 1
obstetrical diagnosis, book review, 74
temperomandibular joint disease, 603*

Radioimmunoassay
alpha-fetoprotein, in cancer, 372*, 467*
antibody to hepatitis-B-core antigen, 467*, 676*
atropine, plasma, 366
automatic reservoir for serial pipetting, 262
beta thromboglobulin, 664*
bile acids, 676*
book review, 811, 1003, 1107, 1218
carcinoembryonic antigen, in cancer, 232, 264, 813*, 1007*
digoxin, stat procedure, 664*
enzyme-, L-Dopa, dopamine, 3-O-methyldopamine, 664*
forensic, 796
gastrin, 617*
human chorionic gonadotropin, testicular tumors, 467*
kits, control sera evaluation, 813*
Ligand Assay Interlaboratory Service Programs, 617*
morphine, heroin, in hair, 748, 796
prostatic acid phosphatase, 664*, 909*, 910*, 1222*
serum folate, antineoplastic drug effects, 178*
serum myoglobin, 115, 120, 165, 371*, 664*
staphylococcal antigen, in rabbits, 813*
thyroglobulin, serum and saliva, in thyroid carcinoma, 77*
thyroid stimulating hormone, 615*, 616*, 1124
thyroxine see *Thyroxine*
T_3, age dependence in adults, 1124
T_3, post I-131 therapy, 387
urinary renin activity, 77*

Radiometric assay
aminopyrine breath test, 686*
C-14 fatty acid metabolism, *M. lepraemurium,* 1222*
container geometry, 1090
M. tuberculosis, fatty acid metabolism, 676*
niacin, 419
serum antibiotic activity, 616*
Vitamin B_6 in biological material, 676*
Vitamin B_{12}, folate, in food, 616*

Radium-224
therapy, book review, 175

Receptors
antagonist, H-3 muscarine acetylcholine for heart, distribution, in animals, 865
assays, book review, 1218
beta-adreno, blocking agents, preparation, distribution, 350
beta, I-125 hydroxybenzolpindolol distribution, in mice, 681*
Br-82 steroid analogs binding, for prostate, 683*
dopamine, Br-75, Br-77 bromocriptine, preparation, distribution, in rats, 683*
F-18 deoxyfluoromannose, preparation, metabolism, 672*
F-18 haloperidol, preparation, binding, 671*
Fc-, function in lupus erythematosis, 813*
halogenated estrogen analogs, binding affinity, distribution, in animals, 671*, 761
H-3 dihydroalpernolol, myocardial uptake, in dogs, 683*
H-3 methylquinuclidinyl benzilate binding, for heart, preparation, distribution, in animals, 671*
human chorionic gonadotropin, ovary imaging, in rats, 941
insulin, whole-body in vivo measurement, 605*
iodinated acetylcholinesterase binding, for heart, preparation, distribution, in mice, 671*
kidney, I-123 vasopressin uptake, in animals, 657*
neutrophil binding, N-formyl-selenomethionine-methionine, 681*
transferrin-binding macromolecule, EMT-6 sarcoma, 672*
transferrin binding, normal and virus transformed cell cultures, 672*

Red blood cell see *Blood; Carbon-11; Chromium-51; Technetium-99m, red blood cells*

Renin
urinary, radioimmunoassay, 77*

Resolution
bar phantom image distortion, 260, 1100, 1315, 1316
Compton scatter tomography, 911*
crystal size effects, 610*, 977, 992
depth, quantitation, 636*
digital camera, 628*
emission computed tomography, 50, 609*
emission tomographic brain scanner, 628*
multi-detector germanium camera, 629*
parallel hole collimator, geometric response, 635*
positron tomography, 628*
proportional gas chamber detector, 335

rotating parallel slit collimator, 610*
scintillation and solid state cameras, 635*
scintillation camera, Ta-178, 538
total imaging systems, Tl-201, 635*
transverse-section brain imager, 319
7 pinhole collimator tomography, 644*
Rubidium-82
generator, alumina, 684*
myocardial positron tomography, 603*
renal blood flow, in dogs, 619*
Rubidium-86
irradiated bone kinetics, in rabbits, 1142
Ruthenium-97
-HIDA, hepatobiliary studies, in animals, 682*
-pharmaceuticals, tumor uptake, in animals, 684*
Ruthenium-103
-HIDA, hepatobiliary studies, in animals, 682*
Salivary glands
imaging, 679*
Scandium-46
-microspheres, renal blood flow, in dogs, 619*
Scanner
rectilinear, depth resolution quantitation, 636*
rectilinear, gray scale, 57, 996, 997, 1211, 1212
whole body, 628*
Selenium-75
-cholic acid analogs for hepatobiliary, dynamics, in rats, 684*
-N-formyl-selenemethionine-methionine, neutrophil binding, 681*
-selenite, -selenomethionine, distribution, in hepatoma-bearing rats, 276*
-selenomethionine, hypothalamic factors effects, in animals, 543
-selenomethionine, long term retention, 365
-selenomethionine, pancreas transplant imaging, 1111*
Skin
dermatomyositis, Ga-67 imaging, 1323*
Spleen
abnormalities, on hepatobiliary studies, 679*
abscess, ultrasound, Ga-67 citrate, Tc-99m S colloid imaging, in child, 1221*
Fc-receptor function in lupus erythematosus, 813*
function, plasma exchange treatment, Cr-51 RBC, Tc-99m damaged RBC, 814*
Ga-67 liposome preparation, distribution, in mice, 680*
Ga-68 microspheres uptake, in rats, 1112*
In-111 oxine-, Tc-99m-DTPA- liposomes, preparation, distribution, in mice, 434
radiation dose, Ga-67 citrate, in children, 637*
-to-liver ratio of colloid uptake, 149
uptake in I-131 iodomethylnorcholesterol in adrenal imaging, 803, 805, 806
Spleen imaging
autologous Tc-99m RBC, 683*
differential diagnosis of tumor, in children, 679*
in malignant melanoma, Tc-99m S colloid, 1232
leukodystrophy, Tc-99m S colloid, 909*
reversible functional asplenia, hepatitis, Tc-99m S colloid, 34
Ta-178, in rabbits, 538
Statistics
use, 550
Steroids
Br-82 analogs for prostate, receptor binding, 683*
Strontium-82
Rb-82 generator, 684*
Strontium-85
bone scanning in thyroid cancer, 999
-microspheres, blood flow, bone retention, in dogs, 413
Strontium-87m
-alginic acid compound, dynamics in gastroesophageal reflux, 1023
Stronium-89
therapy, bone metastases, 371*
Sulfur-35
-thioglucose, pharmacokinetics, pancreas tumor, in hamsters, 753
Surgery
aortocoronary saphenous bypass, Tl-201 perfusion studies, 576
biliary-enteric bypass, cholecystectomy, post-op Tc-99m HIDA studies, 686*
coronary bypass, candidacy, 1206
coronary bypass, perioperative myocardial infarct evaluation, 711
heart, post-surgery function studies, in children, 661*
open heart, damage assessment, Tc-99m pyrophosphate imaging, 275*
recurrent irradiated hemangioma, 901
Synovium see *Joint*
Tantalum-178
lung, liver agents, preparation, distribution, imaging, in animals, 1176
scintillation camera imaging, 538
Technetium-99m
-acetylcysteine, renal extraction efficiency, in dogs, 629*
-acetylcysteine, serum protein interactions, 682*
-aerosol, ventilation in chronic obstructive pulmonary disease, 620*
-agents, brain membrane transport, 1181
-aminoethanethiol complexes, preparation, characterization, 641*
autoirradiation of radiopharmaceuticals, 138, 999
bis(2-mercaptoethyl)amine ligands, for brain, preparation, distribution, in animals, 654*
-bovine thrombin, -streptokinase-activated thrombin, preparation, 967
breast milk secretion, 586*, 799
-cyclam, preparation, distribution, in animals, 641*
-diethyl-IDA, hepatobiliary pharmacokinetics, in vitro model, 642*
-diethyl-IDA, hepatobiliary studies, 171, 685*, 686*
-diethyl-IDA, heptobiliary transport mechanism, in rats, 642*
-diethyl-IDA, liver transplant evaluation, 314
-dihydrothioctic acid, Tc valence, electrophoresis, 871
-diphosphonic acids, effect of structure on bone uptake, in rats, 1066
-DMSA see *Kidney*
electron dose reduction coefficient, 277*
emission computed tomography, 108
-fibrinogen, deep-vein thrombosis detection, 178*
gastrointestinal transport, model, in mice, 606*
-gluceptate, kidney imaging, mass lesions, 1018
-gluconate, Sn vs electrolytic production, kidney imaging, in rabbits, 766
heart tomography, 7 pinhole collimator, 644*
-heparin, leg imaging in thrombosis, 652*
-HIDA see *Hepatobiliary system*
-hydroxymethane diphosphonate, bone imaging, 653*
-hydroxymethane diphosphonate, bone uptake compared to Tc-99m Tc MDP and HEDP, 655*
-hydroxymethane diphosphonate, gentisic acid stabilized, 654*
-3-hydroxy-4-formylpyridine, glutamic acid complex for hepatobiliary, preparation, distribution, imaging, in rabbits, 39
imaging, crystal size effects, 610*
-iminodiphosphonate, myocardial infarct imaging, 1220*
immunoglobulin G labeling, 652*

-leukocytes, labeling, in vivo migration, 1197
lung studies, interference with Xe-133, 268, 270
-oxytechnetium (V) complexes, preparation, characterization, 641*
-parabutyl IDA, hepatobiliary studies, in neonatal jaundice, 637*
-paraisopropyl-IDA, liver retention in hepatobiliary studies, 171
-penicillamine, kidney transport evaluation, 1095
-phosphates, soft tissue tumor uptake, 674*
-phytate, arteriovenous fistula detection, 36
-phytate colloid, lymph node uptake parameters, in rabbits, 1038
-phytate, lymph node imaging, 467*, 585*, 933
-PIPIDA, hepatobiliary pharmacokinetics, in vitro model, 642*
-PIPIDA, hepatobiliary studies, 600*, 680*, 686*
-PIPIDA, radiation dosimetry, 607*
-plasmin, deep vein thrombosis uptake, 633*
-polyphosphate, bone scanning, 1268
-polyphosphate, myocardial contusion imaging, 371*
-pyridoxylidene-isoleucine, hepatobiliary transport mechanism, in rats, 642*
-pyridoxylidene-isoleucine, labeling and storage effects, 1189
-pyridoxylidene glutamate, hepatobiliary imaging, 468*
-pyridoxylidene glutamate, pharmacokinetics, in rats, 45
radiation dose to labeled neutrophils, platelets, 255
reduction methods, comparison, 653*, 766
-Sb colloid, bone marrow imaging, subcapital femoral neck fracture, 673*
-SbS colloid, lymphatic drainage, 645*
-SbS colloid, lymph node imaging, 467*, 585*, 933
-SbS colloid, particle size determination, 133, 1098
single-gamma tomoscanner, 319
-Sn colloid, lymph node uptake parameters, in rabbits, 1038
-$SnPO_4$, para-aortic lymph node imaging, in dogs, 654*
solutions, radiolytic peroxide production, 652*
source, transmission tomography, 665*
-tetradentate ligands, preparation, distribution, in animals, 641*
valence state, 532, 533, 652*, 871
ventricular performance, cold pressor test, 640*
Technetium-99m, albumin
autoirradiation, 138, 999
cisternography, 275*
first-pass and equilibrium characteristics, in dogs, 654*
MAA, intra-arterial hepatic infusion patterns, 675*
MAA, lung imaging, pulmonary artery occlusion, in dogs, 1251
MAA, lung perfusion see *Lung, perfusion; Lung, ventilation-perfusion*
MAA, right to left shunt diagnosis, 75*
MAA, venography, 639*
-microparticles, liver phagocytosis, proteolysis, 606*
myocardial studies; see *Heart*
peritoneo-venous shunt evaluation, 72
Technetium-99m, diphosphonate (HEDP)
bone scanning see *Bone scanning*
bone uptake, compared to Tc-99m HMDP and MPP, in rats, 655*
compared to Tc-99m MDP, 98, 821, 896
gastrointestinal tract infarct imaging, in children, 1006*
gentisic acid stabilized, 654*
infection scanning, disc space, in animals, 1006*
myocardial contusion imaging, 371*
reduction state, 532
renal extraction efficiency, in dogs, 629*
serum protein interactions, 653*
Sn vs electrolytic production, imaging, in rabbits, 766
soft tissue uptake, alcohol induced rhabdomyolysis, 127
Technetium-99m, diphosphonate
uremic pulmonary calcification imaging, 201
Technetium-99m, DTPA
adrenal hemorrhage diagnosis, 521
aerosol lung clearance, 613*
arteriovenous fistula between internal iliac vessels, detection, 36
brain imaging, mycosis fungoides, 240
cisternography, 1101
inflammatory lesion uptake, in rabbits, 173
kidney studies see *Kidney*
kit tagging yields, 652*
-liposomes, preparation, distribution, in mice, 434
multiple chemodectoma imaging, 904
pharmacokinetics, in dogs, 1273
renal extraction efficiency, in dogs, 629*
Sn vs electrolytic reduction, preparation, imaging, in rabbits, 766
Technetium-99m, glucoheptonate
brain imaging, 287, 1101
compared to I-131 Hippuran for kidney studies, 623*
kidney angiography, 1106
kidney imaging, acute pyelonephritis, 623*
myocardial contusion imaging, 371*
renal extraction efficiency, in dogs, 629*
Technetium-99m, methylene diphosphonate (MDP)
blood flow, bone uptake, in dogs, 413, 1257
bone scanning see *Bone scanning*
compared to Tc-99m HEDP, HMDP, 655*, 821
kidney blood flow, imaging, excretion, 623*
kidney uptake post radiation therapy, 32
liver metastases uptake, 303
myocardial infarct imaging, 402, 1220*
pericardial effusion accumulation, 1102
reduction state, 532, 871
renal extraction efficiency, in dogs, 629*
serum protein interactions, 652*
stomach content, stability, 791
Technetium-99m, microspheres
aerosol, mucociliary lung clearance, 613*
inflammatory lesion uptake, in rabbits, 173
lung imaging, pulmonary embolism, in dogs, 407
lung perfusion, 612*, 613*, 638*, 950, 1005*
right-to-left shunt quantitation, 670*
venography, in pulmonary embolism, 291
Technetium-99m, pertechnetate
see also *Brain, blood flow; Brain imaging*
aerosol, lung clearance, 613*
angiography, reimplanted digits, 674*
arthritic joint uptake, in rabbits, 673*
CSF shunt evaluation, 621*
first-pass ventriculography, false left ventricular aneurysm, 851
gastrointestinal imaging, 586*, 888
inflammatory lesion uptake, in rabbits, 173
kidney, dynamic imaging, 11, 1029, 1095
left-to-right shunt quantitation, in dogs, 502
mean transit time, cerebral anastomosis, 611*
myocardial angiography, 276*, 670*, 724
testes imaging, torsion diagnosis, 173, 1221*
thyroid imaging, 345, 678*, 904, 909*
thyroid trap kinetics, 219, 944
tumor uptake and vascularity, 612*
Technetium-99m, pyrophosphate
autoirradiation, 138, 999
arthritic joint uptake, in rabbits, 673*
blood kinetics, renal osteodystrophy, 1321*
bone studies see *Bone; Bone scanning*
joint imaging, rheumatoid arthritis, 467*
muscle imaging, 469*, 646*, 1322*
myocardial calcification uptake, 178*
myocardial contusion imaging, 371*

myocardial damage, uptake mechanism, 650*
myocardial imaging, muscular dystrophy, in children, 1321*
myocardial infarct imaging see *Heart, infarct*
myopericarditis, heart uptake, in mice, 1047
pericardial effusion imaging, 392
pleural effusion accumulation, 276*
renal extraction efficiency, in dogs, 629*
serum protein interactions, 652*
Sn vs electrolytic preparation, 766
tissue uptake parameters, in rats, 76*

Technetium-99m, Red blood cells
arteriovenous fistula diagnosis, 36
autologous, labeling, spleen scanning, 683*
first-pass and equilibrium characteristics, in dogs, 654*
gastrointestinal bleeding evaluation, 631*, 1080
heart studies see *Heart*
heat damaged, spleen function in plasma exchange treatment, 814*
in vivo labeled, compared to Tc-99m HSA for heart, 1210
in vivo labeling, 877, 1071
pacemaker rate optimization, 660*
venous volume change imaging, 633*

Technetium-99m, Sulfur colloid
bone marrow imaging, 675*
gastroesophageal reflux evaluation, 636*, 637*, 1023
gastrointestinal clearance and transit, cholinergic effects, 685*
intestinal bleeding demonstration, 631*
liver clearance rate, 586*
liver imaging see *Liver*
liver perfusion, post-partial hepatectomy, in rats, 26
liver volume, 514
lymphangiography, 275*, 905
lymph node imaging, 467*, 646*
lymph node uptake parameters, in rabbits, 1038
particle size determination, 133, 1098
peritoneo-venous shunt evaluation, 72
pulmonary aspiration detection, in children, 636*, 637*
spleen imaging, 34, 909*, 1221*, 1232
spleen-to-liver uptake ratio, 149
thrombosis uptake, deep vein, in dogs, 633*
vascular trauma imaging, 633*

Terminology
equilibrium, radioactive decay, 162
international, book review, 465
radiopharmaceutical classification, 364
radiotracer classification, 364
use of statistics, 550

Testes
adenoma, I-131 cholesterol image, 307
torsion, $^{99m}TcO_4^-$ dynamic imaging, 173, 1221*
tumor, I-131 iodomethylnorcholesterol uptake, 677*, 1322*
tumor, therapy monitoring, alpha-fetoprotein, chorionic gonadotropin RIA, 467*

Thallium-200
Tl-201 contaminant, 607*

Thallium-201
bone imaging, 815*
carrier content, radiochemical purity, 684*
contaminants, radiation dosimetry, 607*
heart studies see *Heart*
imaging, crystal size effects, 610*
lung uptake, stress myocardial imaging, 649*
myocardial uptake, subcellular, exercise effects, in rats, 1136
peripheral vascular perfusion imaging, 634*, 1005*
renal blood flow, acute tubular necrosis, in rats, 630*
thyroid uptake, 678*, 827
total imaging system performance index, 635*

Thallium-202
Tl-201 contaminant, 607*

Therapy
actinide decorporation, Ca-, Zn-DTPA, 73
alginic acid compound, in gastroesophageal reflux, 1023
antithyroid drugs, goiter, 624*, 1263
calcitonin in osteoporosis, bone mass determination, 677*
cancer, hyperthermia, radiation, book review, 1218
growth hormone, T_4, effect on metaphyseal bone uptake, in children, 678*
immuno-, Pd-109 hematoporphyrin, heart allograft, in rats, 659*
I-125, thyrotoxicosis, 815*
I-131 thyroid see *Thyroid*
L-dopa, reserpine effect on brain uptake of C-14 methionine, -phenylalanine, in rats, 76*
P-32 for bone, effect of hormone pretreatment, 684*
Sr-89, bone metastases, 371*
stanozolol in osteoporosis, bone mass determination, 677*
thyroxine, TRH test, *I uptake, 177*
tumor calcinosis, bone scan monitoring, 675*
Y-90 resin spheres, intra-arterial, liver cancer, 674*

Thermography
in breast cancer, book review, 1319

Thrombus see *Vascular system*

Thyroid
carcinoma, autonomously functioning nodule, 1001
cancer, bone scanning, Tc-99m pyrophosphate, I-131, 271,999
cancer, book review, 811
cancer, I-131 dose distribution, 92, 1099, 1100
cancer, serum and salivary thyroglobulin radioimmunoassay, 77*
cancer, T_3 therapy withdrawal, TSH levels, 928
function tests, age-dependent effects, 1124
gland volume, with imaging and ultrasound, 585*
I-125 therapy, 815*
Marine–Lenhart syndrome, 624*
medullary carcinoma, CEA and calcitonin levels, 813*
screening, neonates, 615*, 616*
Tl-201 uptake, 678*, 827
tomography, seven pinhole collimator, 643*
total binding capacity of thyroxine binding globulin, 67, 995, 997
trap, kinetics, 219, 944
TRH test, *I uptake, thyroid therapy, 177*
uptake of volatile I-131, 362, 363, 995

Thyroid, I-131 therapy
combined with drugs, toxic diffuse goiter, 624*, 1263
dose distribution, 92, 1099, 1100
effect on T_3, T_4 serum levels, 387, 928
for hyperthyroidism, 624*, 890
for thyrotoxicosis, 366, 1110*
posttreatment thyroid disease, 267, 847, 890
radioactivity in perspiration, 469*

Thyroid imaging
abscess, 1051
comparison of $^{99m}TcO_4^-$ and I-123, 678*
comparison of $^{99m}TcO_4^-$ and I-125, 909*
hyperfunctioning nodule disappearance, 579
mediastinal goiter, I-131, 177*
multiple chemodectomas, $^{99m}TcO_4^-$, 904
proportional gas chamber detector, in animals, 335
remote childhood neck radiation, cold defects, 678*
time-coded aperture, 345

Thyroid stimulating hormone
assays, precision, 617*
effect on thyroid trap, 944
effect on thyroid uptake of Tl-201, 678*
levels, age dependency, in adults, 1124
levels, post T_3 therapy in thyroid carcinoma, 928

neonatal cord blood, 616*
radioimmunoassay, 615*, 616*, 813*
stimulation thyroid imaging, 624*
thyroxine therapy, TRH test, *I uptake, 177*
Thyrotropin see *Thyroid stimulating hormone*
Thyroxine
assay, precision, 617*
-binding globulin, total binding capacity, 67, 995, 996
free, comparison of methods, 626*, 627*
free, drug interference, protein matrix effects, 627*
free, effect of clinical states, 627*
free, kinetic reaction rate technique, 627*
free, radioimmunoassay, prebound T_4 microcapsules, 956
free, single tube radioimmunoassay, 615*
levels, age effects in adults, 1124
levels, Marine-Lenhart syndrome, 624*
radioimmunoassay kit evaluation, 615*, 813*
radioimmunoassay, micro-, premature infants, 615*
radioimmunoassay, neonatal cord blood, 616*
serum levels, post I-131 therapy, 387
therapy, effect on metaphyseal bone uptake, in children, 678*
therapy, TRH test, *I uptake, 177*
Tin
(II)-pyrophosphate, effect on red cell survival, in rabbits, 294
Tomography, computerized axial
abdominal abscess, compared to Ga-67 imaging, 469*
acoustic neurinoma, 275*
bone, compared to Tc-99m imaging, radiography, 1006*
book review, 1108
brain and orbit anatomy, book review, 908
brain, compared to radionuclide methods, 319, 462, 1221*
brain, complementary to scanning, 1117
brain, leukodystrophy, 909*
brain, metastatic lung cancer, 644*
cerebral venous angioma, 1166
compared to radionuclide methods, book review, 1320
gynecologic pelvic masses, 815*
hemangioma, 901
kidney, polycystic, 470*
liver tumor, compared to ultrasound, scintigraphy, 1111*
pediatric tumor, compared to scanning, 1110*
pulmonary arterial occlusion imaging, in dogs, 601*, 1251
salivary glands, 679*
Tomography, emission computed
acute myocardial infarction, Tc-99m pyrophosphate, in dogs, 50
cerebral blood flow, regional, continuous Kr-81m, 611*
cerebral blood volume, C-11, Cr-51 RBC, 328
liver hematoma, in dogs, 448
liver volume, Tc-99m S colloid, 514
sampling requirements, 609*
single photon, attenuation compensation, 658*
single vs multiple slice, 799, 800
transaxial, Tl-201, myocardial infarct, 736
whole-body system, 102, 108
Tomography, positron
accidental coincidences effects, 634*
brain, C-11 carboxyhemoglobin, $^{15}O_2$, 628*
brain, heart, F-18 fluorodeoxyglucose, in dogs, 606*
circular, optimization of shielding depth, 635*
^{11}CO inhalation, regional cerebral blood volume, 370*
$C^{15}O_2$ inhalation, cerebral blood flow, 606*
coincident scatter analysis, 635*
coronary artery disease, N-13 ammonia, 604*
heart infarct imaging, F-18, in dogs, 1013
heart, Rb-82, 603*
myocardial blood flow, regional, Cu-62, in dogs, 648*
myocardial infarct, Mn-52m, in dogs, 648*
noise propagation, 609*
pancreas, C-11 amino acids, 507, 778
retroperitoneal tumor differentiation, 631*
single vs multiple slice, 799, 800
Tomography, radionuclide
brain scanner performance, 628*
compared to adrenal imaging, I-131 iodomethylnorcholesterol, 609*
depth resolution quantitation, 636*
focal plane, simultaneous multiplane deconvolution, 666*
Fourier multiaperture technique, 986
gated blood pool imaging, 628*, 644*
glucose metabolism rate, brain, heart, 605*
lung cancer staging, 644*
multi-detector tomoscanner, 319
multiplane scanner, off-plane blurring correction, 1194
optical back-projection, 7 pinhole collimator images, 608*
retroperitoneal fibrosis, Ga-67 citrate, 238
seven pinhole collimator, status, 643*
single photon, pancreas, C-11 tryptophan, 632*
transaxial, Compton scatter effects, 608*
Tomography, transmission
brain, mycosis fungoides, 240
Compton scatter, 911*
dynamic lung, Tc-99m source, 665*
liver hematoma, in dogs, 448
Toxicity
asbestos, lung function, 621*
C-11 tryptophan, -valine, in dogs, 507
doxorubicin, 910*
microspheres, 613*, 899
particles for lung studies, 1098, 1099
Sn(II)-pyrophosphate, red cell survival, in rabbits, 294
Zn-DTPA, 73
Transmission
see also *Tomography, transmission*
absorption edge, stable I determination, 1286
Trauma
biliary tract hemorrhage diagnosis, 1112*
bone fracture scanning, 647*, 1227
bone imaging, child abuse recognition, 675*
bone, stress fracture imaging, 1271
electrical, Tc-99m pyrophosphate muscle imaging, 646*, 1322*
epigastric, ultrasound, 1324*
myocardial contusion, Tc-99m scanning, 371*
subcapital femoral neck fracture, Tc-99m Sb colloid bone marrow imaging, 673*
vascular, Tc-99m S colloid imaging, 633*
Triiodothyronine (T_3)
assays, precision, 617*
levels, age dependency, in adults, 1124
levels, Marine-Lenhart syndrome, 624*
levels, neck abscess, 1051
radioimmunoassay kit evaluation, 813*
serum levels, post I-131 therapy, 387
therapy, in thyroid carcinoma, 928
Tuberculosis
extra-pulmonary, Ga-67 citrate scanning, 833, 1111*
Tumor
see also *specific organ*
abdominal, differential diagnosis, in children, 679*
alpha-fetoprotein radioimmunoassay, 372*, 467*
C-11 aminocyclobutane carboxylic acid, preparation, distribution, imaging, in animals, 1055
carcinoembryonic antigen radioimmunoassay, 232
chemodectoma, multiple, 904
chorionic gonadotropin radioimmunoassay, 467*

culture, anti-human chorionic gonadotropin uptake, 656*
differentiation, P-32 uptake, choroidal lesions, 1322*
EMT-6 sarcoma, transferrin-mediated Ga-67 citrate uptake, 837, 843
EMT-6, transferrin-binding macromolecular component, 672*
F-18 fluorouracil imaging, 645*
F-18 glucose analog uptake, imaging, in animals, 662*
Ga-67 citrate studies see *Gallium-67, citrate*
gynecologic, book review, 175
gynecologic, ultrasound, 372*, 912*
HeLaS3 cells, In-111 oxine labeling damage, 1308
hepatoma, Cd-115m chloride, Co-57 bleomycin, I-125 HSA, Se-75 selenite, Se-75 selenomethionine distribution, in rats, 276*
I-123 fibrinogen imaging, 645*
I-125 and I-131 nucleic acids, preparation, distribution, imaging, in animals, 785
I-131 carcinoembryonic antigen imaging, 645*
lactoferrin content, Hodgkin's and lymphoma, 424
leg, transverse section perfusion imaging, $C^{15}O_2$ inhalation, 619*
mediastinal metastases, Ga-67 citrate scanning, 644*, 645*, 814*
melanoma, spleen imaging, 1232
melanoma, urinary excretion of L-Dopa, dopamine, 3-O-methyl-dopamine, 664*
Mn-54 uptake, carrier effect in rats, 656*
multiple myeloma, skull, bone and brain imaging, 125, 647*
neurofibrosarcoma, Ga-67 citrate scanning, 275*
osteogenic sarcoma, quantitative N-13 glutamate scanning, 782
radionuclide induced, 847, 890
retroperitoneal, differentiation, positron tomography, 631*
Ru-97 agents, uptake studies, in animals, 684*
salivary gland, imaging, 679*
soft tissue, Tc-99m phosphates uptake, 303, 674*
ultrasound detection, 77*, 270, 372*, 470*, 912*, 1111*
vascularity, effect on radiopharmaceutical uptake, 612*, 632*
Y-90 resin sphere intra-arterial therapy, 674*

Ultrasound
abdominal, 175, 179*, 370*, 469*, 601*, 902, 1324*
abscess, 370, 469*, 601*, 1221**
adrenal gland mass, 77*
amniocentesis, 277, 1324**
book review, 74, 175, 1003, 1320
*carotid bifurcation, 911**
compared to computerized axial tomography, 1111*
compared to radionuclide techniques, 270, 469, 651*, 1111*, 1320*
complementary to radionuclide techniques, 601*, 815*, 1221*
cysts, 179, 372*, 469*, 1007**
epigastric trauma, 1324*
*eye, glaucoma, 277**
fetus, 277*, 372*, 815*, 1008*, 1223*, 1323*, 1324*
gallbladder, 179, 1112**
hepatobiliary system, 600*, 686*
inferior vena cava, 77, 1113**
kidney, 77*, 372*, 470*, 815*, 1007*, 1008*, 1113*
*kidney depth correction, renogram, 1007**
liver, 179*, 601*, 814*, 816*, 1111*
myocardial, 600, 651**
ovarian tumor, 912*
pancreas, 77, 469*, 1222**
parathyroid adenoma, compared to I-123 scan, 270
*parenchymal gas, 1113**
pelvic masses, 370*, 372*, 815*
*pericholecystic abscess, 911**
placenta, 470*, 587*, 1223*
obstetrics, 74, 77, 470*, 588*, 912*, 1222**
pulmonary arteriovenous fistula diagnosis, 76*
retroperitoneal fibrosis, 238
salivary gland, 679*
spleen, 1221*
thyroid volume, 585*
tumor, 77*, 270, 470*, 814*, 912*, 1111*, 1113*
uterus, 372*, 587*, 1008*

Urinary tract
obstruction, Tc-99m DTPA imaging, 236, 623*

Uterus
Adnexal thickening, ultrasound, 1324*
cyst, tumor, ultrasound, 372*
in renal agenesis, ultrasound, 587*
endometriosis, adenomyosis, ultrasound, 1008*

Vascular system
arteriovenous fistula between internal iliac vessels, 36
capillary permeability, effect on Ga-67 citrate uptake, in rabbits, 660*
carotid bifurcation, ultrasound, 911*
coronary bypass graft evaluation, 604*, 1111*
deep vein thrombosis detection, Tc-99m fibrinogen, 178*
*deep vein thrombosis, Tc-99m plasmin, I-125 fibrinogen uptake, 633**
*deep vein thrombosis, Tc-99m S colloid uptake, in dogs, 633**
false aneurysms, Tc-99m flow study, 808
inferior vena cava, ultrasound assessment, 77, 1113**
markers, first-pass and equilibrium characteristics, in dogs, 654*
peripheral Tc-99m angiography, 652*
peripheral Tl-201 angiography, 634*, 1005*
peritoneo-venous shunt evaluation, Tc-99m S colloid, HSA, 72
pulmonary arteriovenous fistula diagnosis, 76*
pulmonary artery occlusion imaging, in dogs, 601*, 1251
pulmonary embolism see also *Lung*
pulmonary embolism, Tc-99m microsphere venography, 291
right-to-left shunt, patent ductus arteriosus with Eisenmeyer physiology, Tc-99m MAA imaging, 75*
superior vena caval obstruction, Tc-99m glucoheptonate kidney angiography, 1106
Tc-99m MAA venography, simultaneous with lung study, 639*
thrombophlebitis, false-positive I-131 fibrinogen study, dermatitis, 808
thrombophlebitis, I-123 fibrinogen imaging, radiopaque venography, 633*
thrombosis, Tc-99m heparin imaging, 652*
thrombus, intracardiac, I-123 fibrinogen imaging, in dogs, 604*
trauma, Tc-99m S colloid imaging, 633*
venous blood flow, tourniquet effects, Tc-99m MAA, 639*

Vitamin B_6
radiometric assay, 676*

Vitamin B_{12}
assay, precision, 617*
in food, radiometric assay, 616*
*radiodilution assay, false-negative, pernicious anemia, 1007**

Whole-body
see also *Bone scanning; Ga-67, citrate*
neutron activation analysis, bidirectional scanning, 277*
scanner for quantitative distribution measurement, 628*

Xenon
regional ventilatory clearance methods, 703

Xenon-127
lung ventilation, compared to Xe-133, 460, 461
shielding, 171

Xenon-133
air contamination measurement, 981
air monitoring, 159
compared to Xe-127, 460, 461
*hepatic blood flow, in dogs, 1323**
liver retention, steatosis, 397, 450

lung ventilation see *Lung ventilation; Lung, ventilation-perfusion*
pulmonary arterial pressure estimation, in dogs, 923
quantitative lung volume, 620*
Ytterbium-169
electron dose reduction coefficient, 277*
Yttrium-90
-resin spheres, intra-arterial radiation therapy, liver cancer, 674*
Zinc
-DTPA, actinide decorporation therapy, 73

THE SOCIETY OF NUCLEAR MEDICINE
27th ANNUAL MEETING

June 24-27, 1980 **Cobo Hall** **Detroit, Michigan**

CALL FOR ABSTRACTS FOR SCIENTIFIC PROGRAM

The Scientific Program Committee solicits the submission of abstracts from members and nonmembers of the Society of Nuclear Medicine for the 27th Annual Meeting to be held in Detroit, Michigan. Abstracts accepted for the program will be published in the June issue of the *Journal of Nuclear Medicine*. Original contributions, in three specific categories (Basic Science, Clinical Science and Clinical Practice) on a variety of topics related to nuclear medicine will be considered.

Only abstracts prepared on the official abstract form will be considered. The official abstract form may be obtained from the NOVEMBER issue of JNM or from the Society at the address below

CALL FOR ABSTRACTS FOR RADIOPHARMACEUTICAL SYMPOSIA

The Scientific Program Committee urges members and nonmembers of the Society to submit abstracts for two Radiopharmaceutical Symposia to be held at the 27th Annual Meeting. The two special topics will be

- Bio-inorganic chemistry
- Therapeutic applications

The submission procedure remains the same as above except that authors are requested to type the word "SYMPOSIA" above and outside the box on the official abstract form. Abstracts accepted for the symposia will be published in the June JNM. The official abstract form may be obtained from the November issue of JNM or from

Mr. Dennis L. Park
The Society of Nuclear Medicine
475 Park Avenue South
New York, NY 10016
(212) 889-0717
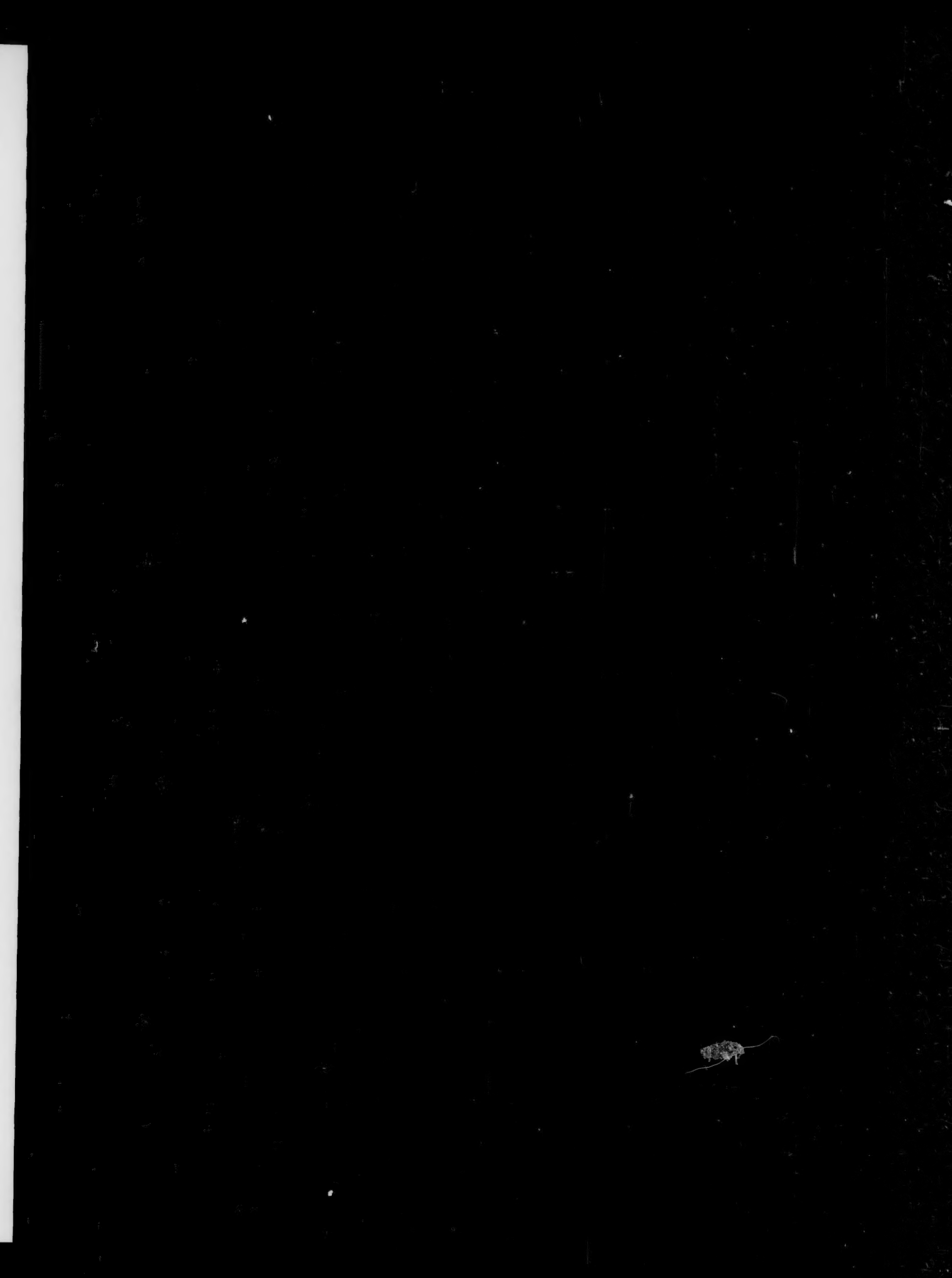
DEADLINE FOR RECEIPT OF ABSTRACTS IS TUESDAY, JANUARY 15, 1980.